

# **Structure and function of the mitochondrial NADH ubiquinone oxidoreductase of *Arabidopsis thaliana***

Von der Naturwissenschaftlichen Fakultät  
der Gottfried Wilhelm Leibniz Universität Hannover  
zur Erlangung des Grades  
Doktorin der Naturwissenschaften  
Dr. rer. nat.

genehmigte Dissertation  
von  
M. Sc. Jennifer Klodmann  
geboren am 9. Dezember 1981 in Hannover

Referent: Prof. Dr. Hans-Peter Braun  
Koreferent: Prof. Dr. Christoph Peterhänsel  
Tag der Promotion: 30. August 2012

**Parts of this work contributed to the following publications:**

Schertl, P., Sunderhaus, S., Klodmann, J., Grozeff, G.E., Bartoli, C.G. and Braun, H.P. (2012)  
L-galactono-1,4-lactone dehydrogenase (GLDH) forms part of three subcomplexes of  
mitochondrial complex I in *Arabidopsis thaliana*.  
*J. Biol. Chem.* 287: 14412-14419.

Klodmann, J. and Braun, H.P. (2011)  
Proteomic approach to characterize mitochondrial complex I from plants.  
*Phytochemistry* 72: 1071-1080.

Klodmann, J., Lewejohann, D. and Braun, H.P. (2011)  
Low-SDS Blue native PAGE.  
*Proteomics* 11: 1834-1839.

Klodmann, J., Senkler, M., Rode, C. and Braun, H.P. (2011)  
Defining the protein complex proteome of plant mitochondria.  
*Plant Physiol.* 157: 587-598.

Rode, C., Senkler, M., Klodmann, J., Winkelmann, T. and Braun, H.P. (2011)  
GelMap – a novel software tool for building and presenting proteome reference maps.  
*J. Proteomics* 74: 2214-2219.

Welchen, E., Klodmann, J. and Braun, H.P. (2011)  
Biogenesis and supermolecular organization of the oxidative phosphorylation system in  
plants.  
*In: Plant Mitochondria. Edited by Kempken, F. pp. 327–355. Springer Science + Business  
Media LLC, New York, NY.*

Klodmann, J., Sunderhaus, S., Nimtz, M., Jansch, L. and Braun, H.P. (2010)  
Internal architecture of mitochondrial complex I from *Arabidopsis thaliana*.  
*Plant Cell* 22: 797-810.

Sunderhaus, S., Klodmann, J., Lenz, C. and Braun, H.P. (2010)  
Supramolecular structure of the OXPHOS system in highly thermogenic tissue of *Arum  
maculatum*.  
*Plant Physiol. Biochem.* 48: 265-272.



## Abstract

The “oxidative phosphorylation” (OXPHOS) system is essential for the majority of energy dependent cellular processes in most species and therefore is a keystone of life. One of the core components of this system is the NADH (ubi-)quinone oxidoreductase (complex I). Despite 50 years of research on its structure and function, the complex still has its secrets. Due to its size and hydrophobicity, structural characterization is challenging. Very recently, the research group of Leonid A. Sazanov finally succeeded in resolving the structure of the major parts of prokaryotic complex I (the hydrophilic “peripheral arm” and the hydrophobic “membrane arm”). Still, crystallization of the holo enzyme and elucidation of the atomic structure of the more intricate eukaryotic complex remain ambitious challenges for future research. Besides its structural analysis, also the functional role of complex I needs to be further characterized. Complex I not only introduces electrons into the respiratory chain but also transfers protons across the membrane, thereby contributing to the proton motif force used for ADP phosphorylation. The way of coupling of these two processes within complex I is still not precisely understood. Furthermore, many accessory subunits are present in eukaryotic complex I, which possibly introduce side functions into the enzyme complex. Research on plant complex I not only deals with these major challenges. Complex I from plants is especially large since it comprises more specific subunits than complex I of any of the other groups of organisms analyzed so far. Most remarkably, it exhibits an additional structural domain of special functional relevance.

In the course of this thesis, the unique architecture of plant complex I was investigated (section 2.1). Based on this project, a first model on the internal subunit arrangement of plant complex I was proposed. The study was facilitated by application of a novel strategy to topologically analyze large membrane-bound protein complexes (section 2.3). Due to fast progress in the field of complex I research, recent data on the plant enzyme were reviewed and functional roles of prominent plant specific complex I subunits were discussed (section 2.2). Finally, subunits of plant complex I separated by two dimensional Blue native / SDS PAGE were annotated at the “GelMap” web portal (section 2.4). In-depth data evaluation not only revealed new putative complex I subunits but also allowed to detect assembly intermediates of complex I which are of low abundance. The novel results on plant complex I support the recently suggested hypothesis that this enzyme complex, besides its role in respiration, is involved in the recycling of mitochondrial CO<sub>2</sub> for carbon fixation in chloroplasts.

Keywords: OXPHOS system, plant mitochondria, complex I

## Zusammenfassung

Das Oxidative Phosphorylierungs- (OXPHOS) System ist für die meisten energieabhängigen Prozesse von Zellen essentiell. Eine zentrale Komponente dieses Systems ist die NADH (Ubi-) quinon Oxidoreduktase (Komplex I). Obwohl dieser Komplex bereits seit fünf Jahrzehnten untersucht wird, ist seine Funktionsweise noch immer weitgehend unklar. Aufgrund seiner Größe und Hydrophobizität ist die strukturelle Analyse des Komplex I schwierig. Dennoch gelang kürzlich der Forschergruppe um Leonid A. Sazanov die Aufklärung der Struktur der Hauptkomponenten des prokaryotischen Komplexes. Als wichtige Aufgaben zukünftiger Forschung an Komplex I verbleiben die Kristallisierung des Holoenzym sowie die Ermittlung der atomaren Struktur des komplexeren eukaryotischen Enzyms. Auch die Charakterisierung der funktionellen Rolle des Komplex I, welcher nicht nur Elektronen in die Atmungskette einschleust, sondern auch Protonen über die Membran transferiert, ist notwendig. Die Kopplung beider Prozesse innerhalb des Komplexes ist noch immer nicht vollständig verstanden. Das eukaryotische Enzym besitzt im Gegensatz zum prokaryotischen viele zusätzliche Untereinheiten, die möglicherweise weitere Funktionen in diesen Komplex integrieren. Insbesondere der pflanzliche Komplex I ist auffällig groß und besitzt im Vergleich zu Komplex I aus anderen Organismengruppen eine besonders hohe Anzahl von Extra-Untereinheiten. Auffällig ist vor allem eine zusätzliche Domäne des pflanzlichen Komplex I, welche vermutlich eine besondere funktionelle Relevanz besitzt.

In der vorliegenden Arbeit wurde die einzigartige Architektur des pflanzlichen Komplex I untersucht (Kapitel 2.1). Mithilfe dieses Projektes konnte erstmalig ein Modell zur Anordnung der Untereinheiten innerhalb des Enzyms erstellt werden. Dazu wurde eine neue experimentelle Strategie zur Ermittlung der Topologie großer Proteinkomplexe entwickelt (Kapitel 2.3). Der große Erkenntnisgewinn zum pflanzlichen Komplex I, der in den vergangenen Jahren erzielt werden konnte, wurde in einem Übersichtsartikels zusammengefasst, in welchem insbesondere neue Ergebnisse zur Funktion der Extra-Untereinheiten besprochen werden (Kapitel 2.2). Schließlich wurden unsere Ergebnisse zum pflanzlichen Komplex I, die auf der Basis von 2D Gelelektrophoresen und massenspektrometrischen Proteinidentifizierungen erzielt wurden, mit Hilfe des Webportals „GelMap“ annotiert und evaluiert, wodurch neue Untereinheiten sowie niedrig-abundante Assemblierungsintermediate entdeckt werden konnten. Die neuen Ergebnisse zum pflanzlichen Komplex I unterstützen die vor kurzem aufgestellte Hypothese, dass dieser Enzymkomplex, neben seiner Rolle für die Zellatmung, an der Wiederverwertung des mitochondrialen CO<sub>2</sub> für die Kohlenstoff-Fixierung in den Chloroplasten beteiligt ist.

Schlagworte: OXPHOS System, pflanzliche Mitochondrien, Komplex I

# Contents

<b>Abbreviations</b>	1
----------------------	---

## Section 1

### **The mitochondrial NADH ubiquinone oxidoreductase of *Arabidopsis thaliana*: An overview**

1.1	The mitochondrial Oxidative Phosphorylation system	2
	General features	
	Structural organization	
	Oxidative Phosphorylation in plants	
1.2	The NADH ubiquinone oxidoreductase (complex I)	7
1.3	Complex I in plants	12
	Investigation of plant complex I	
	Plant specific subunits and function	
	Enigmatic features of plant complex I	
1.4	Objective of the thesis	19
1.5	References	21

## Section 2

### **The mitochondrial NADH ubiquinone oxidoreductase of *Arabidopsis thaliana*: Publications**

2.1	Internal architecture of mitochondrial complex I from <i>A. thaliana</i>	31
	<i>Plant Cell</i> 22: 797-810.	
2.2	Proteomic approach to characterize mitochondrial complex I from plants	45
	<i>Phytochemistry</i> 72: 1071-1080.	
2.3	Low-SDS Blue native PAGE	51
	<i>Proteomics</i> 11: 1834-1839.	
2.4	Defining the <i>protein complex proteome</i> of plant mitochondria	61
	<i>Plant Physiology</i> 157: 587-598.	

<b>Affix</b>	73
Curriculum Vitae	
Publications and conference contributions	
Danksagung	
Eidesstattliche Erklärung	

## Abbreviations

1D	one-dimensional
2D	two-dimensional
3D	three-dimensional
AOX	alternative oxidase
ADP	adenosine diphosphate
ATP	adenosine triphosphate
BN	blue native
CA	carbonic anhydrase
$\gamma$ CA	gamma-type carbonic anhydrase
$\gamma$ CAL	gamma-type carbonic anhydrase like
CAM	carbonic anhydrase of <i>Methanosarcina thermophila</i>
CCM	CO <sub>2</sub> concentrating mechanism
Complex I	NADH dehydrogenase
Complex II	succinate dehydrogenase
Complex III	cytochrome c reductase
Complex IV	cytochrome c oxidase
Complex V	ATP synthase
COX	cytochrome c oxidase
DDM	dodecyl maltoside
e <sup>-</sup>	electron
EM	electron microscopy
ETF-UQ OR	electron transfer flavoprotein ubiquinone oxidoreductase
FADH <sub>2</sub>	flavin adenine dinucleotide; reduced form
FeS cluster	iron sulfur cluster
FMN	flavin mononucleotide
GLDH	L-galactono-1,4 lactone dehydrogenase
GRAVY	grand average of hydropathicity
H <sup>+</sup>	proton
IM	inner mitochondrial membrane
IMS	intermembrane space
kDa	kilo Dalton
MPP	mitochondrial processing peptidase
MS	mass spectrometry
NAD(P) <sup>+</sup>	nicotinamide adenine dinucleotide (phosphate); oxidized form
NAD(P)H	nicotinamide adenine dinucleotide (phosphate); reduced form
OXPHOS	oxidative phosphorylation
PAGE	polyacrylamide gel electrophoresis
P <sub>i</sub>	inorganic phosphate
PMF	proton motive force
(U)Q	(ubi-) quinone (oxidized form)
(U)QH <sub>2</sub>	(ubi-) quinol (reduced form)
ROS	reactive oxygen species
SDS	sodium dodecyl sulfate
TCA cycle	tricarboxylic acid cycle
TIM	translocases of the inner mitochondrial membrane
TOM	translocases of the outer mitochondrial membrane
WT	wild type



## Section 1

# The mitochondrial NADH ubiquinone oxidoreductase of *Arabidopsis thaliana*: An overview

Section 1 provides the theoretical background of the thesis. It outlines general and plant specific features of the mitochondrial oxidative phosphorylation (OXPHOS) system. Special emphasis is placed on one of its key components – the NADH ubiquinone oxidoreductase (complex I). Furthermore, recent findings of complex I research are presented and discussed.

## 1.1 The mitochondrial Oxidative Phosphorylation system

### General features

In most eukaryotic organisms, mitochondria are the energy producing site of the cell and therefore represent an irreplaceable keystone of life. The central suborganellar compartment for energy maintenance in mitochondria is the inner mitochondrial membrane (IM) where the system of Oxidative Phosphorylation (OXPHOS) is localized.

The OXPHOS system (Figure 1) can functionally and physically be divided into the respiratory chain (complexes I - IV, ubiquinone and cytochrome c) and the ATP synthase (complex V).

The respiratory chain transfers electrons from organic compounds to molecular oxygen. Four integral membrane protein complexes catalyze this process: NADH ubiquinone oxidoreductase (complex I) and succinate dehydrogenase (complex II) feed electrons into the system. Electron donors for complexes I and II are NADH and FADH<sub>2</sub>, respectively, which are products of the tricarboxylic acid (TCA) cycle. Both protein complexes transfer electrons to a ubiquinone pool in the IM. The reduced ubiquinol is oxidized by cytochrome c reductase (complex III) which subsequently reduces cytochrome c in the intermembrane space (IMS). Finally, cytochrome c oxidase (complex IV) oxidizes cytochrome c and transfers electrons to molecular oxygen, thereby producing water.

The exergonic reactions of complexes I, III and IV are coupled to a transfer of protons from the mitochondrial matrix into the intermembrane space which creates an electrochemical gradient across the IM and thereby generates a proton motive force. The ATP synthase

(complex V) can use this force to produce the energy rich compound adenosine triphosphate (ATP) by channeling protons from the IMS back into the matrix. ATP can be exported from the mitochondria and is used to drive many energy dependent biochemical processes within the entire cell.

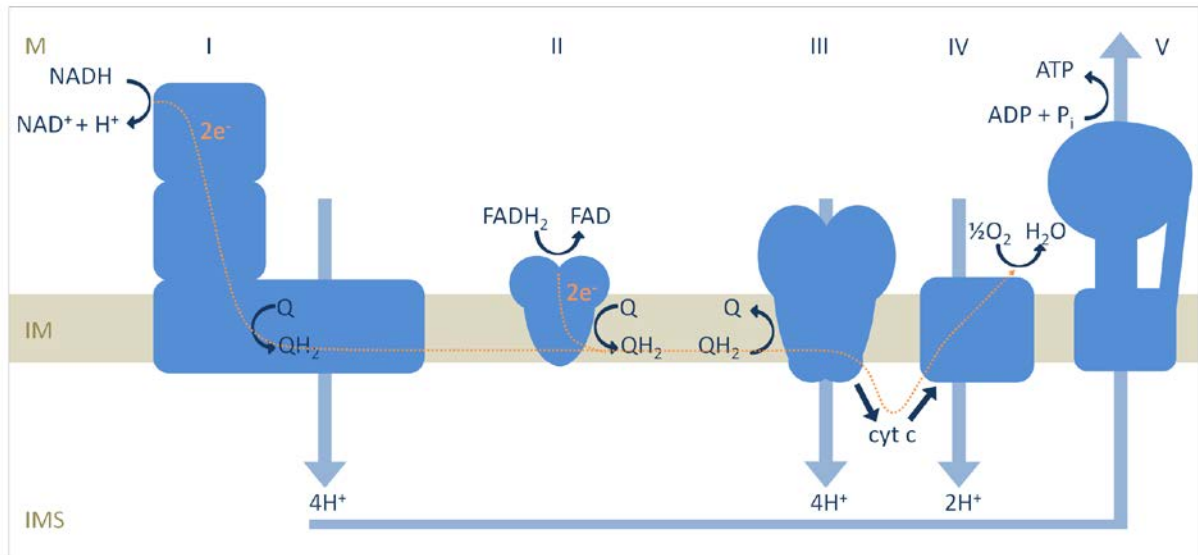


**Figure 1)** Mitochondrial oxidative phosphorylation (OXPHOS) system. Identities of complexes are indicated above. Electrons ( $e^-$ ) are taken up by complexes I and II, transferred through the respiratory chain (orange dotted line) and are finally transmitted to molecular oxygen. The exergonic electron transfer is coupled to proton ( $\text{H}^+$ ) translocation from the matrix (M) through the inner mitochondrial membrane (IM) to the intermembrane space (IMS) (blue arrows). Protons are channeled back into the matrix via complex V which uses the proton flow for phosphorylation of ADP to ATP.  $\text{P}_i$  (inorganic phosphate), Q (quinone, oxidized),  $\text{QH}_2$  (quinol, reduced), cyt c (cytochrome c).

## Structural organization

The protein complexes of the OXPHOS system are embedded in the inner mitochondrial membrane. This mitochondrial compartment remarkably differs from the outer mitochondrial membrane regarding protein content, lipid composition, and permeability. Transfer of organic compounds and ions is directed by specific channels and transporters. The inner mitochondrial membrane therefore represents the major barrier between cytosol and mitochondrial matrix.

The molecular constitution of the inner mitochondrial membrane results in the formation of the so-called “cristae” which are invaginations of the membrane and highly enlarge its overall surface. The inner membrane can be further subdivided into the “inner boundary membrane”

(adjacent and parallel to the outer membrane) and the “cristal membranes” (invaginated inner mitochondrial membranes). The space between the cristal membranes is connected to the intermembrane space only via thin tubes called “cristae junctions”. It therefore represents another subcompartment, the so called “intracristal space” ([Logan 2006](#) and references therein).

Discussions about the arrangement of respiratory chain complexes in the IM are as old as the discovery of the complexes themselves. Two models were proposed, the “solid state model” ([Fowler and Richardson 1963](#)) and the “random collision model” ([Hackenbrock et al 1986](#)). Corresponding to the solid state model, membrane proteins and protein complexes stably interact with each other. In contrast, according to the random collision model, proteins and complexes are diffusing and electron transfer between respiratory chain complexes takes place via random collisions of the reaction partners.

The discovery of “respiratory supercomplexes” is generally interpreted as support for the solid state model ([Wittig and Schagger 2009](#)). Respiratory supercomplexes are stoichiometric assemblies of two or more protein complexes.

Recently, based on structural data mainly generated by native gel electrophoresis and by single particle electron microscopy, an integrated model for the structure of the OXPHOS system was suggested. It proposes that singular protein complexes and supercomplexes co-exist in a dynamically way (reviewed in [Welchen et al 2011](#)).

Various stoichiometric assemblies of OXPHOS complexes have been found: I+III<sub>2</sub> (complex I with a dimeric form of complex III), III<sub>2</sub>+IV<sub>1-2</sub> (dimeric complex III with one or two copies of complex IV), I+III<sub>2</sub>+IV<sub>1-4</sub> (complex I with dimeric complex III and up to four copies of complex IV) and V<sub>2</sub> (dimeric complex V) ([Dudkina et al 2010](#)). Furthermore, adding another level of complexity, these supercomplexes were found to form even larger structures. The I+III<sub>2</sub>+IV<sub>1-4</sub> supercomplex represents a functional respiratory unit, which also is termed “respirasome”. Assemblies of respirasomes into rows have been termed “respiratory strings” ([Bultema et al 2009](#)).

Dimerization of ATP synthase complexes to form V<sub>2</sub> supercomplexes leads to bending of the IM. Evidence based on electron cryotomography experiments suggests that this process induces cristae formation ([Strauss et al 2008](#), [Davies et al 2011](#)).

## Oxidative phosphorylation in plants

The physiological conditions given in photosynthetically active organisms require a flexible OXPHOS system. It therefore is especially dynamic and intricate in plants.

Besides the core respiratory chain complexes, plants possess additional enzymes, like alternative NAD(P)H dehydrogenases and the alternative oxidase (AOX). These enzymes respond to different physiological states of the plant cell and protect it from harmful overreduction (for review see [Rasmusson et al 2008](#)).

Three types of alternative type II NAD(P)H dehydrogenases are present in the IM of plant mitochondria (see Figure 2): NDA, NDB, and NDC. The four presently known isoforms of NDB (NDB1, NDB2, NDB3 and NDB4) are localized on the IMS surface of the IM. NDB1 and NDB2 have been shown to be  $\text{Ca}^{2+}$  dependent whereas NDB4 is  $\text{Ca}^{2+}$  independent ([Michalecka et al 2004](#), [Geisler et al 2007](#)). NDA1, NDA2, and NDC1 are localized on the matrix-directed side of the IM. NDB1 and NDC1 function as NADPH dehydrogenases whereas NDB3, NDB4, NDA1 and NDA2 resemble NADH dehydrogenases ([Rasmusson and Møller 2011](#)).

Alternative NAD(P)H dehydrogenases introduce additional electrons to the ubiquinone pool of the IM and therefore allow a better response to high reduction states of the plant cell. Their activities have been shown to be up-regulated in response to stress, low nitrogen supply and photorespiration ([Rasmusson and Wallström 2010](#)). However, the alternative NAD(P)H dehydrogenases do not contribute to ATP synthesis as their electron transfer reaction is not coupled to a proton translocation across the IM.

*Arabidopsis* possesses five homologues of the alternative oxidase (AOX): AOX1a, AOX1b, AOX1c, AOX1d, and AOX2 ([Thirkettle-Watts 2003](#)). AOX re-oxidizes the ubiquinone pool and transfers electrons directly to molecular oxygen, thereby protecting complexes III and IV from overreduction. A role of AOX beyond protection of respiratory chain complexes has been postulated, for example in response to different types of stresses ([Rasmusson and Møller 2011](#)).

Electron flux through the respiratory chain is not only affected by the major and the alternative enzymes. Additionally, enzymes of other metabolic pathways (e.g. amino acid metabolism) functionally interact with the ubiquinone pool of the inner membrane, thereby

affecting the redox state of the system (Figure 2). The respiratory chain, especially the one of plants, therefore not only is the major site of cellular energy maintenance but also represents an important junction of diverse energy related metabolic pathways.

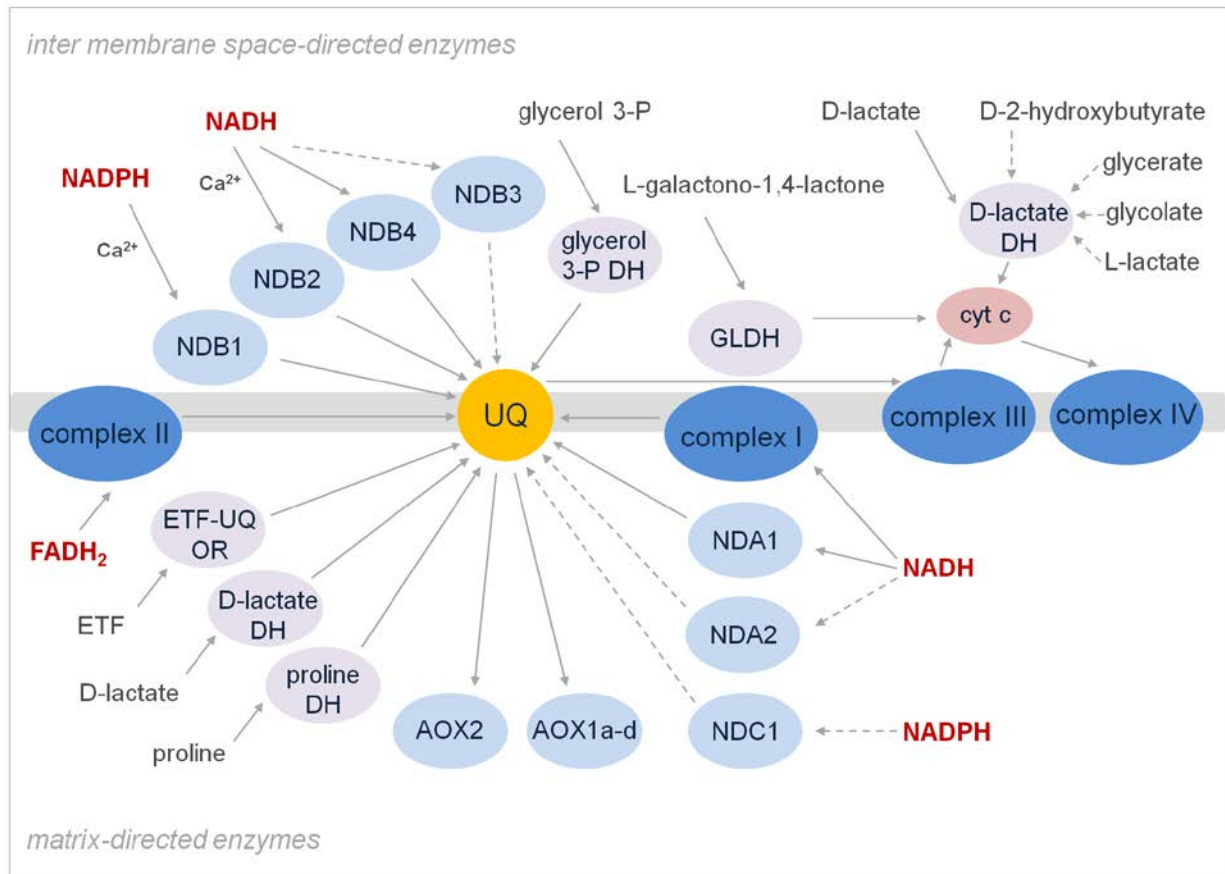


**Figure 2)** Electron flow into and through the respiratory chain, modified from [Rasmusson et al 2008](#).

Ubiquinone (UQ, yellow) constitutes the central component of the system. The gray bar in the center divides inter membrane space- and matrix-directed enzymes. Major respiratory chain complexes (dark blue): complex I (NADH ubiquinone oxidoreductase), complex II (succinate dehydrogenase), complex III (cytochrome c reductase), complex IV (cytochrome c oxidase); alternative enzymes (light blue): NDB1, NDB2, NDB3, NDB4 (NADH dehydrogenase B1, B2, B3, B4), NDA1, NDA2 (NADH dehydrogenase A1, A2), NDC1 (NADH dehydrogenase C1), and AOX1a-d (alternative oxidase 1a-d), AOX2 (alternative oxidase 2). Further enzymes (light purple): ETF-UQ OR (electron-transfer flavoprotein ubiquinone oxidoreductase), D-lactate DH (D-lactate dehydrogenase) (substrates for cytosolic enzyme taken from [Engvist et al 2009](#)), proline DH (proline dehydrogenase), GLDH (L-galactono 1,4 lactone dehydrogenase); cyt c (cytochrome c, light red); dashed arrows: experimental evidence limited.

In plants, also the classical respiratory chain complexes show special features since they possess several additional subunits.

- Plant complex I comprises more subunits than its counterparts in all other groups of organisms. Most notably, it has an additional domain attached to its membrane arm, which protrudes into the mitochondrial matrix. This domain will be discussed in detail in section 1.2.
- Complex II of plants consists of eight subunits, twice as many as in other eukaryotes ([Eubel et al 2003](#), [Millar et al 2004](#)). The function of the additional subunits still needs to be elucidated.
- Complex III of plants possesses the mitochondrial processing peptidase (MPP) which is represented by its two “core subunits”. MPP is involved in cleavage of mitochondrial targeting presequences and introduces an important additional function to this respiratory complex in plants ([Braun et al 1992](#)).

## 1.2 The NADH ubiquinone oxidoreductase (complex I)

The NADH ubiquinone oxidoreductase (complex I) is the largest enzyme of the mitochondrial OXPHOS system. Comprising about 45 different subunits in eukaryotes, it is much more intricate than all other OXPHOS complexes and about half of all proteins present in the OXPHOS system belong to complex I.

Major function of complex I is the reduction of ubiquinone by oxidation of NADH (generated in the TCA cycle). This oxidoreduction is coupled to the translocation of four protons from the mitochondrial matrix into the IMS. It is a major source of reactive oxygen species (ROS) and dysfunction of human complex I is associated with several neurodegenerative diseases as well as aging ([Efremov and Sazanov 2011a](#) and references therein).

First analyses of complex I were performed 50 years ago by Hatefi and co-workers ([Hatefi et al 1962](#)). Due to its shape, complexity and hydrophobicity, attempts to resolve the atomic crystal structure of complex I for a long time were not successful. Therefore, structural data were restricted to single-particle electron microscopy analysis as well as two-dimensional crystallography ([Böttcher et al 2002](#), [Djafarzadeh et al 2000](#), [Grigorieff 1998](#), [Leonard et al 1987](#), [Peng et al 2003](#)). Analysis by electron microscopy revealed a conserved L-like shape of the enzyme in all organisms investigated, where one arm is embedded in the IM (membrane arm), while the other one extends into the mitochondrial matrix (peripheral arm) (Figure 3).

Eukaryotic complex I has a molecular mass of approximately 1000 kDa. In bacteria, a "minimal enzyme" is present (~550 kDa, termed NADH dehydrogenase 1 (NDH-1)), which consists of only 14 subunits. These subunits are conserved throughout species and represent the core subunits required for electron transport and proton translocation. Each arm of the complex contains seven core subunits.

Based on different evolutionary origins, which correlate to functional properties, complex I can be subdivided into three major modules ([Brandt 2006](#), [Friedrich and Scheide, 2000](#), [Efremov and Sazanov 2012](#)): the N-module (NADH oxidation module), the Q-module (quinone reduction module), and the P-module (proton translocation module).

N- and Q-module are located within the peripheral arm and contain all redox prosthetic groups (one FMN, and eight to nine iron-sulfur (FeS) clusters), necessary for electron transfer from NADH to ubiquinone. Subunits of the N-module are homologous to subunits of bacterial NAD<sup>+</sup> reducing hydrogenases, subunits of the Q-module are homologous to subunits of bacterial NiFe hydrogenases ([Brandt 2006](#) and references therein).

The P-module is located in the membrane arm. Here, three subunits show homology to Na<sup>+</sup>/H<sup>+</sup> antiporters and have been postulated to be involved in proton translocation.

In 2006, Hinchliffe and Sazanov succeeded in the crystallization of the peripheral arm of complex I from the bacterium *Thermus thermophilus* at 3.3 Å resolution, uncovering the arrangement of the electron transferring elements within the complex ([Sazanov and Hinchliffe 2006](#), [Hinchliffe and Sazanov 2005](#), at 3.1 Å resolution: [Berrisford and Sazanov 2009](#)).

The N-module includes the electron entrance site (flavin mononucleotide, FMN) which oxidizes NADH and is attached to the so-called 51 kDa subunit. It represents the starting point of the electron transfer chain through the complex which is represented by an 84 Å long row of seven FeS clusters (N3, N1b, N5, N4, N6a, N6b, N2). The first cluster (N3) is located in the 51 kDa subunit. Clusters N1b, N5, and N4 are part of the 75 kDa subunit. The Q-module contains three clusters, two of which (N6a and N6b) are present in the TYKY subunit. The final cluster N2 is located in the PSST subunit (Figure 3). Here, electrons are transferred to ubiquinone by a so far unknown mechanism. N2 is located in direct vicinity to the "quinone binding pocket" between PSST and 49 kDa subunit.

An eighth cluster (N1a) does not form part of the electron transfer chain due to its distant position. It is assembled in the 24 kDa subunit and located near FMN. As the chain only can transfer one electron at a time, this eighth cluster was postulated to function as a temporary store for one of the two electrons transferred from NADH to FMN.



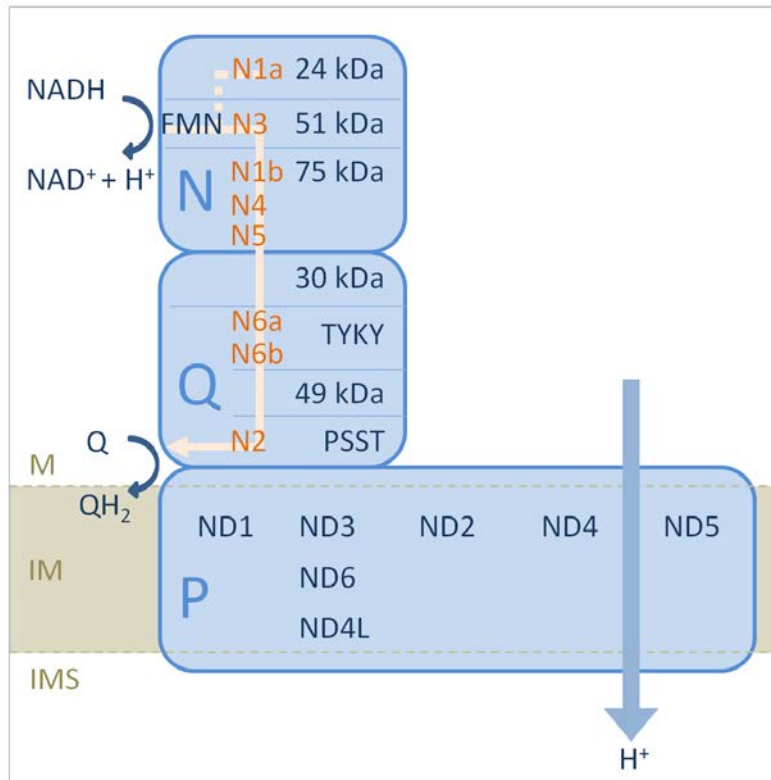


**Figure 3)** Modular design of mitochondrial complex I. N = N-module, Q = Q-module, P = P-module. Core subunits of each module are indicated (dark blue) as well as respective FeS cluster(s) (orange). The NADH oxidation site (FMN) belongs to the 51 kDa subunit. Electron flow through the peripheral arm is indicated by a beige arrow, proton translocation is indicated by a blue arrow. M (matrix), IM (inner membrane), IMS (inter-membrane space).

While electron transfer is realized by subunits and redox prosthetic groups of the peripheral arm, translocation of protons from the mitochondrial matrix into the intermembrane space is carried out by subunits of the membrane arm. Due to its size and hydrophobicity its structural analysis is challenging and only recently, Efremov and co-workers finally succeeded in obtaining the crystal structure of the membrane arm of *T. thermophilus* (Efremov et al 2010) and *E. coli* (Efremov and Sazanov 2011b).

The crystal structure allowed discovering a unique structural arrangement of the membrane arm subunits. As already mentioned above, three subunits show homology to Na<sup>+</sup>/H<sup>+</sup> antiporters (ND5, ND4, ND2). Their crystallization uncovered presence of remarkable structural elements: each of the three subunits comprises a highly similar core of 14 transmembrane helices including two discontinuous helices which introduce charge and flexibility into the center of the membrane arm. Similar motifs can be found in channels or transporters and are assumed to be involved in ion transfer.

Interestingly, a special C-terminal extension could be obtained in subunit ND5 (NuoL in *E. coli*). ND5 is located at the tip of the membrane arm at maximum distance to the connection with the peripheral arm. Its extension is a 110 Å long amphipathic helix (named “HL”) which runs parallel to the membrane surface and spans almost the entire length of the membrane arm



(180 Å). It is in contact with the discontinuous helices in each antiporter-like subunit and links the subunits of the membrane arm.

Subunits of the membrane arm are arranged from its distal tip to the connecting site with the peripheral arm in the following order: ND5, ND4, ND2, ND4L, ND6, ND3, and finally ND1 which might represent an important connecting element between both arms.

Shortly after the elucidation of the bacterial membrane arm structure (Efremov et al 2010), complex I from the obligate heterotrophic yeast *Yarrowia lipolytica* was analyzed by X ray crystallography at 6.3 Å resolution (Hunte et al 2010). It includes discontinuous helices like the bacterial enzyme and a long amphipathic helix HL could be identified as well.

Comparison of electron density maps from the prokaryotic and eukaryotic enzyme (Efremov and Sazanov 2011a) reveals a remarkable high degree of structural conservation between both species. Not only are the discontinuous helices of the antiporter like subunits perfectly conserved. Also, Efremov and Sazanov found that helix HL of the *Yarrowia* complex I exhibits the same length (110 Å) as in bacteria.

Fitting of the *T. thermophilus* structure into the electron density map of complex I from *Y. lipolytica* revealed the positions of accessory eukaryotic subunits as additional densities (Figure 4).

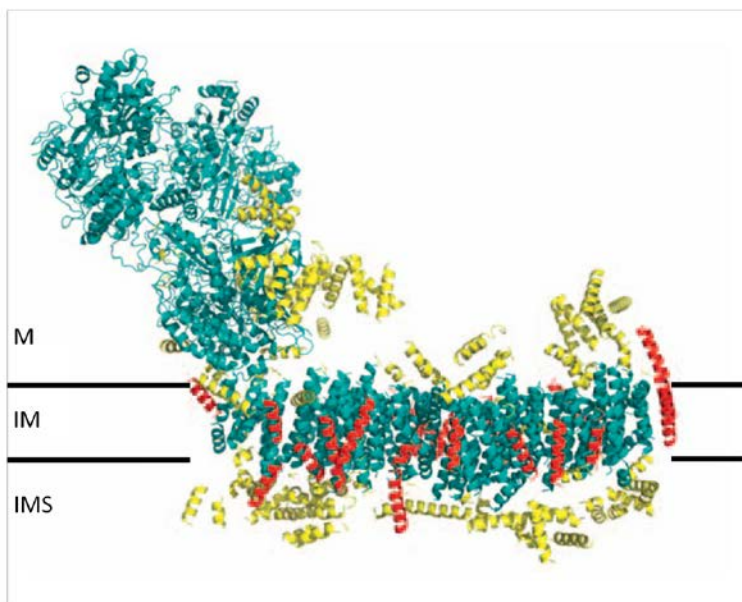


**Figure 4)** Helix arrangement in complex I from *Y. lipolytica*. It was derived from the fitting of complex I structure from *T. thermophilus* into the electron density map of *Y. lipolytica* complex I. Core subunits are highly conserved (green). Accessory subunits can be identified as extra densities (transmembrane helices in red, others in yellow). Modified from Efremov and Sazanov 2011a.

The accessory subunits present in eukaryotic complex I account for approximately 50 % of its molecular mass. However, many of their functions remain enigmatic as the 14 core subunits fulfill all major tasks of complex I. Roles in assembly and stabilization of the holo complex as

well as side functions due to homology to known enzymes have been proposed ([Klodmann et al 2011a](#), section 2.2 and references therein). New experimental data support the hypothesis that several accessory subunits are necessary for stabilization and structural organization of the holo complex ([Angerer et al 2011](#), [Zickermann et al 2010](#)).

Of the 31 additional subunits present in the well characterized bovine complex I ([Carroll et al 2002, 2003, 2006](#), [Hirst et al 2003](#)) 18 have homologues in other eukaryotic species, like *N. crassa*, *Y. lipolytica*, *C. reinhardtii*, and *A. thaliana* ([Cardol et al 2004](#), [Morgner et al 2008](#), [Gawryluk and Gray 2010](#)). Furthermore, specific subunits have been identified in every phylogenetic group analyzed so far.

Recently, an extensive bioinformatics study of accessory subunits was carried out ([Cardol 2011](#)). Based on homology searches and comparison of structural protein data, Cardol postulated presence of homologous proteins for over 40 mammalian subunits in multiple other eukaryotic lineages, thus minimizing the number of lineage specific subunits.

Electron transfer in the peripheral arm is coupled to proton translocation in the membrane arm. The coupling mechanism has been a matter of debate for years. Direct, redox-driven coupling as well as indirect coupling via conformational changes has been discussed.

Several studies based on cross-linkers and proteolysis suggest an indirect coupling mechanism ([Efremov and Sazanov 2011a](#) and references therein). Elucidation of the membrane arm structure from bacteria gave strong evidence for conformational coupling of electron transfer and proton translocation ([Efremov et al 2010, 2011b](#)).

Conformational changes during complex I activity can be observed in both arms. In the N module, binding of NADH and reduction of FMN induces conformational changes which shield the FMN site and drastically reduce the amount of ROS production.

Reduction of FeS cluster N2, which represents the final cluster of the electron transfer path in the Q module, induces a movement of a bundle of helices towards the membrane arm as well as movement of two helices parallel to the membrane arm ([Berrisford and Sazanov 2009](#)).

Conformational changes around cluster N2 could be transferred to nearby subunits of the membrane arm (ND1, ND3, ND6, ND4L) thereby coupling the reduction state of the peripheral arm to the proton transfer state of the membrane arm. Also, binding, reduction and release of quinone might be involved in the coupling process.

In the membrane arm of the reduced complex, the most obvious coupling element is the long amphipathic helix HL which is connected to the discontinuous helices of the three antiporter like subunits ND2, 4 and 5. The C terminal end of HL is located near the interface of ND6

and ND4L with ND2 and therefore could be moved by the conformational changes induced at cluster N2. A piston like movement of HL along the membrane domain would then move the discontinuous helices depending on the reduction state of the complex (model illustrated in [Efremov and Sazanov 2011b](#)). Movement of the discontinuous helices leads to simultaneously opening / closing of channels represented by the 14 transmembrane segments of the antiporter like subunits at the matrix / inter membrane space site of the complex. This action could facilitate proton transfer through the membrane arm of the complex as a result of reduction status / electron transfer activity at cluster N2.

The exact coupling mechanism still needs further investigation. Nevertheless, several models have been proposed recently ([Brandt 2011](#), [Gonzalez-Halphen et al 2011](#), [Efremov and Sazanov 2012](#)) which not only consider the different evolutionary origins of the functional modules of complex I but also point towards a key role of ubiquinone for the coupling mechanism.

### 1.3 Complex I in plants

#### Investigation of plant complex I

With almost 50 subunits, plant complex I is even more intricate than its counterparts in other eukaryotes, implying several additional functions of the plant system.

Section 2.2 includes a comprehensive review on plant complex I, its proteomic investigation as well as its plant specific features ([Klodmann and Braun 2011](#)). The following section is meant to give a short overview. It also introduces data published very recently, which are not included in the research publications (section 2).

Purification and analysis of complex I from different plant species already started two decades ago, applying procedures such as ion-exchange and immunoaffinity chromatography. Subunits were separated by SDS polyacrylamide gel electrophoresis (PAGE) and protein identification was carried out by Edman degradation. ([Leterme and Boutry 1993](#) (*Vicia faba*), [Herz et al 1994](#) (potato), [Rasmusson et al 1994](#) (red beet), [Trost et al 1995](#) (sugar beet), [Combettes and Grienberger 1999](#) (wheat)).

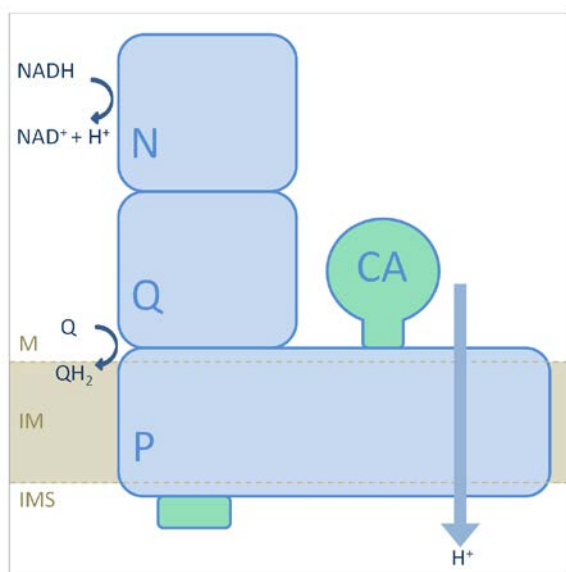
The analysis of complex I composition was accompanied by the elucidation of the plant mitochondrial genome. Thereby, not only the seven hydrophobic core subunits of the

membrane arm were identified on the mitochondrial DNA. Also, genes for two subunits of the Q module, the 30 kDa and 49 kDa subunit, were found to be mitochondrially encoded. They were therefore named ND9 and ND7, respectively, in plants (Unsel et al 1997).

More recently, analyses by different 2D gel electrophoresis techniques combined with mass spectrometry (MS) considerably increased the number of identified subunits of plant complex I (Heazlewood et al 2003 (*A. thaliana*, rice), Cardol et al 2004 (*Chlamydomonas reinhardtii*), Sunderhaus et al 2006 (*A. thaliana*)). In 2008, a 3D gel electrophoretic separation of *Arabidopsis* complex I resolved 37 distinct spots, leading to the identification of 42 different complex I subunits (Meyer et al 2008).

Beside biochemical analyses of plant complex I, also single particle electron microscopy (EM) was used to define its structure. Surprisingly, the shape of plant complex I remarkably differs from its counterparts in other species. An additional domain was found to be attached to the membrane arm on its matrix exposed side (Dudkina et al 2005). This domain could be identified in all plant species analyzed by EM so far, including potato, maize and *Polytomella* (Bultema et al 2009, Peters et al 2008, Sunderhaus et al 2006). Biochemical analysis of the complex I membrane arm of *Arabidopsis* shows that carbonic anhydrases are localized within this extra domain (Sunderhaus et al 2006). These carbonic anhydrases have been found in different plants before (Eubel et al 2003, Heazlewood et al 2003, Cardol et al 2004). Phylogenetic analyses identified them as gamma type carbonic anhydrases ( $\gamma$ CA) (Parisi et al 2004). The prototype of these enzymes is present in the archaebacterium *Methanosarcina thermophila* ( $\gamma$  carbonic anhydrase of *M. thermophila*, CAM) (Alber and Ferry 1994).

Figure 5 shows a schematic view of the shape of complex I from plants with the carbonic anhydrase domain indicated in green. Another plant specific domain can be identified at the



IMS directed side of the membrane arm of complex I. Its subunit composition could not be clarified so far.

**Figure 5)** Shape of complex I from plants. Plant specific domains are highlighted in green. N = N-module, Q = Q-module, P = P-module, CA = plant-specific carbonic anhydrase domain. M = matrix, IM = inner mitochondrial membrane, IMS = inter-membrane space.

A comprehensive topological analysis of complex I from plants was performed in 2010. It is based on a novel biochemical strategy which allows purification of complex I in its native conformation ([Klodmann et al 2010](#), see section 2.1). Treatment of the purified enzyme with low SDS concentrations induced its disaggregation into 10 different subcomplexes which subsequently were analyzed by 2D Blue native (BN) SDS PAGE and tandem mass spectrometry. Analysis of the subunit composition of each subcomplex allowed the construction of a first model for the internal architecture of plant complex I (section 2.1).

Remarkably, a subcomplex was identified which exclusively consists of carbonic anhydrases. During the destabilization process, it immediately detaches from the membrane arm. These findings are consistent with the conclusion of Sunderhaus and co-workers ([Sunderhaus et al 2006](#)).

Not only disassembly of complex I but also its assembly has recently been analyzed ([Meyer et al 2011](#)). In their study, Meyer and co-workers performed blue native PAGE of mitochondrial proteins from seven complex I knock-out mutants deficient in different subunits of the enzyme. Immunoblots of the native gels with antibodies directed against seven different complex I subunits allowed to detect complex I subcomplexes in the mutants. Data were further complemented by mass spectrometry and 2D Tricine SDS PAGE of a major subcomplex of 650 kDa identified in the 18 kDa subunit knock out mutant. This approach led to the identification of four putative assembly intermediates of the membrane arm. Carbonic anhydrases were found to be present in every identified subcomplex indicating their early integration during assembly of complex I.

### **Plant specific subunits and function**

As described above, investigation of plant mitochondrial complex I led to the discovery of gamma carbonic anhydrases attached to the membrane arm.

Five proteins of approximately 30 kDa have been identified in complex I from *Arabidopsis*, named CA1, CA2, CA3, CAL1 and CAL2 ([Eubel et al 2003](#), [Heazlewood et al 2003](#), [Parisi et al 2004](#)). Homology of the two latter proteins to the enzyme found in *M. thermophila* is lower and active site residues are less conserved compared to the CAs. Therefore, they were named “Carbonic anhydrase like” (CAL).

Function of the carbonic anhydrase domain of plant complex I has not been elucidated so far. Nevertheless, experimental data of recent years point towards a role in assembly and stabilization of the enzyme as well as involvement in one carbon metabolism of plants.

Analyses of *A. thaliana* CA2 knock-out mutants revealed a reduction in the amount of complex I of about 80% (Perales et al 2005). This indicates an important role during assembly of the enzyme and is in line with the presence of CA2 in all investigated assembly subcomplexes (Meyer et al 2011).

Involvement of the gamma carbonic anhydrases in carbon metabolism not only is supported by their homology to CAM. Also, presence of complex I was shown to be critical for plant CO<sub>2</sub> metabolism. Analysis of complex I deficient *Nicotiana sylvestris* plants revealed a decreased photosynthetic performance which could be compensated by increasing the CO<sub>2</sub> concentration (Dutilleul et al 2003). Recently, analysis of OXPHOS complex abundances in different tissues of Arabidopsis plants revealed that amount of complex I is increased in photosynthetic active organs (flowers, leaves and stems) compared to non-green tissues (roots, seeds and callus) (Peters et al 2012).

A different study showed that under decreased CO<sub>2</sub> concentrations the photosynthesis rate of protoplast is higher than that of isolated chloroplasts. Addition of carbonic anhydrase inhibitor to the protoplasts abolishes this effect (Riazunnisa et al 2006).

Furthermore, microarray gene expression studies revealed that expression of the CA2 gene is reduced in plants grown at elevated CO<sub>2</sub> (Perales et al 2005). Recently, characterization of recombinantly expressed gamma CA2 showed that it can efficiently bind CO<sub>2</sub>/HCO<sub>3</sub><sup>-</sup> (Martin et al 2009).

All these data strongly indicate an involvement of plant complex I and its carbonic anhydrases in CO<sub>2</sub>/HCO<sub>3</sub><sup>-</sup> metabolism of plants. Plant specific gamma carbonic anhydrases seem to represent a linkage of respiratory complex I and photosynthesis thereby possibly constituting a basic component of a so far uncharacterized interaction between mitochondria and chloroplasts. In 2007, Braun and Zabaleta proposed complex I / gamma CA involvement in a CO<sub>2</sub> recycling mechanism which transfers CO<sub>2</sub> generated in mitochondria (especially during photorespiration) into the chloroplast, making it available for carbon fixation by RubisCO (Braun and Zabaleta 2007). In cyanobacteria an analogous system, the carbon concentrating mechanism (CCM), also was shown to involve cyanobacterial complex I (reviewed in Badger and Price 2003). Most recently, Zabaleta et al discussed carbonic anhydrase function in plant carbon metabolism and proposed a basal carbon concentrating mechanism (bCCM) to be present plants (Zabaleta et al 2012).



Presence of active mechanisms for CO<sub>2</sub> recycling would be highly beneficial, especially in C3 plants. However, further research is needed to test this postulated interaction between mitochondria and chloroplasts.

Besides carbonic anhydrases, complex I from plants comprises several additional unique subunits. For the majority of these subunits, no function could be obtained so far. However, due to homology to proteins of known functions, several side functions for complex I subunits have been proposed (reviewed in [Remacle et al 2008](#)), like involvement in apoptosis (B16.6 subunit/GRIM19 in humans) and additional translocation activity (subunits of the TIM family, like B14.7). An acyl carrier subunit which is known to be present in mammalian and fungal complex I could not be identified as part of plant complex I so far ([Meyer et al 2007](#)). Independent from lineage specific backgrounds, accessory subunits were generally proposed to fulfill functions in assembly and stabilization ([Brandt 2006](#), [Angerer et al 2011](#)). For example, involvement of the L-galactono 1,4 lactone dehydrogenase (GLDH) in assembly of plant complex I has also been proposed. GLDH is the terminal enzyme of the ascorbate biosynthesis pathway. It was first identified as a subunit of a minor form of complex I ([Heazlewood et al 2003](#), [Millar et al 2003](#)). Experimental analysis of an *Arabidopsis* GLDH insertion mutant showed that presence of the enzyme is critical for complex I assembly ([Pineau et al 2008](#)). These findings were further supported by a biochemical analysis of GLDH in plant mitochondria ([Schertl et al 2012](#)). In gel activity assay and immunodetection of GLDH in *Arabidopsis* mitochondria revealed presence of three low-abundant subcomplexes which not only include GLDH but also contain known membrane arm subunits of complex I. They most likely represent assembly intermediates of complex I which suggests a direct involvement of GLDH in the assembly process. As its ascorbate forming activity could be demonstrated by in gel activity assays, it might functionally connect complex I with ascorbate synthesis in plants.

Actual data on complex I subunits have been integrated into an up-to-date schematic model of plant complex I (Figure 6). According to data of the Brandt group, the P-module can be divided in a proximal (P<sub>P</sub>) and distal (P<sub>D</sub>) domain (with respect to the relative positions of these domains to the connection between both arms).

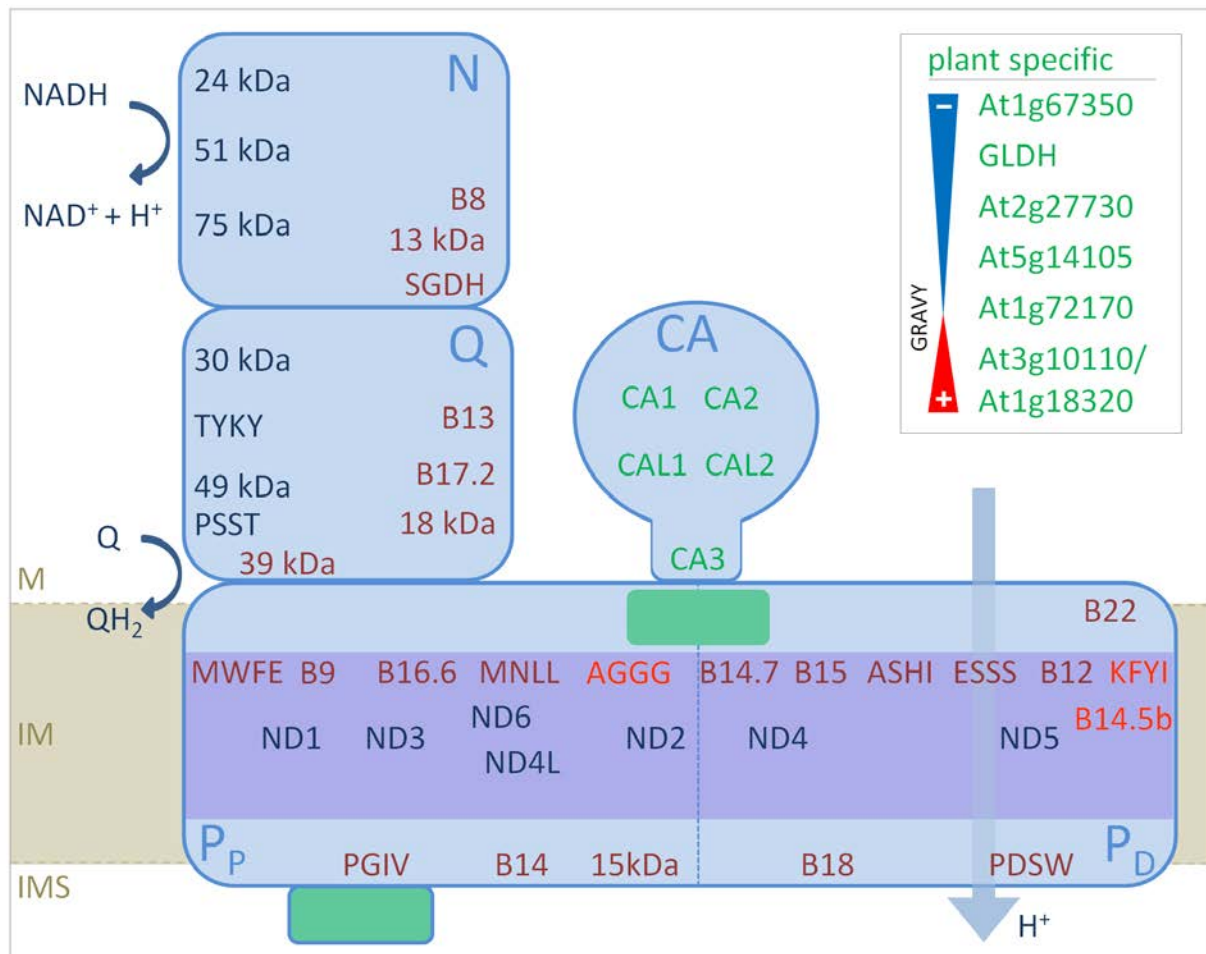


**Figure 6)** Model of the internal subunit arrangement of plant complex I. For abbreviations see Figure 3. The P-module is separated into two domains: one is located proximal to the peripheral arm (P<sub>P</sub>) the other one is distal (P<sub>D</sub>). Core subunits are indicated in dark blue, eukaryotic subunits in red (dark red: position taken from Angerer et al 2011, light red: exact positions unclear), plant specific in green. Membrane-spanning subunits have a purple background. Carbonic anhydrases are localized in the carbonic anhydrase domain. Positions of the other plant specific subunits are not exactly clear. At1g67350, At2g27730 and At5g14105 have been found in membrane arm subcomplexes (Klodmann and Braun 2011), the remaining have only been identified in the holo complex I so far. Most likely, plant specific subunits are positioned in areas of additional densities of the EM structure of plant complex I or adjacent to them (indicated in green). Furthermore, the hydrophobicity of a protein (expressed by the GRAVY score) can indicate if its position is rather membrane integral or surface directed. Therefore, the plant specific subunits have been listed in order of their relative GRAVY scores (on the right). The model integrates data from Angerer et al 2011, Brandt 2006, Cardol 2011, Efremov et al 2010, Efremov and Sazanov 2011a, Efremov and Sazanov 2011b, Klodmann and Braun 2011, Klodmann et al 2011a.



## Enigmatic features of plant complex I

In recent years, progress in complex I research remarkably increased and led to the elucidation of its membrane arm crystal structure in bacteria. Still, further efforts are needed to finally resolve the structure of the holo complex. Another major focus in the complex I field will be the elucidation of the coupling of electron transfer and proton translocation within complex I.

Considering the very special shape of complex I from plants, a more extended function of this enzyme seems likely, especially in the light of the additional carbonic anhydrase subunits and their proposed role in CO<sub>2</sub> recycling. Does the plant complex carry out an even more complicated coupling mechanism?

Further steps for plant complex I research seem clear. Carbonic anhydrases and their proposed metabolic role need to be further characterized. Functional classification of all other plant specific subunits will help to gain a more comprehensive view on the unique role of complex I in plants.

Besides physiological analyses, one key element for research is in-depth data evaluation. Recently, the new web based software “GelMap” has been developed for annotation of two-dimensional gels and interactive illustration of biochemical pathways (Senkler and Braun 2012, <http://gelmap.de>). It already has been used for annotation of several gel based proteomic studies, among them the annotation of the protein complex proteome of *Arabidopsis* mitochondria (Klodmann et al 2011a, see section 2.4).

Most recently, data on complex I subunit composition have been integrated into GelMap (Figure 7, <http://gelmap.de/complex-i>). The gel shows 2D BN SDS PAGE of the holo complex I (left) and SDS-induced subcomplexes (method described in section 2.1). In contrast to experimentally driven projects, it rather aims to give an overview on information about complex I subunits. As shown by the enlargement of the popup window (Figure 7), names of homologous subunits from other organisms are indicated. The annotation of the complex I subcomplexes in GelMap is still under preparation and integration of further functional details as well as experimental data is planned to provide a freely accessible source of information on complex I from plants.

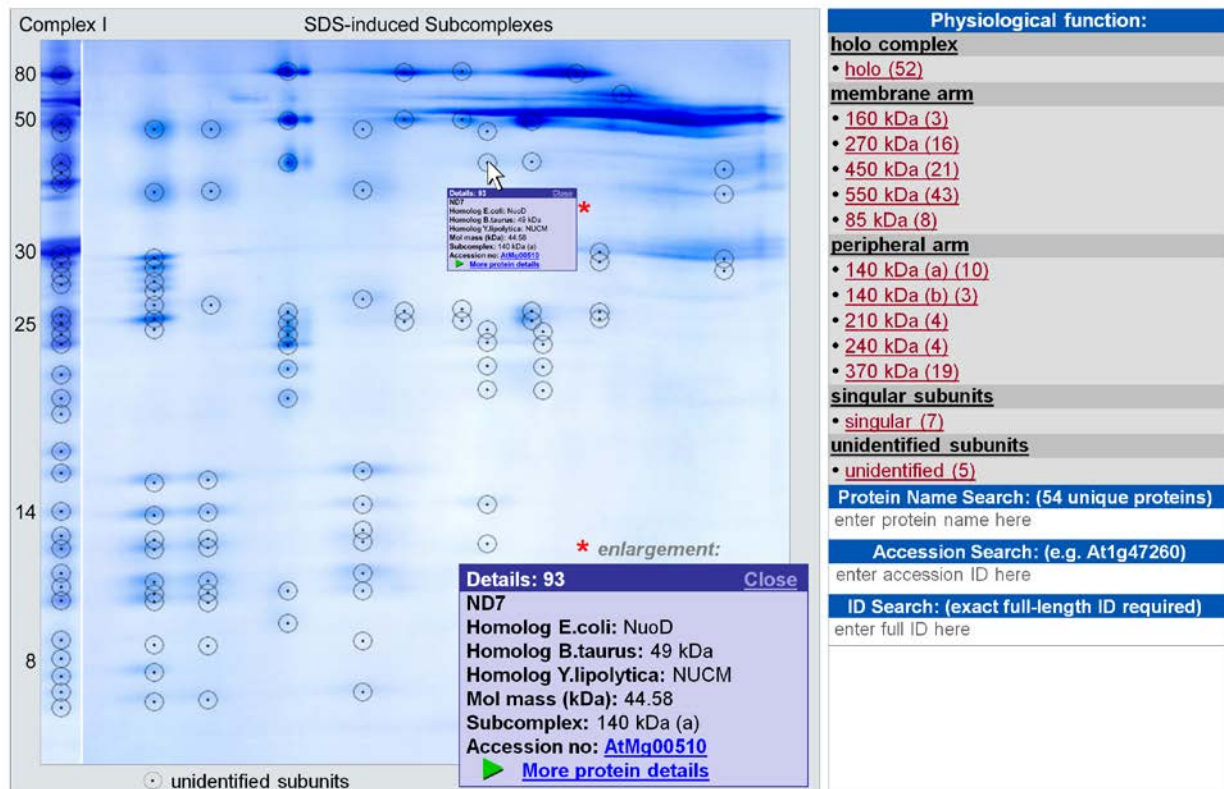


**Figure 7)** Subcomplexes of mitochondrial complex I from *Arabidopsis* as shown by GelMap. The Map shows a 2D BN SDS gel of holo complex I (left) as well as SDS induced subcomplexes. Numbers left to the map indicate molecular masses in kDa. Proteins on the gel are categorized (menu to the right) into holo complex (including all subunits) membrane and peripheral arm subcomplexes, as well as singular subunits (directly detached from the holo enzyme). Unidentified subunits are accessible via an artificial “spot” below the gel. Upon clicking a spot, a popup window will open which offers information on the respective protein (here: ND7). Information in the popup is (from top to bottom): Subunit name, name of homologous subunit in *E.coli*, *B. taurus*, and *Y. lipolytica*, molecular mass (kDa), subcomplex including the subunit, accession number according to the tair database ([www.arabidopsis.org](http://www.arabidopsis.org)) which is linked to the database entry, and a link to a table giving more information about the complex I subunit. Data can be directly viewed at the GelMap homepage: <http://gelmap.de/complex-i>.

## 1.4 Objective of the thesis

Alice Barkan recently designated complex I the “center of the universe” of the plant mitochondrial research field (Alice Barkan, final discussion of the ICPMB 2009, Lake Tahoe, California, USA).

While this statement is of course slightly disproportionate, mitochondrial complex I is indeed very interesting in several respects:

- Its subunits are encoded by two genomes, the mitochondrial and the nuclear one.
- Coupling of electron transfer and proton translocation seems to be based on an especially sophisticated mechanism, which so far is only partially understood.
- It has exceptionally many subunits and the physiological role of most of them is largely unknown.
- Complex I is speculated to have several side functions.

In plants, the enzyme is of even more interest as the presence of carbonic anhydrases within the complex strongly points to a unique role in  $\text{CO}_2/\text{HCO}_3^-$  metabolism.

The general aim of this work was to increase our knowledge of the structure and function of plant complex I to reveal novel insights into the special physiological role of this enzyme in photosynthetic active organisms.

Special focus was placed on the elucidation of the internal architecture of the complex (Klodmann et al 2010, section 2.1). For this purpose, a novel purification strategy was developed, which allows to obtain native complex I for topological studies. A new biochemical approach, based on controlled subcomplex generation and subsequent analyses of their subunit compositions, was chosen to get insights into the internal subunit arrangement of plant complex I. Applying this strategy, ten distinct complex I subcomplexes were generated and analyzed which resulted in the first topological model for the plant enzyme. The protocol can also be applied for structural analysis of other protein complexes and has been published recently (Klodmann et al 2011b, section 2.3).

Fast progress in the field of complex I research implicated to review recent data on the plant enzyme (Klodmann and Braun 2011, section 2.2). In parallel, also new proteomic data were generated and subsequently summarized.

Finally, using the recently developed GelMap software, the protein complex proteome of plant mitochondria was annotated (Klodmann et al 2011b, section 2.4). This project was initially aimed to annotate complex I subunits in a whole mitochondrial protein fraction. However, annotation of the entire fraction not only identified several new complex I subunits. Careful data evaluation using the filter options of GelMap revealed the presence of several low abundant complex I subcomplexes in the mitochondrial fraction which most likely represent assembly intermediates. Furthermore, the study also revealed presence of numerous so far undiscovered mitochondrial protein complexes.



## References

- Angerer, H., Zwicker, K., Wumaier, Z., Sokolova, L., Heide, H., Steger, M., Kaiser, S., Nübel, E., Brutschy, B., Radermacher, M., Brandt, U. and Zickermann, V. (2011) A scaffold of accessory subunits links the peripheral arm and the distal proton-pumping module of mitochondrial complex I. *Biochem J.* 437: 279-288.
- Alber, B.E., and Ferry, J.G. (1994) A carbonic anhydrase from the archaeon *Methanosarcina thermophila*. *Proc. Natl. Acad. Sci. USA* 91: 6909–6913.
- Badger, M.R. and Price, G.D. (2003) CO<sub>2</sub> concentrating mechanisms in cyanobacteria: molecular components, their diversity and evolution. *J. Exp. Bot.* 54: 609–622.
- Berrisford, J.M. and Sazanov, L.A. (2009) Structural basis for the mechanism of respiratory complex I. *J. Biol. Chem.* 284: 29773–29783.
- Brandt, U. (2006) Energy converting NADH:quinone oxidoreductase (complex I). *Annu. Rev. Biochem* 75: 69–92.
- Brandt, U. (2011) A two-state stabilization-change mechanism for proton-pumping complex I. *Biochim Biophys Acta.* 1807: 1364-1369.
- Braun, H.-P. and Zabaleta, E. (2007) Carbonic anhydrase subunits of the mitochondrial NADH dehydrogenase complex (complex I) in plants. *Physiol Plant* 129: 114–122.
- Braun, H.-P., Emmermann, M., Kruft, V. and Schmitz, U.K. (1992) The general mitochondrial processing peptidase from potato is an integral part of cytochrome c reductase of the respiratory chain. *EMBO J* 11: 3219–3227.
- Böttcher, B., Scheide, D., Hesterberg, M., Nagel-Steger, L. and Friedrich, T. (2002) A novel, enzymatically active conformation of the *Escherichia coli* NADH:ubiquinone oxidoreductase (complex I). *J. Biol. Chem.* 277: 17970–17977.
- Bultema, J., Braun, H.-P., Boekema, E. and Kouril, R. (2009) Megacomplex organization of the oxidative phosphorylation system by structural analysis of respiratory supercomplexes from potato. *Biochim Biophys Acta* 1787: 60–67.
- Cardol P. (2011) Mitochondrial NADH:ubiquinone oxidoreductase (complex I) in eukaryotes: a highly conserved subunit composition highlighted by mining of protein databases. *Biochim Biophys Acta.* 1807: 1390-1397.
- Cardol, P., Vanrobaeys, F., Devreese, B., Van Beeumen, J., Matagne, R.F. and Remacle, C. (2004) Higher plant-like subunit composition of mitochondrial complex I from

- Chlamydomonas reinhardtii*: 31 conserved components among eukaryotes. *Biochim. Biophys. Acta* 1658: 212–224.
- Carroll, J., Shannon, R.J., Fearnley, I.M., Walker, J.E. and Hirst, J. (2002) Definition of the nuclear encoded protein composition of bovine heart mitochondrial complex I. Identification of two new subunits. *J. Biol. Chem.* 277: 50311–50317.
- Carroll, J., Fearnley, I.M., Shannon, R.J., Hirst, J. and Walker, J.E. (2003) Analysis of the subunit composition of complex I from bovine heart mitochondria. *Mol. Cell. Proteomics* 2: 117–126.
- Carroll, J., Fearnley, I.M., Skehel, J.M., Shannon, R.J., Hirst, J. and Walker, J.E. (2006) Bovine complex I is a complex of 45 different subunits. *J. Biol. Chem.* 281: 32724–32727.
- Combettes, B. and Grienemberger, J.M. (1999) Analysis of wheat mitochondrial complex I purified by a one-step immunoaffinity chromatography. *Biochimie* 81, 645–653.
- Davies, K.M., Strauss, M., Daum, B., Kief, J.H., Osiewacz, H.D., Rycovska, A., Zickermann, V. and Kuhlbrandt, W. (2011) Macromolecular organization of ATP synthase and complex I in whole mitochondria. *Proceedings of the National Academy of Sciences* 108: 14121–14126.
- Djafarzadeh, R., Kerscher, S., Zwicker, K., Radermacher, M., Lindahl, M., Schagger H. and Brandt U. (2000) Biophysical and structural characterization of proton-translocating NADH-dehydrogenase (complex I) from the strictly aerobic yeast *Yarrowia lipolytica*. *Biochim. Biophys. Acta* 1459: 230–238.
- Dudkina, N.V., Eubel, H., Keegstra, W., Boekema, E.J. and Braun, H.-P. (2005) Structure of a mitochondrial supercomplex formed by respiratory-chain complexes I and III. *Proc. Natl. Acad. Sci. U.S.A* 102: 3225–3229.
- Dudkina, N.V., Kouril, R., Peters, K., Braun, H.-P. and Boekema, E.J. (2010) Structure and function of mitochondrial supercomplexes. *Biochim. Biophys. Acta* 1797: 664–670.
- Dutilleul, C., Driscoll, S., Cornic, G., Paepe, R. de, Foyer, C.H. and Noctor, G. (2003a) Functional mitochondrial complex I is required by tobacco leaves for optimal photosynthetic performance in photorespiratory conditions and during transients. *Plant Physiol* 131: 264–275.
- Efremov, R.G. and Sazanov, L.A. (2011a) Respiratory complex I: 'steam engine' of the cell? *Curr Opin. Struct. Biol.* 21: 532–540.

- Efremov, R.G. and Sazanov, L.A. (2011b) Structure of the membrane domain of respiratory complex I. *Nature* 476: 414–420.
- Efremov, R.G. and Sazanov, L.A. (2012) The coupling mechanism of respiratory complex I - A structural and evolutionary perspective. *Biochim Biophys Acta*. In press.
- Efremov, R.G., Baradaran, R. and Sazanov, L.A. (2010) The architecture of respiratory complex I. *Nature* 465: 441–445.
- Engqvist, M., Drincovich, M.F., Flüge, U.I. and Maurino, V.G. (2009) Two D-2-hydroxy-acid dehydrogenases in *Arabidopsis thaliana* with catalytic capacities to participate in the last reactions of the methylglyoxal and beta-oxidation pathways. *J. Biol. Chem.* 284: 25026–25037.
- Eubel, H., Jansch, L. and Braun, H.-P. (2003) New insights into the respiratory chain of plant mitochondria. Supercomplexes and a unique composition of complex II. *Plant Physiol* 133: 274–286.
- Fowler, L.R. and Richardson, S.H. (1963) Studies on the electron transfer system. L. On the mechanism of reconstitution of the mitochondrial electron transfer system. *J Biol Chem* 238: 456–463.
- Friedrich, T. and Scheide, D. (2000) The respiratory complex I of bacteria, archaea and eukarya and its module common with membrane-bound multisubunit hydrogenases. *FEBS Lett.* 479: 1–5.
- Gawryluk, R.M. and Gray, M.W. (2010) Evidence for an early evolutionary emergence of gamma-type carbonic anhydrases as components of mitochondrial respiratory complex I. *BMC Evol. Biol.* 10: 176.
- Geisler, D.A., Broselid, C., Hederstedt, L. and Rasmusson, A.G. (2007) Ca<sup>2+</sup>-binding and Ca<sup>2+</sup>-independent respiratory NADH and NADPH dehydrogenases of *Arabidopsis thaliana*. *J. Biol. Chem.* 282: 28455–28464.
- Grigorieff, N. (1998) Three-dimensional structure of bovine NADH:ubiquinone oxidoreductase (complex I) at 2.2 Å in ice. *J. Mol. Biol.* 277: 1033–1046.
- Gonzalez-Halphen, D., Ghelli, A., Iommarini, L., Carelli, V. and Esposti, M.D. (2011) Mitochondrial complex I and cell death: a semi-automatic shotgun model. *Cell Death Dis.* 2: e222 (PMID 22030538).

- Hackenbrock, C.R., Chazotte, B. and Gupte, S.S. (1986) The random collision model and a critical assessment of diffusion and collision in mitochondrial electron transport. *J Bioenerg Biomembr* 18: 331–368.
- Hatefi, Y., Haavik, A.G., and Griffiths, D.E. (1962) Studies on the electron transfer system. XL. Preparation and properties of mitochondrial DPNH-coenzyme Q reductase. *J Biol Chem* 237: 1676–1680.
- Heazlewood, J., Howell, K. and Millar, A. (2003) Mitochondrial complex I from *Arabidopsis* and rice: orthologs of mammalian and fungal components coupled with plant-specific subunits. *Biochim Biophys Acta* 1604: 159–169.
- Herz, U., Schröder, W., Liddell, A., Leaver, C.J., Brennicke, A. and Grohmann, L. (1994) Purification of the NADH:ubiquinone oxidoreductase (complex I) of the respiratory chain from the inner mitochondrial membrane of *Solanum tuberosum*. *J. Biol. Chem.* 269, 2263–2269.
- Hinchliffe, P. and Sazanov, L.A. (2005) Organization of iron–sulfur clusters in respiratory complex I. *Science* 309: 771–774.
- Hirst, J., Carroll, J., Fearnley, I.M., Shannon, R.J. and Walker, J.E. (2003) The nuclear encoded subunits of complex I from bovine heart mitochondria. *Biochim. Biophys. Acta* 1604: 135–150.
- Hunte, C., Zickermann, V. and Brandt, U. (2010) Functional modules and structural basis of conformational coupling in mitochondrial complex I. *Science* 329: 448–451.
- Klodmann, J. and Braun, H.P. (2011) Proteomic approach to characterize mitochondrial complex I from plants. *Phytochemistry* 72: 1071–1080.
- Klodmann, J., Lewejohann, D. and Braun, H.P. (2011) Low-SDS Blue native PAGE. *Proteomics*. 11: 1834-1839.
- Klodmann, J., Senkler, M., Rode, C. and Braun, H.P. (2011a) Defining the protein complex proteome of plant mitochondria. *Plant Physiol.* 157: 587-598.
- Klodmann, J., Sunderhaus, S., Nimtz, M., Jansch, L. and Braun, H.P. (2010) Internal architecture of mitochondrial complex I from *Arabidopsis thaliana*. *Plant Cell* 22: 797–810.
- Leonard, K., Haikerm, H. and Weiss, H. (1987) Three-dimensional structure of NADH: ubiquinone reductase (complex I) from *Neurospora* mitochondria determined by electron microscopy of membrane crystals. *J. Mol. Biol.* 194: 277–286.



- Leterme, S. and Boutry, M. (1993) Purification and preliminary characterization of mitochondrial complex I (NADH: ubiquinone reductase) from broad bean (*Vicia faba* L.). *Plant Physiol.* 102, 435–443.
- Logan, D.C. (2006) The mitochondrial compartment. *Journal of Experimental Botany* 57: 1225–1243.
- Martin, V., Villarreal, F., Miras, I., Navaza, A., Haouz, A., González-Lebrero, R.M., Kaufman, S.B. and Zabaleta, E. (2009) Recombinant plant gamma carbonic anhydrase homotrimers bind inorganic carbon. *FEBS Lett.* 583, 3425–3430.
- Meyer, E.H., Heazlewood, J.L. and Millar, A.H. (2007) Mitochondrial acyl carrier proteins in *Arabidopsis thaliana* are predominantly soluble matrix proteins and none can be confirmed as subunits of respiratory Complex I. *Plant Mol. Biol.* 64: 319–327.
- Meyer, E.H., Solheim, C., Tanz, S.K., Bonnard, G. and Millar, A.H. (2011) Insights into the composition and assembly of the membrane arm of plant complex I through analysis of subcomplexes in *Arabidopsis* mutant lines. *J. Biol. Chem.* 286: 26081–26092.
- Meyer, E.H., Taylor, N.L. and Millar, A.H. (2008) Resolving and identifying protein components of plant mitochondrial respiratory complexes using three dimensions of gel electrophoresis. *J. Proteome Res.* 2: 786–794.
- Michalecka, A.M., Agius, S.C., Møller, I.M. and Rasmusson, A.G. (2004) Identification of a mitochondrial external NADPH dehydrogenase by overexpression in transgenic *Nicotiana sylvestris*. *Plant J.* 37: 415–425.
- Millar, A., Mittova, V., Kiddle, G., Heazlewood, J., Bartoli, C., Theodoulou, F. and Foyer, C. (2003) Control of ascorbate synthesis by respiration and its implications for stress responses. *Plant Physiol* 133: 443–447.
- Millar, A.H., Eubel, H., Jansch, L., Kruff, V., Heazlewood, J.L. and Braun, H.P. (2004) Mitochondrial cytochrome c oxidase and succinate dehydrogenase complexes contain plant specific subunits. *Plant Mol. Biol* 56: 77–90.
- Parisi, G., Perales, M., Fornasari, M.S., Colaneri, A., González-Schain, N., Gómez-Casati, D., Zimmermann, S., Brennicke, A., Araya, A., Ferry, J.G., Echave, J. and Zabaleta, E. (2004) Gamma carbonic anhydrases in plant mitochondria, *Plant Mol. Biol.* 55: 193–207.
- Peng, G., Fritsch, G., Zickermann, V., Schagger, H., Mentele, R., Lottspeich, F., Bostina, M., Radermacher, M., Huber, R., Stetter, K.O. and Michel, H. (2003) Isolation,

characterization and electron microscopic single particle analysis of the NADH:ubiquinone oxidoreductase (complex I) from the hyperthermophilic eubacterium *Aquifex aeolicus*. *Biochemistry* 42: 3032–3039.

Perales, M., Eubel, H., Heinemeyer, J., Colaneri, A., Zabaleta, E. and Braun, H.P. (2005) Disruption of a Nuclear Gene Encoding a Mitochondrial Gamma Carbonic Anhydrase Reduces Complex I and Supercomplex I+III<sub>2</sub> Levels and Alters Mitochondrial Physiology in *Arabidopsis*. *Journal of Molecular Biology* 350: 263–277.

Peters, K., Dudkina, N.V., Jansch, L., Braun, H.P. and Boekema, E.J. (2008) A structural investigation of complex I and I+III<sub>2</sub> supercomplex from *Zea mays* at 11-13 Å resolution: assignment of the carbonic anhydrase domain and evidence for structural heterogeneity within complex I. *Biochim. Biophys. Acta* 1777: 84–93.

Peters, K., Nießen, M., Peterhänsel, C., Späth, B., Hölzle, A., Binder, S., Marchfelder, A. and Braun, H.P. (2012) Complex I-complex II ratio strongly differs in various organs of *Arabidopsis thaliana*. *Plant Mol Biol*. 79: 273-284.

Pineau, B., Layoune, O., Danon, A. and De Paepe, R. (2008) L-galactono-1,4-lactone dehydrogenase is required for the accumulation of plant respiratory complex I. *J Biol Chem* 283: 32500–32505.

Rasmusson, A.G. and Møller, I.M. (2011) Mitochondrial electron transport and plant stress. In *Plant Mitochondria*. Edited by Kempken, F. pp. 357–381. Springer Science+Business Media LLC, New York, NY.

Rasmusson, A.G. and Wallström, S.V. (2010) Involvement of mitochondria in the control of plant cell NAD(P)H reduction levels. *Biochem. Soc. Trans* 38: 661–666.

Rasmusson, A.G., Geisler, D.A. and Møller, I.M. (2008) The multiplicity of dehydrogenases in the electron transport chain of plant mitochondria. *Mitochondrion* 8: 47–60.

Rasmusson, A.G., Mendel-Hartvig, J., Møller, I.M. and Wiskich, J.T. (1994) Isolation of the rotenone-sensitive NADH-ubiquinone reductase (Complex I) from red beet mitochondria. *Physiol. Plantarum* 90, 607–615.

Remacle, C., Barbieri, M.R., Cardol, P. and Hamel, P.P. (2008) Eukaryotic complex I: functional diversity and experimental systems to unravel the assembly process. *Mol. Genet. Genomics* 280: 93–110.

- Riazunnisa, K., Padmavathi, L., Bauwe, H. and Raghavendra, A.S. (2006) Markedly low requirement of added CO<sub>2</sub> for photosynthesis by mesophyll protoplasts of pea (*Pisum sativum*): Possible roles of photorespiratory CO<sub>2</sub> and carbonic anhydrase. *Physiologia Plantarum* 128: 763-772.
- Sazanov, L.A. and Hinchliffe, P. (2006) Structure of the hydrophilic domain of respiratory complex I from *Thermus thermophilus*. *Science* 311: 1430-1436.
- Schertl, P., Sunderhaus, S., Klodmann, J., Grozeff, G.E., Bartoli, C.G. and Braun, H.P. (2012) L-galactono-1,4-lactone dehydrogenase (GLDH) forms part of three subcomplexes of mitochondrial complex I in *Arabidopsis thaliana*. *J. Biol. Chem.* 287: 14412-14419.
- Senkler, M. and Braun, H.P. (2012) Functional Annotation of 2D Protein Maps: The GelMap Portal. *Front. Plant Sci.* 3: 87.
- Strauss, M., Hofhaus, G., Schröder, R.R. and Kühlbrandt, W. (2008) Dimer ribbons of ATP synthase shape the inner mitochondrial membrane. *EMBO J* 27: 1154-1160.
- Sunderhaus, S., Dudkina, N., Jansch, L., Klodmann, J., Heinemeyer, J., Perales, M., Zabaleta, E., Boekema, E. and Braun, H.P. (2006) Carbonic anhydrase subunits form a matrix-exposed domain attached to the membrane arm of mitochondrial complex I in plants. *J Biol Chem* 281: 6482-6488.
- Thirkettle-Watts, D. (2003) Analysis of the Alternative Oxidase Promoters from Soybean. *Plant Physiol* 133: 1158-1169.
- Trost, P., Bonora, P., Scagliarini, S. and Pupillo, P. (1995) Purification and properties of NAD(P)H: (quinone-acceptor) oxidoreductase of sugarbeet cells. *Eur J Biochem.* 234: 452-458.
- Unsold, M., Marienfeld, J.R., Brandt, P. and Brennicke, A. (1997) The mitochondrial genome of *Arabidopsis thaliana* contains 57 genes in 366, 924 nucleotides. *Nat. Genet.* 15, 57-61.
- Welchen, E., Klodmann, J. and Braun, H.P. (2011) Biogenesis and supermolecular organization of the oxidative phosphorylation system in plants. In *Plant Mitochondria*. Edited by Kempken, F. pp. 327-355. Springer Science+Business Media LLC, New York, NY.
- Wittig, I. and Schägger, H. (2009) Supramolecular organization of ATP synthase and respiratory chain in mitochondrial membranes. *Biochim. Biophys. Acta* 1787: 672-680.
- Zabaleta, E., Martin, M.V. and Braun, H.P. (2012) A basal carbon concentrating mechanism in plants? *Plant Sci.* 187: 97-104.

Zickermann, V., Angerer, H., Ding, M.G., Nübel, E. and Brandt, U. (2010) Small single transmembrane domain (STMD) proteins organize the hydrophobic subunits of large membrane protein complexes. FEBS Lett. 584: 2516-2525.

## Section 2

## The mitochondrial NADH ubiquinone oxidoreductase of *Arabidopsis thaliana*: Publications

This thesis contains four manuscripts. Major contents and my contributions to the manuscripts are given below.

### 1) **Internal architecture of mitochondrial complex I from *A. thaliana* (2010)**

**Plant Cell 22: 797-810.**

*Arabidopsis* complex I was purified by a new, very mild strategy which preserved its native state. Subsequently, the purified enzyme was destabilized using low concentrations of SDS, thereby inducing its disaggregation into up to ten distinct subcomplexes. Subunit composition of the subcomplexes was analyzed by 2D BN / SDS PAGE and tandem mass spectrometry. Results were evaluated with respect to published structural data and allowed us to propose a first topological model on the subunit arrangement within plant complex I.

The novel purification strategy was proposed by Hans-Peter Braun and Stephanie Sunderhaus. All biochemical experiments of the study were carried out by me. Protein identifications by mass spectrometry were carried out at the Helmholtz Zentrum für Infektionsforschung (HZI) in Braunschweig with the help of Manfred Nimtz and Lothar Jänsch. Database searches were carried out by me. Data evaluation was performed by Hans-Peter Braun and me. Figures of the manuscript were prepared by me. The manuscript was written by Hans Peter Braun and me.

### 2) **Proteomic approach to characterize mitochondrial complex I from plants (2011)**

**Phytochemistry 72: 1071-1080.**

This review gives an overview on complex I in plants and discusses putative roles of the plant specific subunits of the complex. Furthermore, a systematic approach to identify subunits of complex I from *Arabidopsis* is reported which is based on protein separation by Blue native / SDS PAGE in combination with protein identification by ESI-MS/MS. An up-to-date structural model on complex I from plants is presented. Finally, a new functional mechanism involving the plant specific carbonic anhydrase domain is suggested.

All experiments were carried out by me. Major parts of the manuscript were written by me. Figures were developed by me and optimized after discussions with Hans-Peter Braun.

### **3) Low-SDS Blue native PAGE (2011)**

**Proteomics 11: 1834-1839.**

This manuscript describes a new method for the topological characterization of large protein complexes, which is based on their gentle dissection into functional modules by low concentrations of SDS and on a subsequent investigation of the modules by BN / SDS PAGE and tandem mass spectrometry. Different variants of the method are presented and discussed.

Gels were prepared by Dagmar Lewejohann and me. Figures were prepared by me. The manuscript was written by Hans-Peter Braun and me.

### **4) Defining the protein complex proteome of plant mitochondria. (2011)**

**Plant Physiology 157: 587-598.**

In this work, a whole mitochondrial protein fraction of Arabidopsis mitochondria was separated by Blue native / SDS PAGE. Protein spots were analyzed by tandem mass spectrometry. Results were used for data annotation using the novel software “GelMap”. Usage of the filter options of the software allowed identifying numerous mitochondrial protein complexes, many of which were described for the first time. In the course of the study, new putative complex I subunits were identified and low abundant complex I subcomplexes were detected which most likely represent assembly intermediates of the complex.

Spot picking and digestion, mass spectrometry, database searches and evaluation of the identified proteins were carried out by me. Construction of the protein and peptide table as well as their uploading into GelMap was done by me with the help of Michael Senkler. Further development of GelMap for annotation and evaluation of Blue native / SDS gels was carried out by Hans-Peter Braun and Michael Senkler. A first general functional classification of all identified proteins was carried out by me with the help of Hans-Peter Braun. Assignment and definition of mitochondrial protein complexes was performed by Hans-Peter Braun. Figures were prepared by me with the help of Hans-Peter Braun. The manuscript was written by Hans-Peter Braun.

# Internal Architecture of Mitochondrial Complex I from *Arabidopsis thaliana*

Jennifer Klodmann,<sup>a</sup> Stephanie Sunderhaus,<sup>a</sup> Manfred Nimtz,<sup>b</sup> Lothar Jänsch,<sup>b</sup> and Hans-Peter Braun<sup>a,1</sup>

<sup>a</sup>Institute for Plant Genetics, Faculty of Natural Sciences, Leibniz Universität Hannover, D-30419 Hannover, Germany

<sup>b</sup>Proteome Research Group, Division of Cell and Immune Biology, Helmholtz Centre for Infection Research, D-38124 Braunschweig, Germany

The NADH dehydrogenase complex (complex I) of the respiratory chain has unique features in plants. It is the main entrance site for electrons into the respiratory electron transfer chain, has a role in maintaining the redox balance of the entire plant cell and additionally comprises enzymatic side activities essential for other metabolic pathways. Here, we present a proteomic investigation to elucidate its internal structure. *Arabidopsis thaliana* complex I was purified by a gentle biochemical procedure that includes a cytochrome c-mediated depletion of other respiratory protein complexes. To examine its internal subunit arrangement, isolated complex I was dissected into subcomplexes. Controlled disassembly of the holo complex (1000 kD) by low-concentration SDS treatment produced 10 subcomplexes of 550, 450, 370, 270, 240, 210, 160, 140, 140, and 85 kD. Systematic analyses of subunit composition by mass spectrometry gave insights into subunit arrangement within complex I. Overall, *Arabidopsis* complex I includes at least 49 subunits, 17 of which are unique to plants. Subunits form subcomplexes analogous to the known functional modules of complex I from heterotrophic eukaryotes (the so-called N-, Q-, and P-modules), but also additional modules, most notably an 85-kD domain including  $\gamma$ -type carbonic anhydrases. Based on topological information for many of its subunits, we present a model of the internal architecture of plant complex I.

## INTRODUCTION

Oxidative phosphorylation (OXPHOS) is the ATP formation driven by oxidative reactions of the respiratory chain. The process is based on the presence of a so-called OXPHOS system localized in specialized biomembranes (e.g., the plasma membrane in oxygenic prokaryotes and the inner mitochondrial membrane in eukaryotes). Complex I is the largest protein complex of the OXPHOS system (for reviews, see Friedrich and Böttcher, 2004; Brandt, 2006; Vogel et al., 2007; Remacle et al., 2008; Zickermann et al., 2008, 2009; Lazarou et al., 2009). It catalyzes NADH-quinone oxidoreduction and in many systems represents the main entrance site for electrons into the respiratory electron transfer chain. Coupled to this oxidoreduction, complex I translocates protons across the inner mitochondrial membrane or the plasma membrane of bacteria. The precise mechanism of complex I function is still not completely understood (reviewed in Zickermann et al., 2009).

Analyses by electron microscopy (EM) revealed that complex I is composed of two arms arranged in orthogonal configuration to form an L-shaped particle (Guénebaut et al., 1997, 1998; Grigorieff, 1998; Böttcher et al., 2002; Peng et al., 2003; Dudkina

et al., 2005; Radermacher et al., 2006; Morgan and Sazanov, 2008; Clason et al., 2010). One arm is hydrophobic and embedded within the membrane (membrane arm); the other is hydrophilic and protrudes into the mitochondrial matrix or the lumen of a bacterial cell (peripheral arm). In *Escherichia coli*, complex I is composed of 14 subunits but in mitochondria complex I contains up to 31 additional subunits. The structure of the peripheral arm of the archaeobacterium *Thermus thermophilus* complex I was recently solved by x-ray crystallography. It includes eight subunits that bind one flavine mononucleotide and nine iron-sulfur clusters as redox prosthetic groups involved in electron transfer from NADH to quinone (Hinchliffe and Sazanov, 2005; Sazanov and Hinchliffe, 2006; Sazanov, 2007; Berrisford and Sazanov, 2009). By contrast, the inner architecture of the membrane arm, which is responsible for proton translocation, is less well understood. Locations of some subunits have been deduced by single particle electron microscopy using complex I subcomplexes or by immune-electron microscopy (Abdrakhmanova et al., 2004; Baranova et al., 2007a, 2007b; Clason et al., 2007). Overall, the subunits of the prokaryotic membrane arm are predicted to include >50 membrane-spanning helices. Even more membrane-spanning helices are predicted to be present within the membrane arm of eukaryotic complex I. Seven of the most hydrophobic subunits of the membrane arm in eukaryotes are encoded by the mitochondrial genome in most organisms investigated.

Nomenclature of complex I subunits unfortunately differs among the organisms investigated, although a large number of subunits likewise are present in different species. In this work,

<sup>1</sup> Address correspondence to braun@genetik.uni-hannover.de. The author responsible for distribution of materials integral to the findings presented in this article in accordance with the policy described in the Instructions for Authors (www.plantcell.org) is: Hans-Peter Braun (braun@genetik.uni-hannover.de).  
www.plantcell.org/cgi/doi/10.1105/tpc.109.073726

the bovine nomenclature is used for all homologous complex I subunits of *Arabidopsis* because bovine complex I is particularly well-investigated (Carroll et al., 2003, 2006; Hirst et al., 2003). Subunits specific to complex I of plant mitochondria are named according to the corresponding genes annotated by The Arabidopsis Information Resource (TAIR; www.Arabidopsis.org).

The OXPHOS system of plant mitochondria is more complicated compared with its counterparts in heterotrophic eukaryotes. First of all, quite a large number of alternative oxidoreductases are present in the inner mitochondrial membrane; these participate in respiratory electron transport without contributing to the proton gradient across the inner mitochondrial membrane (reviewed in Rasmussen et al., 2008). Furthermore, the classical protein complexes of the OXPHOS system have several special features. Complex I of *Arabidopsis*, rice (*Oryza sativa*), and *Chlamydomonas reinhardtii* was reported to include plant-specific subunits (Heazlewood et al., 2003; Millar et al., 2003; Cardol et al., 2004; Sunderhaus et al., 2006; Meyer et al., 2008). So far, 13 complex I subunits of *Arabidopsis* that have no counterparts in complex I of mammals or fungi have been described. Some of these subunits introduce side activities into complex I, for example, subunits resembling  $\gamma$ -type carbonic anhydrases (CAs) and an L-galactone-1,4-lactone dehydrogenase (GLDH), which is associated with complex I in plants.

In plants, mitochondrial complex I has additional functions that are of great importance for the entire cell, e.g., in maintaining the redox balance during photosynthesis (Dutilleul et al., 2003). Also, plant complex I has a unique shape as revealed by single-particle EM (Dudkina et al., 2005; Sunderhaus et al., 2006; Peters et al., 2008; Bultema et al., 2009). In contrast with all other investigated organisms, it comprises an additional peripheral domain that is attached to the membrane arm at a central position on its matrix-exposed side (Figure 1). The extra domain has a spherical shape, is estimated to have a molecular mass of 80 kD, and was shown to include CA subunits specific for plant complex I (Sunderhaus et al., 2006). By analogy with the prototype CA from the archaeobacterium *Methanosarcina thermophila* (CAM) (Alber and Ferry, 1994), the spherical extra domain probably represents a CA trimer. Three distinct CAs have been found to be present within

*Arabidopsis* complex I and are termed CA1, CA2, and CA3. Furthermore, two CA-like proteins named CAL1 and CAL2 have been described that have altered active sites compared with the one of CAM (reviewed in Braun and Zabaleta, 2007). The physiological role of the CA domain of plant complex I is currently a matter of debate.

To better understand structure and function of plant complex I, we analyzed its internal architecture. The study is based on a biochemical strategy that includes gentle complex I purification, controlled disassembly of the purified complex, separation of the generated subcomplexes by blue native (BN)-PAGE, separation of the subunits of the subcomplexes by SDS-PAGE, and, finally, subunit identification by tandem mass spectrometry. Integration of the obtained results is used to deduce the internal architecture of plant complex I.

## RESULTS

### Purification of Complex I from *Arabidopsis*

Biochemical analysis of the subunit arrangement within complex I first requires its gentle purification in the native conformation. A new three-step purification strategy was developed for complex I isolation, based on (1) purification of mitochondrial membranes, (2) separation of mitochondrial membrane protein complexes by sucrose gradient ultracentrifugation, and, finally, (3) cytochrome c affinity chromatography to remove complex III and complex III-containing supercomplexes from complex I-enriched fractions (Figure 2). The outcome of each purification step can be monitored by one-dimensional (1D) BN-PAGE.

The starting point for the complex I purification was mitochondria isolated from *Arabidopsis* cell suspension cultures. The organelle fraction included all five OXPHOS complexes, the I+III<sub>2</sub> supercomplex and the F1 part of complex V (Figure 2A). Since complex I is the largest enzyme of the OXPHOS system, a size-based separation by sucrose gradient ultracentrifugation was employed to separate the solubilized complexes of the mitochondrial membranes. Under the conditions applied, complex I-enriched fractions were located close the bottom of the centrifugation tube (Figure 2B, fractions 2 and 3). The only visible contaminations within these fractions were dimeric complex III and the I+III<sub>2</sub> supercomplex.

Finally, cytochrome c affinity chromatography was applied to specifically remove complex III<sub>2</sub> and the I+III<sub>2</sub> supercomplex from complex I-enriched fractions. Originally, this procedure was developed to purify complex III<sub>2</sub> by the binding to its natural substrate cytochrome c (Weiss and Juchs, 1978; Braun and Schmitz, 1992). Binding of complex III<sub>2</sub> is most efficient if cytochrome c is in the oxidized state. Upon reduction of cytochrome c by ascorbate, affinity decreases and allows elution of complex III by a salt gradient of low ionic strength (Weiss and Juchs, 1978). No salt gradient is necessary to detach complex I from the cytochrome c sepharose because it simply passes through the column without interactions and therefore can be obtained in the flow-through fraction. Low salt conditions during purification ensure optimal integrity and native conformation of complex I (Figure 2C).

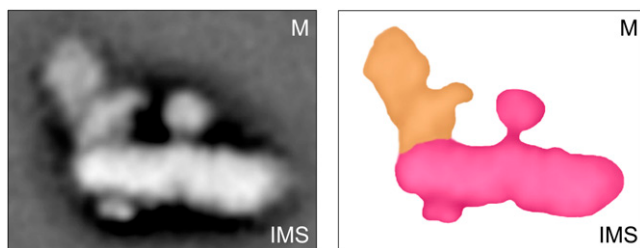


**Figure 1.** EM Average Structure and Scheme of Mitochondrial Complex I from *Arabidopsis*.

The EM average structure (left) was taken from Dudkina et al. (2005). The deduced scheme (right) shows the membrane arm of complex I in red and the peripheral arm in orange. The membrane arm is inserted into the inner mitochondrial membrane. M, matrix side; IMS, intermembrane space side.



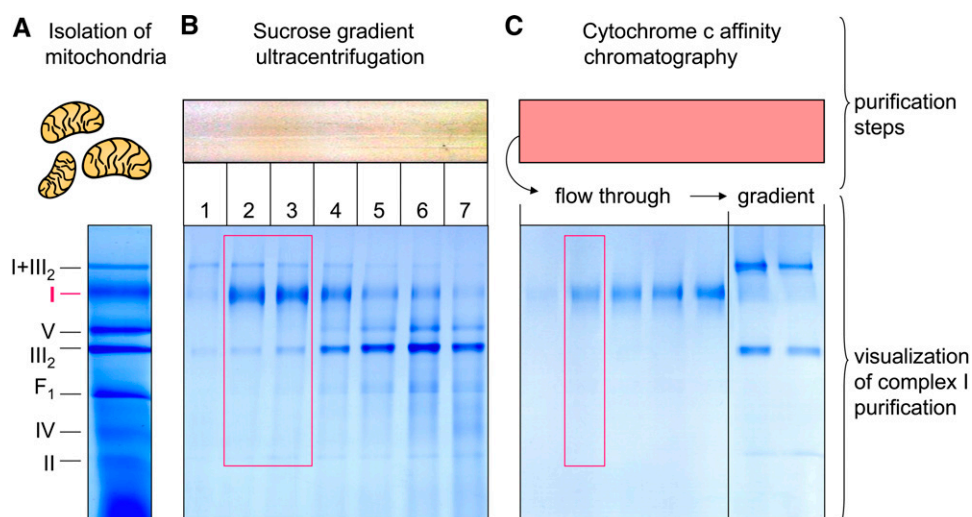


**Figure 2.** Purification Strategy for Mitochondrial Complex I of *Arabidopsis*.

The three purification steps are shown at the top; after each step, complex I purity was visualized by BN-PAGE and Coomassie blue staining.

**(A)** Mitochondria were isolated from *Arabidopsis* suspension culture, and total membrane protein was extracted. All OXPHOS complexes are present within this fraction as monitored by BN-PAGE (gel below). Identification of bands was based on subunit composition of the complexes as revealed by second gel dimensions (for comparison, see Eubel et al., 2003). I, II, IV, and V, complexes I, II, IV, and V; F<sub>1</sub>, F<sub>1</sub> part of complex V; III<sub>2</sub>, dimeric complex III; I+III<sub>2</sub>, supercomplex composed of complex I and dimeric complex III.

**(B)** The membrane proteins were subsequently separated by sucrose gradient ultracentrifugation. The top of the gradient (small protein complexes) is to the right and the bottom (large protein complexes) to the left. Complex I-containing fractions were identified by BN-PAGE (gel below, rectangle).

**(C)** These fractions were used for cytochrome c affinity chromatography. Complex I was obtained in the flow-through as revealed by BN-PAGE (gel below, rectangle). Finally, complex III<sub>2</sub> and the I+III<sub>2</sub> supercomplex were eluted from the column with a salt gradient as visible on the BN gel shown below.

### Controlled Disassembly of *Arabidopsis* Complex I

To obtain information on subunit localizations within complex I, the isolated protein complex was destabilized using defined biochemical conditions to generate complex I subcomplexes and finally analyze their subunit composition. Several destabilization conditions were tested, such as temperature, urea, and detergent treatment or mild proteolysis. Results of experiments were monitored by 1D BN-PAGE. Many conditions allowed dissecting complex I (1000 kD) into a large membrane arm of 550 kD and a 370-kD subcomplex that represents the peripheral arm. Dissection of isolated complex I from *Arabidopsis* into subcomplexes of similar sizes was previously reported by the use of two-dimensional (2D) BN/PAGE, if digitonin used for solubilization is replaced by dodecylmaltoside during the electrophoresis run of the second native gel dimension (Sunderhaus et al., 2006). However, slightly harsher conditions than these destabilization treatments consistently caused complete disassembly of complex I into its subunits.

We finally tested destabilization of isolated complex I by treatment with SDS at very low concentrations. Indeed, several additional complex I subcomplexes became visible upon analysis by 1D BN-PAGE and subsequent Coomassie blue or NADH activity staining (Figure 3). Treatment of complex I with only 0.01% SDS caused its partial dissociation into the 550- and 370-kD subcomplexes. Also, the molecular mass of the holocomplex is slightly reduced by ~80 kD in the presence of 0.01% SDS,

indicating loss of a few individual subunits (Figure 3). Increase of the SDS concentration to 0.04% and up to 0.12% generates further subcomplexes of 240, 210, and 140 kD, all of which can oxidize NADH as monitored by an in-gel activity assay. Therefore, they were considered to represent subcomplexes of the peripheral arm, which is known to include the NADH oxidation domain of complex I.

2D BN/SDS-PAGE analyses were performed to further examine SDS-induced subcomplex generation (Figure 4). In the absence of SDS, the subunits of the complex I holoenzyme form a vertical row of spots in the 1000-kD gel region (Figure 4, left gel). Treatment of intact complex I with 0.015% SDS leads to its partial dissection into the 550- and 370-kD complexes, which clearly are composed of distinct subunits (Figure 4, middle gel). Further increase of the SDS concentration to 0.04% leads to the generation of several additional subcomplexes, which are separated into vertical rows of subunits upon analysis by 2D BN/SDS-PAGE. Besides the NADH oxidizing 240-, 210-, and 140-kD subcomplexes detected on 1D BN gels, further subcomplexes are visible at 450, 270, 160, and 85 kD.

### Subunit Composition of Complex I Subcomplexes from *Arabidopsis*

Subunits of complex I subcomplexes resolved by 2D BN/SDS-PAGE were systematically identified by mass spectrometry (MS)

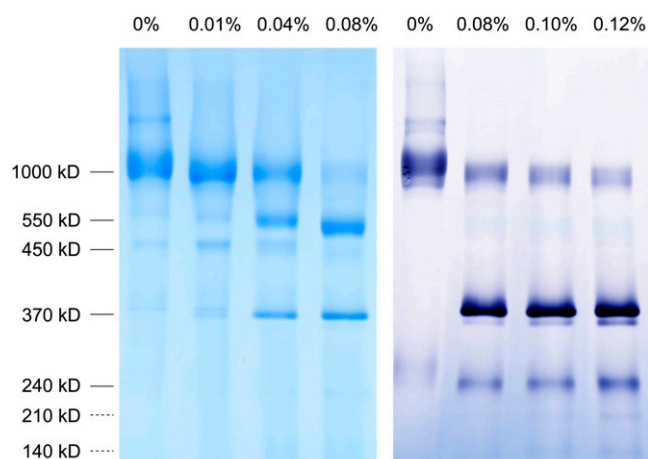


**Figure 3.** Controlled Disassembly of Complex I from *Arabidopsis* by SDS Treatment.

Purified complex I was treated with different SDS concentrations to induce its dissection into subcomplexes. The fractions were separated via BN-PAGE. Gels were either stained with Coomassie blue colloidal (left) or by an in-gel activity stain for NADH-dehydrogenase (right). Molecular masses are indicated on the left (in kD), and the SDS-concentrations used for complex I disassembly are given on top of the gels.

to determine the protein composition of the subcomplexes (Figure 5). Overall, 50 gel spots were analyzed, representing 40 different complex I subunits and a few contaminating proteins like prohibitin, the  $\beta$ -subunit of ATP synthase (complex V), Ser hydroxymethyltransferase, and lipoamide dehydrogenase (Table 1). Protein determinations revealed that the 550-, 450-, 270-, 160-, and 85-kD subcomplexes are related to the membrane arm

(indicated in red on Figure 5) and the 370-, 240-, 210-, and two 140-kD subcomplexes to the peripheral arm (indicated in orange on Figure 5). MS-based protein identifications gave insights into the subunit compositions of 10 different complex I subcomplexes (first given for the peripheral arm and afterwards for the membrane arm).

(1) The 370-kD subcomplex represents the entire peripheral arm. It includes at least 11 subunits: the so-called 75-kD, 51-kD, 49-kD (ND7), 30-kD (ND9), 24-kD, TYKY, B13, PSST, and B8 subunits (bovine nomenclature), the plant-specific subunit At1g67785 (~12 kD), and the previously not described *Arabidopsis* complex I subunit At3g03070 (~10 kD), which is homologous to the 13-kD subunit of the bovine enzyme (Figure 6).

(2) The 240-kD subcomplex represents the so-called NADH oxidation-module (N-module) of the peripheral arm, which previously was identified after pH- and Triton X-100-induced destabilization of complex I isolated from *E. coli* (Leif et al., 1995). It is composed of at least four proteins: the 51-kD subunit, which includes the NADH oxidation domain, the 75-kD subunit, the 24-kD subunit, the B8 subunit, and/or the plant-specific At1g67785 protein.

(3) The slightly smaller 210-kD subcomplex comprises only the three core subunits of the N-module, namely, the 75-, 51-, and 24-kD subunits.

(4) and (5) Careful inspection of the 2D gel in Figure 5 revealed that the 140-kD subcomplex consists of two distinct comigrating subcomplexes termed 140a and 140b. Assignment of subunits to the two subcomplexes is based on spot shape (barbell shaped in the case of subcomplex 140a and round in the case of subcomplex 140b). Subcomplex 140b includes the 51- and 24-kD subunits. Due to the presence of the NADH binding 51-kD subunit, it becomes visible upon in-gel NADH staining like the 240- and 210-kD subcomplexes (Figure 3).

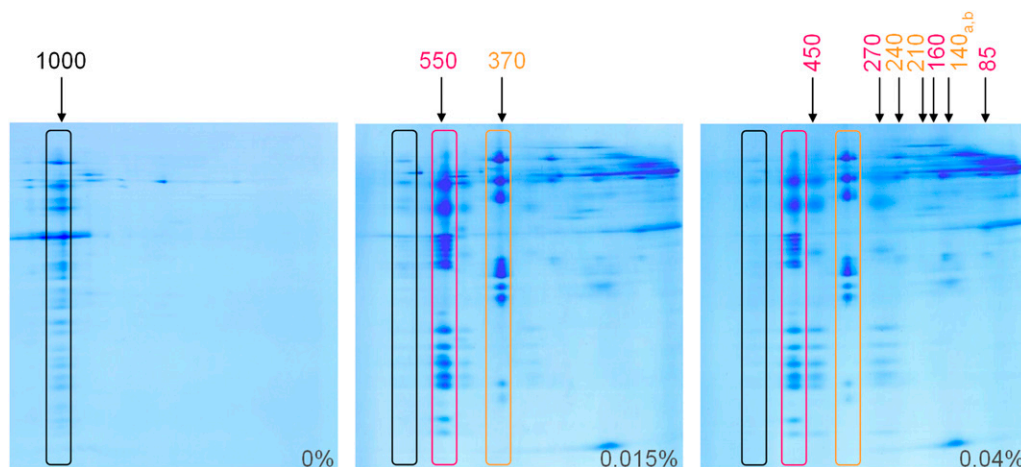


**Figure 4.** Analysis of Complex I Subcomplexes by 2D Gel Electrophoresis.

Purified complex I was treated with different SDS concentrations as indicated on each gel. Subcomplexes of complex I were separated by 2D BN/SDS-PAGE and visualized by Coomassie blue staining. The holocomplex (1000 kD) is indicated by a black box, and the primarily induced 550-kD subcomplex (representing the membrane arm of complex I) and 370-kD subcomplex (the peripheral arm) are marked by red and orange boxes. Secondary subcomplexes induced by increased destabilization are indicated by arrows above the gel to the right. Their estimated molecular masses are given in orange or red according to their assignment to one of the two primarily induced subcomplexes (see Figures 5 and 8).

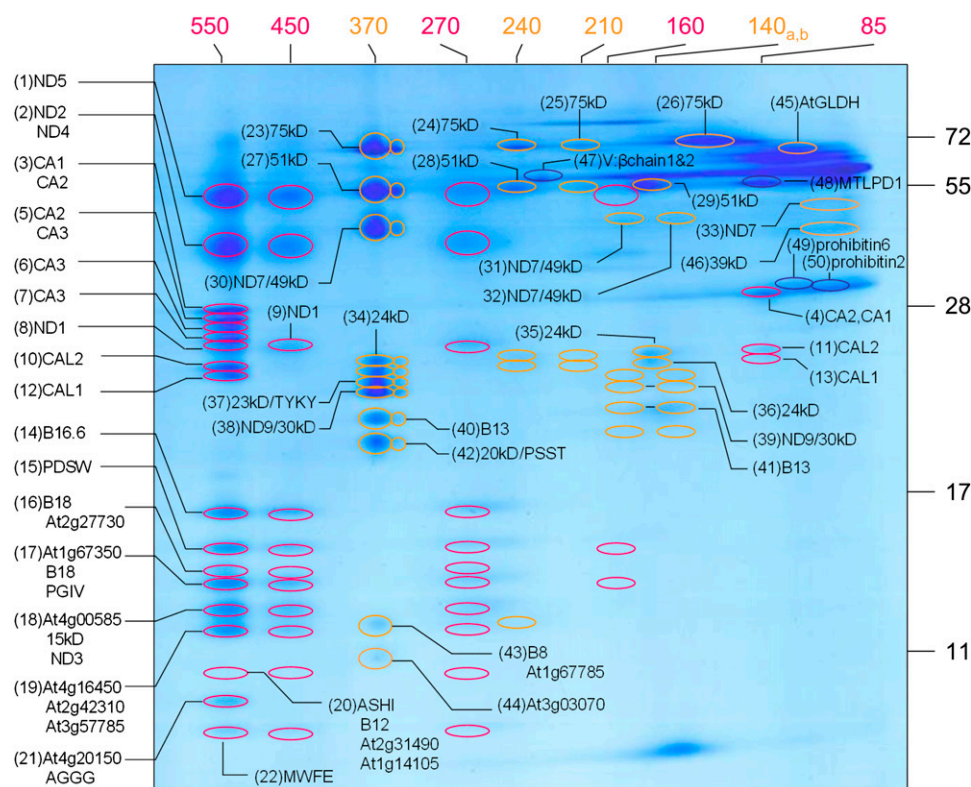


**Figure 5.** Identification of Subunits of Complex I Subcomplexes by MS.

The complex I fraction was pretreated with 0.04% SDS; subsequently, proteins were resolved by 2D BN/SDS-PAGE. Protein spots were cut out of the gel, digested with trypsin, and analyzed by MS. Spot numbers (in parentheses) refer to those given in Table 1; designations behind the spot numbers correspond to the names of the subunits (see Table 1). Subunits of membrane-embedded complex I subcomplexes are indicated in red, subunits of subcomplexes derived from the peripheral arm in orange, and proteins not belonging to complex I in blue. The sizes of the subcomplexes are indicated above the gel (in kD; red numbers, membrane arm of complex I and subcomplexes; orange, peripheral arm and subcomplexes; 140a,b, two different 140-kD subcomplexes that comigrate on the native gel dimension). The molecular masses of standard proteins are given to the right of the gel.

The 140a subcomplex includes subunits previously reported to form the so-called Q-reduction module (Q-module) of the peripheral arm in *E. coli* (Leif et al., 1995). It is composed of the 49-kD (ND7), 30-kD (ND9), TYKY, PSST, and B13 subunits.

(6) The 550-kD subcomplex represents the membrane arm of *Arabidopsis* complex I. It includes at least 27 subunits, 13 of which are homologous to known subunits of the membrane arm from bovine complex I (ND1, ND2, ND3, ND4, ND5, PDSW, B18, PGIV, 15 kD, B12, ASH1, AGGG, and MWFE). Additionally, the membrane arm of *Arabidopsis* complex I includes a bovine homolog known to be present in the peripheral arm, the so-called 16.6-kD subunit (GRIM19). Thirteen further subunits of the *Arabidopsis* membrane arm are plant-specific proteins, eight of which are rather small and hydrophobic (At4g16450, At2g27730, At2g42310/At3g57785, At4g00585, At4g20150, At2g31490, At1g67350, and the previously not described complex I subunit At5g14105). The five remaining plant-specific subunits of the membrane arm represent the CA subunits CA1, CA2, CA3, CAL1, and CAL2.

(7) The 450-kD subcomplex is a subcomplex of the membrane arm generated most efficiently at a slightly higher SDS concentration. The subunit composition resembles the one of the 550-

kD complex, but it lacks all five CA subunits and some of the smaller subunits of the membrane arm.

(8) and (9) The 270- and 160-kD subcomplexes represent smaller forms of the 450-kD subcomplex that lack so far unknown subunits. The 160-kD subcomplex includes the ND5 subunit, the B18 subunit, and/or At2g27730 as well as the PGIV subunit and/or At1g67350.

(10) Finally, an 85-kD subcomplex includes the CA subunits present within plant complex I, the CA1, CA2, CAL1, and CAL2 proteins. Slightly differing horizontal positions of the CAL1 and CAL2 proteins with respect to the CA1 and CA2 subunits indicate that they might not be simultaneously present within individual CA subcomplexes.

The GLDH, which is associated to complex I in plants, and the so-called 39-kD subunit were identified as separate proteins on BN/SDS gels (Figure 5), which do not form part of complex I subcomplexes upon SDS treatment of any concentration and therefore are assumed to be either peripherally localized or at the interphase of the membrane and the peripheral arm.

Elucidation of subunit compositions of complex I subcomplexes allows us to deduce a model of internal subunit arrangement within plant complex I as discussed below.

**Table 1.** Proteins Identified by MS

## Complex I-Related Proteins

Spot <sup>a</sup>	Identity in <i>Arabidopsis</i>		Homologs in			Mass (kD) <sup>b</sup>	GRAVY <sup>c</sup>	Score <sup>d</sup>	No MP <sup>e</sup>	Coverage (%) <sup>f</sup>
	Accession No. <sup>g</sup>	Name <sup>h</sup>	<i>E. coli</i>	<i>B. taurus</i>	<i>Y. lipolytica</i>					
1	AtMg00060/AtMg00513/AtMg00665	ND5	NUOL	ND5	NU5M	73.91	0.585	40	5	7
2	AtMg00580	ND4	NUOM	ND4	NU4M	55.23	0.687	7	2	6
	AtMg00285/AtMg01320	ND2	NUON	ND2	NU2M	54.88	0.727	22	3	5
3	At1g47260	CA2	–	–	–	30.07	–0.157	231	21	70
	At1g19580	CA1	–	–	–	29.97	–0.223	82	10	47
4	At1g47260	CA2	–	–	–	30.07	–0.157	216	18	71
	At1g19580	CA1	–	–	–	29.97	–0.223	123	12	53
5	At1g47260	CA2	–	–	–	30.07	–0.157	217	18	70
6	At5g66510.1	CA3	–	–	–	27.84	–0.293	126	11	56
7	At5g66510.1	CA3	–	–	–	27.84	–0.293	208	17	69
8	AtMg00516/AtMg01120/AtMg01275	ND1	NUOH	ND1	NU1M	35.68	0.773	95	2	7
9	AtMg00516/AtMg01120/AtMg01275	ND1	NUOH	ND1	NU1M	35.68	0.773	31	1	4
10	At3g48680	CAL2	–	–	–	27.96	0.041	175	12	51
11	At3g48680	CAL2	–	–	–	27.96	0.041	154	11	46
12	At5g63510	CAL1	–	–	–	27.57	0.06	195	14	58
13	At5g63510	CAL1	–	–	–	27.57	0.06	122	10	49
14	At2g33220	B16.6	–	B16.6	NB6M	16.12	–0.472	932	12	63
15	At3g18410/	PDSW	–	PDSW	NIDM	12.44	–0.956	314	11	83
	At1g49140	PDSW	–	PDSW	NIDM	12.53	–0.88	312	10	78
16	At2g02050	B18	–	B18	NB8M	11.74	–0.428	398	10	73
	At2g27730	At2g27730	–	–	–	11.95	–0.467	266	7	45
17	At2g02050	B18	–	B18	NB8M	11.74	–0.428	408	8	70
	At1g67350	At1g67350	–	–	–	15.25	0.615	299	9	76
	At5g18800/	PGIV	–	PGIV	NUPM	11.97	–0.492	84	2	16
	At3g06310	PGIV	–	PGIV	NUPM	12.16	–0.456	46	2	15
18	At4g00585	At4g00585	–	–	–	9.86	–0.592	142	6	69
	At2g47690	15 kD	–	15 kD	–	13.97	–0.918	49	1	14
	AtMg00990	ND3	NuoA	ND3	NU3M	13.66	0.590	83	2	17
19	At4g16450	At4g16450	–	–	–	11.35	0.024	463	6	61
	At2g42310/	At2g42310	–	–	–	12.63	–0.539	281	4	33
	At3g57785	At3g57785	–	–	–	12.66	–0.521	117	3	29
20	At5g47570	ASHI	–	ASHI	NIAM	13.21	0.061	85	4	24
	At2g02510	B12	–	B12	NB2M	8.05	–0.503	51	1	16
	At2g31490	At2g31490	–	–	–	8.29	–0.5	43	1	12
	At5g14105	At5g14105	–	–	–	8.44	–0.247	36	1	17
21	At4g20150	At4g20150	–	–	–	9.21	–0.2	328	6	83
	At1g76200	AGGG	–	AGGG	–	7.57	–0.536	113	4	55
22	At3g08610	MWFE	–	MWFE	NIMM	7.34	–0.189	31	2	21
23	At5g37510	75 kD	NUOG	75 kD	NUAM	81.18	–0.154	2147	35	52
24	At5g37510	75 kD	NUOG	75 kD	NUAM	81.18	–0.154	154	19	35
25	At5g37510	75 kD	NUOG	75 kD	NUAM	81.18	–0.154	133	16	28
26	At5g37510	75 kD	NUOG	75 kD	NUAM	81.18	–0.154	208	21	35
27	At5g08530	51 kD	NUOF	51 kD	NUBM	53.35	–0.303	226	21	50
28	At5g08530	51 kD	NUOF	51 kD	NUBM	53.35	–0.303	90	9	24
29	At5g08530	51 kD	NUOF	51 kD	NUBM	53.35	–0.303	160	18	35
30	AtMg00510	ND7	NUOD	49 kD	NUCM	44.58	–0.408	83	10	23
31	AtMg00510	ND7	NUOD	49 kD	NUCM	44.58	–0.408	64	10	19
32	AtMg00510	ND7	NUOD	49 kD	NUCM	44.58	–0.408	21	5	13
33	AtMg00510	ND7	NUOD	49 kD	NUCM	44.58	–0.408	48	8	22
34	At4g02580	24 kD	NUOE	24 kD	NUHM	28.39	–0.36	118	10	32
35	At4g02580	24 kD	NUOE	24 kD	NUHM	28.39	–0.36	95	9	31
36	At4g02580	24 kD	NUOE	24 kD	NUHM	28.39	–0.36	120	9	30
37	At1g79010	TYKY	NUOI	TYKY	NUKM	25.50	–0.559	84	9	40
38	AtMg00070	ND9	NUOC	30 kD	NUGM	22.69	–0.676	76	8	42
39	AtMg00070	ND9	NUOC	30 kD	NUGM	22.69	–0.676	78	9	44

(Continued)

**Table 1.** (continued).

## Complex I-Related Proteins

Spot <sup>a</sup>	Identity in <i>Arabidopsis</i>		Homologs in			Mass (kD) <sup>b</sup>	GRAVY <sup>c</sup>	Score <sup>d</sup>	No MP <sup>e</sup>	Coverage (%) <sup>f</sup>
	Accession No. <sup>g</sup>	Name <sup>h</sup>	<i>E. coli</i>	<i>B. taurus</i>	<i>Y. lipolytica</i>					
40	At5g52840	B13	–	B13	NUFM	19.34	–0.478	119	10	56
41	At5g52840	B13	–	B13	NUFM	19.34	–0.478	116	9	42
42	At5g11770	PSST	NUOB	PSST	NUKM	24.04	–0.123	106	7	33
43	At5g47890	B8	–	B8	NI8M	10.85	–0.289	67	5	59
	At1g67785	At1g67785	–	–	–	7.53	–0.417	35	2	36
44	At3g03070	13 kD	–	13 kD	NUMM	12.23	–0.246	268	4	43
45	At3g47930	GLDH	–	–	–	68.56	–0.479	91	11	30
46	At2g20360	39 kD	–	39 kD	NUEM	43.94	–0.059	192	17	44

## Other Proteins

Spot <sup>a</sup>	Accession No. <sup>g</sup>	Name	Mass (kD) <sup>b</sup>	GRAVY <sup>c</sup>	Score <sup>d</sup>	No MP <sup>e</sup>	Coverage (%) <sup>f</sup>
47	At5g08670/At5g08690	β-Subunit of the mitochondrial ATP-synthase	59.63	−0.152	133	16	33
	At5g26780	Ser-hydroxymethyltransferase 2 (SMH2)	57.34	−0.286	95	14	32
48	At1g48030	Mitochondrial lipoamide DH1 (MTLPD1)	53.99	−0.042	170	23	55
	At3g17240	Mitochondrial lipoamide DH2 (MTLPD2)	53.99	−0.023	130	20	54
49	At2g20530	Prohibitin 6 (AtPHB6)	31.62	−0.140	68	7	32
50	At1g03860	Prohibitin 2 (AtPHB2)	31.79	−0.155	95	13	62

<sup>a</sup>Spot number in accordance with Figure 5. In some cases, more than one complex I subunit was found to be present within a single spot. Furthermore, in some cases, individual subunits of complex I were identified twice in neighboring spots. This is interpreted to be due to spot overlappings on the gel. In most cases, identification of a subunit was most significant for one single spot, allowing unambiguous assignment of spots and subunits.

<sup>b</sup>Calculated molecular mass of the identified protein as deduced from the corresponding gene.

<sup>c</sup>GRAVY (grand average of hydropathy) score of the protein.

<sup>d</sup>Probability score for the protein identification based on MS analysis and MASCOT search.

<sup>e</sup>Number of unique matching peptides.

<sup>f</sup>Sequence coverage of a protein by identified peptides.

<sup>g</sup>Accession numbers as given by TAIR (<http://www.Arabidopsis.org/>). More than one accession number is given in case a subunit is encoded by more than one gene in identical form. In some cases, subunits are present in isoforms. Accessions for all isoforms exactly matching to identified peptides are given. Note that in some cases the identified peptides do not allow us to distinguish between possible isoforms.

<sup>h</sup>Subunits of complex I from *Arabidopsis* are named according to the bovine nomenclature. Subunits specific to complex I of plant mitochondria are named according to the corresponding genes annotated by TAIR ([www.Arabidopsis.org](http://www.Arabidopsis.org/)). Exceptions: the plant-specific CA subunits are named CA1, CA2, CA3, CAL1, and CAL2, and the L-galactone-1,4-lactone dehydrogenase is named GLDH in accordance with the literature. Furthermore, *Arabidopsis* homologs to the 30- and 49-kD subunits of bovine complex I are designated ND9 and ND7 because the corresponding proteins are encoded by the mitochondrial genome in plants.

## DISCUSSION

### Biochemical Procedures to Characterize Complex I

A protocol for complex I isolation is presented that is based on mitochondrial preparation, sucrose gradient ultracentrifugation, and depletion of complex III-related contaminants by cytochrome c affinity chromatography. Protocols previously published for the isolation of complex I from plants include ion-exchange or immunoaffinity chromatography, which require salt gradients or acid treatment for complex I elution (Leterme and Boutry, 1993; Herz et al., 1994; Rasmusson et al., 1994; Trost et al., 1995; Combettes and Grienberger, 1999). By contrast, the protocol presented here completely avoids high salt conditions since complex I passes the cytochrome c affinity column

used for complex III depletion in the flow-through fraction. Complex I therefore can be expected to have optimal integrity for further structural analysis.

Insights into the internal subunit arrangement of complex I were obtained by its careful disassembly and biochemical analysis of the generated disassembly products. Incubation of complex I with low concentrations of SDS proved to be an ideal tool for careful subcomplex generation. It is textbook knowledge that SDS treatment of biochemical fractions is incompatible with native protein characterization. However, SDS concentrations usually employed in protein science often are in the range of 1% or higher (e.g., 5% for sample preparation prior to SDS-PAGE) (Laemmli, 1970; Schägger and von Jagow, 1987). Here, we report use of very low SDS concentrations in the range of 0.01 to 0.04%. Indeed, low SDS conditions cause very distinct



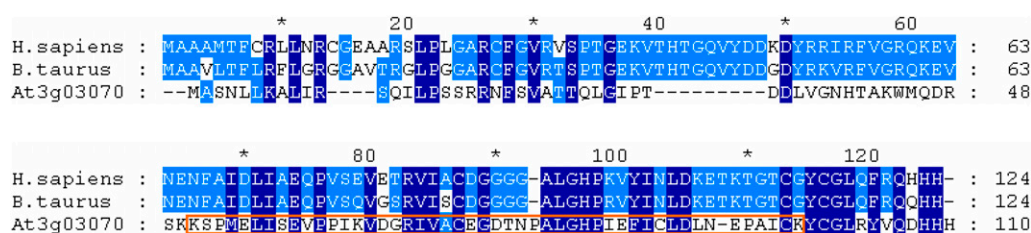


**Figure 6.** Alignment of At3g03070 with the 13-kD Subunit of Human and Beef Complex I.

Amino acid positions identical in all three sequences are highlighted in dark blue and amino acid positions conserved in two sequences in light blue. The orange box indicates peptides identified by MS analyses.

dissection of complex I into functional modules in a highly reproducible way. There are a few examples in the literature on usage of low SDS for native protein analyses, for example, the green native gel electrophoresis system developed for the analysis of protein complexes of the photosynthesis apparatus, which is based on a first gel dimension in the presence of low and a second gel dimension in the presence of high SDS (Thorner, 1986; Allen and Staehelin, 1991). We suggest the use of low SDS concentrations generally as a tool for the biochemical analysis of the internal architecture of protein complexes.

### Subunits of Mitochondrial Complex I from *Arabidopsis*

Forty different complex I subunits were identified by MS analysis of complex I subcomplexes (Figure 5, Table 1). Compared with the most extensive study on complex I subunits in plants (Meyer et al., 2008), which was based on the separation of complex I proteins by three-dimensional BN/SDS/PAGE, six subunits were not detected (the ND6, 18-kD, B17.2, B14.7, B14, and At1g68680 subunits). These subunits probably are lost during low SDS treatment. Indeed, at least five subunits with apparent molecular masses of 39, 19, 16, 8, and 7 kD form part of intact complex I on BN gels but neither are part of the membrane nor the peripheral arm (see Supplemental Figure 1 online). The 39-kD subunit was identified by MS on the 2D BN/SDS gel shown in Figure 5 as a monomer, whereas the other subunits were not detected. On the other hand, four of the 40 subunits identified in our study were not reported in Meyer et al. (2008): the homolog of the bovine 13-kD subunit (At4g03070; Figure 6), ND3, GLDH, and the novel plant-specific subunit At1g14105. Two further complex I subunits (B22 and At1g14450) were identified by another study (Sunderhaus et al., 2006) but not found by Meyer et al. (2008) or within any of the complex I subcomplexes analyzed in this investigation. Overall, 17 plant-specific complex I subunits have now been identified (Heazlewood et al., 2003; Sunderhaus et al., 2006; Meyer et al., 2008; this study). Except for the CA subunits and GLDH, most of them are small hydrophobic subunits forming part of the membrane arm. It currently cannot be excluded that some of these proteins are structural homologs of small subunits additionally present in fungal or mammalian complex I since sequence conservation often is low between related proteins if they are small and hydrophobic (Brandt, 2006).

In addition to the overall 48 MS-identified complex I subunits of *Arabidopsis* (Sunderhaus et al., 2006; Meyer et al., 2008; this

study), the mitochondrial genome of *Arabidopsis* encodes an ND4L homolog that is extremely hydrophobic and most likely difficult to detect by MS. The number of distinct complex I subunits in *Arabidopsis* therefore adds up to at least 49. Bovine complex I, which is the largest complex I particle biochemically characterized so far, has 45 distinct subunits (Carroll et al., 2006), and complex I of the fungus *Yarrowia lipolytica* has 40 subunits (Morgner et al., 2008). Indeed, upon direct size comparison of bovine and potato (*Solanum tuberosum*) complex I by 1D BN-PAGE, the enzyme complex from plants is slightly larger (Jänsch et al., 1995).

For several subunits, pairs of isoforms occur in *Arabidopsis*. MS analysis allowed us to detect isoforms for the PSDW subunit (encoded by At3g18410 and At1g49140), the PGIV subunit (At5g18800 and At3g06310), and a 12.6-kD subunit (At2g42310 and At3g57785; Table 1). For some other subunits, genes encoding isoforms are present in the *Arabidopsis* genome, but the encoded proteins are not distinguishable by the peptide sequences obtained.

### The CA Subunits of Complex I from *Arabidopsis*

The CA1, CA2, CA3, CAL1, and CAL2 proteins also exhibit sequence similarity and might be considered to represent isoforms. However, biochemical evidence indicates the presence of at least three proteins of the CA/CAL family in individual complex I particles because the CA domain attached to complex I has a trimeric structure (Sunderhaus et al., 2006). Unfortunately, despite large efforts, the CA/CAL proteins so far could not be functionally characterized. The genes encoding CA1 and CA2 are downregulated if plants are cultivated in the presence of high CO<sub>2</sub> concentrations (Perales et al., 2005), which is also known for enzymes involved in photorespiration. A role for the CA/CAL proteins in an intracellular CO<sub>2</sub> transfer mechanism from mitochondria to chloroplasts analogous to the cyanobacterial carbon concentration mechanism has been proposed (Braun and Zabaleta, 2007). Recently, overexpressed CA2 was shown to bind CO<sub>2</sub> and/or bicarbonate efficiently (Martin et al., 2009).

For reasons not understood, the five CA/CAL proteins are represented by six protein spots on 2D BN/SDS gels (Figure 5). Since they partially overlap, assignment of the spots to the proteins is difficult. However, the most likely explanation is that CA3 occurs in two versions of ~28 and 29 kD. Interestingly, the corresponding gene also is annotated in two versions (At5g66510.1 and At5g66510.2), which differ in size by ~1.2

kD (27.837 and 29.043 kD) due to a small insertion in At5g66510.2 at a central position. The functional relevance of this possible CA3 heterogeneity is so far unclear.

Mapping of MS-identified peptides for the CA/CAL proteins to the complete amino acid sequences deduced from the corresponding genes indicates the absence of a cleavable presequence for CA1, CA2, and CA3 (Figure 7). In the case of CA3, the N terminus of the primary translation product forms part of the mature protein. For CA1 and CA2, the most N-terminal peptides identified by MS start at amino acid 7 of the translation products. The six N-terminal amino acids of the translation products do not exhibit the typical properties of cleavable mitochondria targeting sequences (Glaser et al., 1998). Also, the apparent molecular masses of CA1 and CA2, which both migrate at 30 kD on 2D BN/SDS gels, exactly fit to the calculated molecular masses of the translation products (29.970 and 30.065 kD). By contrast, the CAL1 and CAL2 sequences have cleavable presequences. Removal of the targeting sequences was previously shown by an in vitro processing assay (Perales et al., 2004). The length of the presequences can be predicted to be 22 amino acids for CAL1 and 26 amino acids for CAL2 on the basis of a sequence comparison to the N-terminal region of a homologous 29-kD subunit of complex I from potato (Herz et al., 1994) (Figure 7). Also, N termini for the mature CAL2 and CAL1 proteins were recently directly determined by an elegant MS-based approach (Huang et al., 2009). The resulting masses of the mature CAL1 and CAL2 subunits are 25.079 and 25.045 kD, which nicely

corresponds to their apparent masses upon separation by BN/SDS-PAGE (Figure 5).

### Internal Architecture of Complex I from *Arabidopsis*

Incubation of isolated complex I from *Arabidopsis* with SDS solutions of low concentration allows the dissection of the complex into 10 defined subcomplexes. At 0.01% SDS, the membrane arm (550 kD) and the peripheral arm (370 kD) are generated. Furthermore, approximately five subunits are detached as monomers during this first dissection step, including the 39-kD subunit, which was identified by MS within the dye front of the BN gel dimension. Increase of SDS to 0.04% further dissects the two arms into secondary subcomplexes of 450, 270, 240, 210, 160, 140, 140, and 85 kD. The proposed disassembly process of complex I from *Arabidopsis* is summarized in Figure 8. Apparent molecular masses of the subcomplexes are in good accordance with calculated masses of the subcomplexes based on the sum of the masses of their subunits. However, in some cases, the calculated masses of the subcomplexes are slightly lower, most likely indicating that further subunits might additionally be present, which are not resolved on the Coomassie blue-stained gel (Figure 5).

Subfractionation procedures were previously used for the analysis of complex I particles from other organisms. In beef, treatment of isolated complex I with the nondenaturing detergent *N,N*-dimethyldodecylamine *N*-oxide dissociates the enzyme

CA1	.....MGT	LGR	AFYSVGF	WIRE	TGQALD	RLGCR	LQGKN	YFRE	QLSRHR	TLMN	VFDKAP	IVDKE	AFVAP											
CA2	.....MGT	LGR	AIYTVGN	WIRGT	GQALD	RVGS	LLQGS	R	IEEHL	SRHR	TLMN	VFDKSP	LVDKD	VFVAP										
CA3	.....MGT	MGK	AFYSVGF	WIRE	TGQALD	RLGCR	LQGKN	HFRE	QLSRHR	TLMN	VFDKTP	NVDK	GAFVAP											
CAL1	MATSIARLSR	R....	GVTSN	LIRRC	FAAEA	ALARK	TELPK	PQFTV	SPSTD	RVK	WDYR	GQR	QIIP	LQGWLP	KVAV	DAYVAP								
CAL2	MATSLARISK	RSITS	AVSSN	LIRRY	FAAEA	VAVAT	TEPK	PKSQVT	SPSD	RVK	WDYR	GQR	QIIP	LQGWLP	KVAV	DAYVAP								
CA1	IVDKE	AFVAP	SASVIG	DVHI	GRGSS	IWYGC	VL	RGD	VNTVS	VGSGT	NIQDN	SLVH	VAKSNL	SGK	VHPTIIG	DNVTIG	SAV							
CA2	LVDKD	VFVAP	SASVIG	DVQI	GKGSS	IWYGC	VL	RGD	VNNIS	VGSGT	NIQDN	TLVH	VAKTNI	SGK	VLPTLIG	DNVTVG	SAV							
CA3	NVDKG	AFVAP	NASLSG	DVHV	GRGSS	IWYGC	VL	RGD	DANSIS	VGAGT	NIQDN	ALVH	VAKTNL	SGK	VLPTVIG	DNVTIG	SAV							
CAL1	KVAV	DAYVAP	NVVL	AGQTV	WDGSS	VWNGA	VL	R	GDLN	KIT	VGFC	SNVQER	CVVH	AAWSSP	TGLPA	ATIID	RYVT	VGAYSL						
CAL2	KVAV	DAYVAP	NVVL	AGQTV	WDGSS	VWNGA	VL	R	GDLN	KIT	VGFC	SNVQER	CVVH	AAWSSP	TGLPA	QTLID	RYVT	VGAYSL						
CA1	LHGCT	VEDET	FIGM	GATLLD	GVVVEK	HGMV	AAGAL	VRQNT	RIP	S	GEVWGG	NPA	RFLR	KLT	DEE	IAFISQS	ATNYS	NLAQA						
CA2	IHGCT	VEBDA	FVGM	GATLLD	GVVVEK	HAMV	AAGS	LVKQNT	RIP	S	GEVWGG	NPA	KFMR	KLT	DEE	I	VYISQS	AKNY	INLAQI					
CA3	LHGCT	VEDEA	YIGT	SATVLD	GAHVEK	HAMV	ASGAL	VRQNT	RIP	S	GEVWGG	NPA	KFLR	KVT	EE	R	VFFSSS	AVEYS	NLAQA					
CAL1	LR	SC	TIEPEC	IIGQ	HSILME	GS	LVETR	SIL	EAGS	V	PPGR	RIP	S	GELWGG	NPA	R	FIR	T	LT	NEET	LEIPKL	AVAIN	HL	SGD
CAL2	LR	SC	TIEPEC	IIGQ	HSILME	GS	LVETR	SIL	EAGS	V	PPGR	RIP	S	GELWGG	NPA	R	FIR	T	LT	NEET	LEIPKL	AVAIN	HL	SGD
CA1	HAAENAK	PLN	VIEFEK	VLRK	KH	ALKDEEYD	SMLG	IVRETP	PE	LN	LPNNIL	PDKE	..TK	RP	SNV	..	..	..	..					
CA2	HASENSK	SFE	QIEVER	ALRK	KY	ARKDEYD	SMLG	ITRETP	PE	L	IPDNV	PGGK	PAK	V	STQY	F	..	..	..					
CA3	HATENAK	NLD	EA	E	FKKLLNK	KN	AR	DTEYD	SVL	.....	DDLT	L	PENVP	KAA	.....	.....	.....	.....	.....					
CAL1	YFSE	FLPYST	Y	LEVEK	FKK	SLG	I	A	V	.....	.....	.....	.....	.....	.....	.....	.....	.....	.....					
CAL2	YFSE	FLPYST	I	Y	LEVEK	FKK	SLG	I	A	I	.....	.....	.....	.....	.....	.....	.....	.....	.....					

**Figure 7.** Coverage of the CA Sequences by Peptides Identified by MS.

The five amino acid sequences of the CA/CA-like subunits of *Arabidopsis* complex I were aligned using ClustalW2 (<http://www.ebi.ac.uk/Tools/clustalw2/index.html>). Identified peptides are highlighted in blue. The sequences correspond to the following accessions: At1g19580 (CA1), At1g47260 (CA2), At5g66510.1 (CA3), At5g63510 (CAL1), and At3g48680 (CAL2). The red arrow indicates the cleavage site for the removal of the presequences in CAL1 and CAL2.

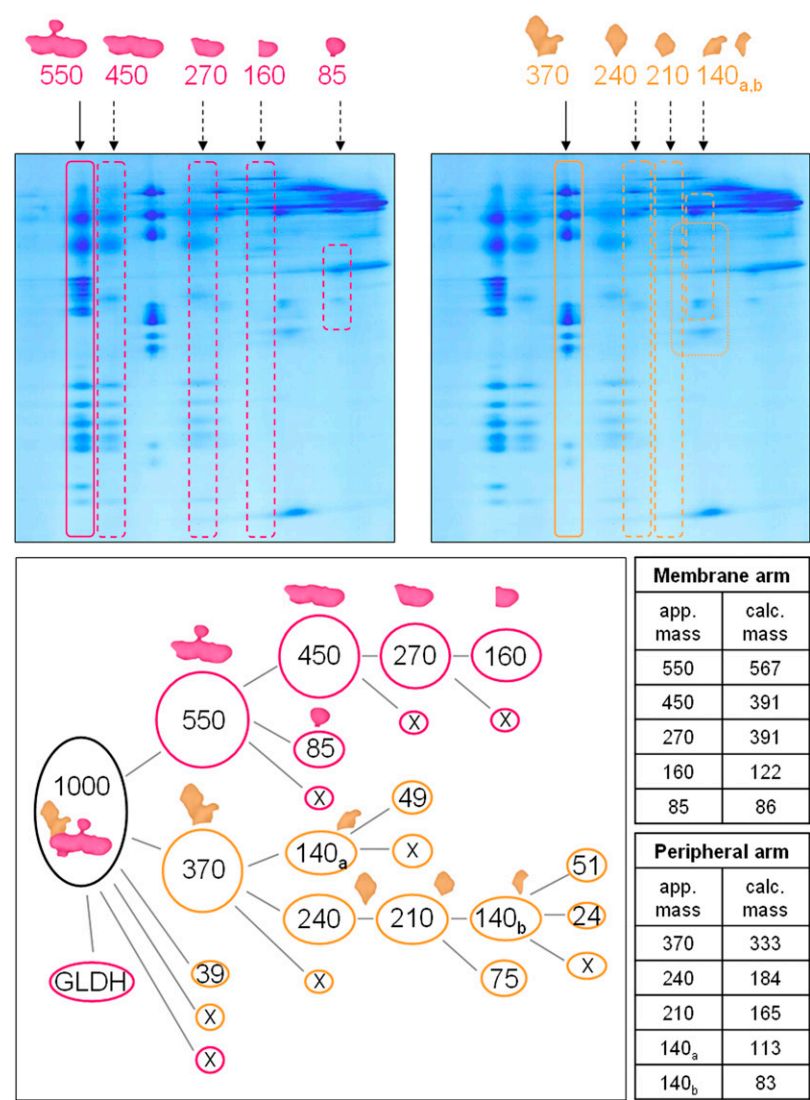


**Figure 8.** Proposed Disassembly Process for *Arabidopsis* Complex I. Top: 2D BN/SDS separations of complex I subcomplexes generated by 0.04% SDS. The membrane arm and its dissection products are indicated on the 2D gel on the left and the peripheral arm and its subcomplexes on the 2D gel to the right. Apparent molecular masses of the subcomplexes are given above the gels (in kD). Bottom: proposed disassembly pathway of *Arabidopsis* complex I. Membrane subcomplexes/subunits are given in red and the ones of the peripheral arm in orange. Numbers indicate apparent molecular masses (in kD). The table to the right of the scheme compares the apparent molecular masses of the generated complex I subcomplexes with the calculated molecular mass of the sum of their protein subunits identified by MS. Since two subcomplexes deduced from the peripheral arm have apparent molecular masses of 140 kD, these are distinguished in the figure and in the table by (a) and (b). For unknown reasons, the calculated molecular mass of the 270 kD complex is too high.

into two parts, an  $\alpha$ -part including the subunits of the peripheral arm as well as adjacent subunits of the membrane arm and a  $\beta$ -part that represents the remaining membrane arm (Finel et al., 1992). Modified procedures allow the purification of a  $\lambda$ -subcomplex including the hydrophilic subunits and a  $\gamma$ -subcomplex that includes the more hydrophobic subunits of the  $\alpha$ -part of beef complex I (Arizmendi et al., 1992; Sazanov et al., 2000; Carroll et al., 2003). In *E. coli*, treatment of complex I with Triton X-100 leads to the dissociation of complex I into a membrane part, a water-soluble NADH dehydrogenase part, and

an amphipathic part that connects the two other parts (Leif et al., 1995). The subunit compositions of the bovine and *E. coli* subcomplexes have been resolved (Leif et al., 1995; Carroll et al., 2003). Based on the protein composition of complex I subcomplexes, functional domains have been defined (reviewed in Brandt, 2006): an NADH oxidation (N) module, a quinone reduction (Q) module, and a proton translocating (P) module. Systematic analysis of the subunit compositions of the 10 complex I subcomplexes generated by SDS treatment gave the following insights into the internal architecture of this protein



complex in *Arabidopsis* (summarized in Figure 9). The 240-kD subcomplex (75-kD, 51-kD, 24-kD, and B8 and/or At1g67785 subunits) represents the N-module and the 140-kD (140a) subcomplex (49-kD/ND7, 30-kD/ND9, TYKY, PSST, and B13 subunits) the Q-module of complex I. Together with the 13-kD subunit (At3g03070), they form the peripheral arm (370 kD). The 240-kD subcomplex can be further dissected into a smaller 140-kD (140b) subcomplex including the 51- and 24-kD subunits and possibly some further subunits. This is the smallest subcomplex exhibiting NADH oxidation activity (Figure 3).

The membrane arm subcomplex (550 kD) includes at least five of the hydrophobic mitochondrially encoded subunits (ND1, ND2, ND3, ND4, and ND5), seven further mainly hydrophobic subunits homologous to nuclear-encoded complex I subunits from beef, eight additional plant-specific subunits, and the five CA/CAL proteins (Figure 9). Arrangement of all these subunits within the membrane arm still is largely unknown because the generation of secondary subcomplexes is difficult. However, based on single particle EM and cross-linking experiments, the location for some proteins is known. For instance, several lines of evidence suggest that the ND4 and ND5 proteins are in close proximity and form the tip of the membrane arm (Holt et al., 2003; Baranova et al., 2007a, 2007b). Analysis of a 210-kD subcomplex derived from the membrane arm of complex I from *Arabidopsis* indicates an association of the PDSW subunit and at least one of the three subunits included in spot 17 (Figure 5, Table 1) with ND5. The ND6 and possibly also the ND4L subunits, which could not be identified within the 550-kD membrane arm of *Arabidopsis* complex I, probably are detached from complex I during initial dissection into the membrane and the peripheral arm at 0.01% SDS and are speculated to represent the end of the membrane

arm at the site of its connection to the peripheral arm. This is in line with detection of ND6 in subcomplex  $\alpha$  of complex I from beef but its absence in subcomplex  $\lambda$  (Carroll et al., 2003). Most interestingly, the B16.6 subunit, which is identical to the GRIM-19 protein involved in apoptosis, forms part of the membrane arm of complex I in *Arabidopsis* but was reported to be part of the peripheral ( $\lambda$ ) arm in beef (Carroll et al., 2003). This most likely points to a location of B16.6 at the intersection of the two complex I arms.

Some subunits were detached from *Arabidopsis* complex I during initial dissociation of the peripheral and the membrane arm (e.g., the 39-kD subunit). However, in a previous investigation (Sunderhaus et al., 2006), this protein was reported to be associated with the peripheral arm in *Arabidopsis*. Also, GLDH, which only in plants is part of complex I (Heazlewood et al., 2003), was not found to be associated with either of its two arms. Since this enzyme catalyzes the terminal step of ascorbic acid biosynthesis, it should be associated with the membrane arm of complex I on the side exposed to the intermembrane space. However, recent findings indicate that GLDH might represent an assembly factor important for complex I biogenesis (Pineau et al., 2008). Indeed, GLDH initially was described as a subunit of an *Arabidopsis* complex I version of slightly reduced molecular mass (Heazlewood et al., 2003; Millar et al., 2003).

Finally, an 85-kD subcomplex is generated if the membrane arm is further destabilized using 0.04% SDS. This complex includes the 30-kD CA1 and CA2 proteins and the 25-kD CAL1 and CAL2 proteins. Based on previous findings that CAs are trimers, we conclude that probably three of the four proteins form a CA domain. The stoichiometry of the four proteins upon analysis by 2D BN/SDS-PAGE (Figure 5) differs: the amount of CA1+CA2 clearly exceeds the one of CAL1+CAL2. We speculate that the CA domain attached to complex I might include two CA proteins (CA1+CA2 or two copies of CA2 or two copies of CA1) and additionally either CAL1 or CAL2. Interestingly, interaction of CA2 with CAL1 and CAL2 was previously proved by a two-hybrid screen (Perales et al., 2004). Furthermore, using the same approach, it was shown that the N-terminal half of CA2 binds to the CAL subunits. By contrast, CA1–CA2 interaction has not been reported. For reasons currently not understood, CA3 was not found to interact with any of the other members of the CA/CAL protein family, neither by two-hybrid screening nor by MS analysis of complex I subcomplexes. Further investigations will be necessary to better understand the composition and function of the CA domain of plant complex I.

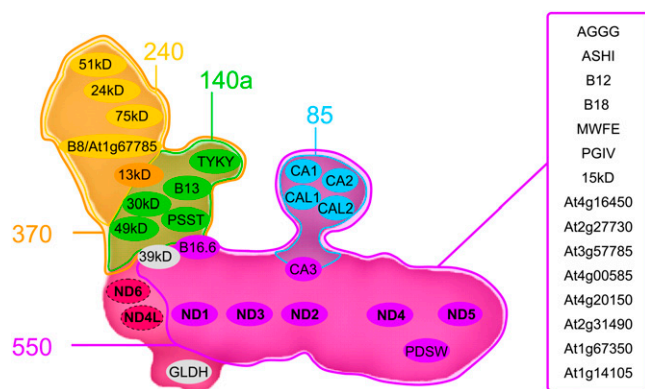


**Figure 9.** Model of the Internal Architecture of Mitochondrial Complex I from *Arabidopsis*.

Based on the presented disassembly analysis and subunit identifications, the 550-, 370-, 240-, 140-, and 85-kD subcomplexes are assigned to the EM average structure of complex I (Figure 1). The approximate localization of subunits within the subcomplexes is given in accordance with further insights based on the presented findings and data available in the literature (Sazanov and Hinchliffe, 2006; Baranova et al., 2007a, 2007b; Zickermann et al., 2009). The localization of several subunits within the membrane arm of complex I so far is unknown (subunits included in box to the right of the model).

## Outlook

The presented biochemical strategy, SDS-mediated dissection of isolated complex I, separation of subcomplexes by BN/SDS-PAGE, and protein identifications by MS, allowed us to achieve insights into the internal architecture of complex I. Since crystallization of the entire complex proved to be intractable, sophisticated biochemical procedures are required to better understand the structure and function of this key enzyme complex of the respiratory chain. Despite large efforts, knowledge on the subunit arrangements within the membrane arm of eukaryotic complex I still is fragmentary. New protocols to generate

additional subcomplexes of this arm will be crucial for a deeper understanding of internal complex I structure. Further progress could also come from combining controlled complex I dissections and cross-link approaches in future experiments. Analysis of complex I certainly will remain one of the most fascinating challenges in biochemistry.

## METHODS

### *Arabidopsis thaliana* Cultivation and Isolation of Mitochondria

Cell cultures of *Arabidopsis* wild type (Columbia-0) were established as described by May and Leaver (1993). Cells were cultivated in a suspension culture maintained as outlined previously (Sunderhaus et al., 2006). Mitochondria were isolated from *Arabidopsis* suspension culture as given by Werhahn et al. (2001).

### Purification of Complex I

Purification of complex I from isolated *Arabidopsis* mitochondria followed a two-step procedure based on (1) sucrose gradient ultracentrifugation to prepare the ~1-MD protein fraction and (2) cytochrome c affinity chromatography to deplete the complex I-enriched 1-MD fraction from remaining contaminations of complex III<sub>2</sub> and supercomplex I+III<sub>2</sub>.

Isolated mitochondria were pelleted by centrifugation and resuspended in digitonin solubilization buffer (30 mM HEPES, 150 mM potassium acetate, 10% [v/v] glycerol, and 5% [w/v] digitonin) at a detergent/protein ratio of 5 mg/mg. Protein complexes were subsequently resolved by sucrose gradient ultracentrifugation. Solubilized mitochondria (~10 mg mitochondrial protein) were loaded onto a 12-mL sucrose gradient (15 mM Tris, 20 mM KCl, 0.2% [w/v] digitonin, and 0.3 to 1.5 M sucrose). Ultracentrifugation was performed at 4°C using Beckmann 9/16 × 3 3/4 Ultra Clear Tubes and the Beckmann SW40Ti rotor (146,000g for 20 h). Afterwards, the gradient was divided into 700-μL fractions, and the protein complex composition of each fraction was analyzed by 1D BN-PAGE (see below). Fractions containing complex I but devoid of complex V were used for a cytochrome c-mediated depletion of complex III contaminations.

For this approach, cytochrome c was coupled to CNBr-activated Sepharose as described by Weiss and Juchs (1978). Before usage, the cytochrome c sepharose was washed with 300 mL oxidation solution (5 mM K<sub>3</sub>[Fe(CN)<sub>6</sub>], 0.5% [v/v] Triton X-100, 0.1 M NaHCO<sub>3</sub>, and 0.5 M NaCl) to oxidize the cytochrome c. Subsequently, this solution was removed by washing the Sepharose with 150 mL washing buffer (20 mM Tris-acetate, pH 7.0, 5% [w/v] sucrose, 0.04% [w/v] digitonin, and 0.2 mM PMSF). Six milliliters of Sepharose was filled into a column (1 cm × 10 cm) and washed with washing buffer another time. Afterwards, the complex I-containing sucrose gradient fractions were transferred on the top of the column, and the flow-through was collected in 1-mL fractions. Additional 2 mL of washing buffer was used to remove remaining complex I from the column. Finally, complex III<sub>2</sub> and the I+III<sub>2</sub> supercomplex were eluted from the column using a salt gradient (20 to 200 mM Tris-acetate, pH 7.0, 5.0% [w/v] sucrose, 0.04% [w/v] digitonin, 0.2 mM PMSF, and 2 mM Na-ascorbate). The eluate was collected in 1-mL fractions. For evaluation of the protein complex content of the fractions, 25 μL of each flow-through fraction and 75 μL of each eluate fraction were analyzed by 1D BN-PAGE (see below). Fractions containing pure complex I were concentrated using an ultra filtration cell (Millipore; polyethersulfone filter; exclusion limit, 100,000 kD) to a final protein concentration of ~5 mg/mL.

### Controlled Disassembly of Complex I

For disassembly experiments, purified complex I (1 mg in 200 μL) was treated with low concentrations of SDS (0.01 to 0.12% [w/v]) for 5 min on

ice. Afterwards, 1 μL BN loading buffer (750 mM aminocaproic acid and 5% [w/v] Coomassie Brilliant Blue G 250) was added.

## Gel Electrophoresis Procedures

1D BN-PAGE was used to separate the generated complex I subcomplexes and 2D BN/SDS-PAGE to analyze their subunit composition. Procedures were performed as outlined previously (Wittig et al., 2006). Proteins were either visualized by Coomassie Brilliant Blue colloidal staining (Neuhoff et al., 1988) or in-gel NADH dehydrogenase activity staining (Zerbetto et al., 1997).

## MS

Tryptic digestion of proteins was performed as follows: Protein spots were cut from 2D BN/SDS gels and destained. Gel pieces were dehydrated using acetonitrile. For alkylation of cysteines, gel pieces were first incubated with 20 mM DTT for 30 min at 56°C, dehydrated, and incubated in 55 mM iodoacetamide at room temperature for the same time in the dark. The dehydrated gel pieces were incubated in 0.1 M NH<sub>4</sub>HCO<sub>3</sub>, and digestion was performed at 37°C overnight using trypsin (2 μg/mL resuspension buffer [Promega] in 0.1 M NH<sub>4</sub>HCO<sub>3</sub>). Tryptic peptides were extracted by incubation with acetonitrile for 15 min at 37°C. Supernatants were kept and basic peptides were extracted with 5% formic acid for 15 min at 37°C. The dehydration step was repeated, and the supernatant was pooled with the first one. Extracted peptides were finally dried via vacuum centrifugation and stored at -20°C.

Protein identification by MS was performed as follows: Tryptic peptides were resuspended in 20 μL of washing solution (2% [v/v] methanol and 0.5% [v/v] formic acid) and desalted using ZipTips (0.2 μL C<sub>18</sub>; Millipore). For matrix-assisted laser desorption ionization (MALDI) analyses, 1 μL of Matrix solution (0.1% [w/v] α-Cyano-4-hydroxy-cinnamic acid, 25% [v/v] acetonitrile, and 0.1% [w/v] trifluoroacetic acid) was mixed with 1 μL of desalted peptide solution and spotted on a MALDI target. MALDI-time of flight (TOF)/TOF-MS analyses were performed with an Ultraflex II mass spectrometer (Bruker Daltonics). Offline electrospray ionization (ESI)-quadrupole (Q)-TOF-MS analyses were performed with a Q-TOF 2 mass spectrometer (Waters).

For liquid chromatography-ESI-Q-TOF-MS analyses, tryptic peptides were resuspended in 15 μL 0.1% [v/v] formic acid. The MS analyses were performed with the EASY-nLC System (Proxeon) coupled to a MicroTOF-Q II mass spectrometer (Bruker Daltonics).

Proteins were identified using the MASCOT search algorithm against (1) the *Arabidopsis* protein database ([www.Arabidopsis.org](http://www.Arabidopsis.org); release TAIR 8), (2) a complex I database generated from the complex I subunits identified by Meyer et al. (2008), and (3) the NCBI nonredundant protein database ([www.ncbi.nih.gov](http://www.ncbi.nih.gov)).

## Accession Numbers

All peptides identified in our study match protein sequences deduced from the *Arabidopsis* genome sequence ([www.Arabidopsis.org](http://www.Arabidopsis.org)). The corresponding accession numbers are listed in Table 1 (column 2).

## Supplemental Data

The following materials are available in the online version of this article.

**Supplemental Figure 1.** Subunits Detached from Complex I upon Treatment with Low Concentrations of SDS.

## ACKNOWLEDGMENT

This research was supported by the Deutsche Forschungsgemeinschaft (Grant Br 1829/10-1).

Received December 23, 2009; revised February 12, 2010; accepted February 18, 2010; published March 2, 2010.

## REFERENCES

- Abdrakhmanova, A., Zickermann, V., Bostina, M., Radermacher, M., Schägger, H., Kerscher, S., and Brandt, U. (2004). Subunit composition of mitochondrial complex I from the yeast *Yarrowia lipolytica*. *Biochim. Biophys. Acta* **1658**: 148–156.
- Alber, B.E., and Ferry, J.G. (1994). A carbonic anhydrase from the archaeon *Methanosarcina thermophila*. *Proc. Natl. Acad. Sci. USA* **91**: 6909–6913.
- Allen, K.D., and Staehelin, L.A. (1991). Resolution of 16 to 20 chlorophyll-protein complexes using a low ionic strength native green gel system. *Anal. Biochem.* **194**: 214–222.
- Arizmendi, J.M., Skehel, J.M., Runswick, M.J., Fearnley, I.M., and Walker, J.E. (1992). Complementary DNA sequences of two 14.5 kDa subunits of NADH:ubiquinone oxidoreductase from bovine heart mitochondria. Completion of the primary structure of the complex? *FEBS Lett.* **313**: 80–84.
- Baranova, E.A., Holt, P.J., and Sazanov, L.A. (2007b). Projection structure of the membrane domain of *Escherichia coli* respiratory complex I at 8 Å resolution. *J. Mol. Biol.* **366**: 140–154.
- Baranova, E.A., Morgan, D.J., and Sazanov, L.A. (2007a). Single particle analysis confirms distal location of subunits NuoL and NuoM in *Escherichia coli* complex I. *J. Struct. Biol.* **159**: 238–242.
- Berrisford, J.M., and Sazanov, L.A. (2009). Structural basis for the mechanism of respiratory complex I. *J. Biol. Chem.* (in press).
- Böttcher, B., Scheide, D., Hesterberg, M., Nagel-Steger, L., and Friedrich, T. (2002). A novel, enzymatically active conformation of the *Escherichia coli* NADH:ubiquinone oxidoreductase (complex I). *J. Biol. Chem.* **277**: 17970–17977.
- Brandt, U. (2006). Energy converting NADH:quinone oxidoreductase (complex I). *Annu. Rev. Biochem.* **75**: 69–92.
- Braun, H.P., and Schmitz, U.K. (1992). Affinity purification of cytochrome c reductase from plant mitochondria. *Eur. J. Biochem.* **208**: 761–767.
- Braun, H.P., and Zabaleta, E. (2007). Carbonic anhydrase subunits of the mitochondrial NADH dehydrogenase complex (complex I) in plants. *Physiol. Plant.* **129**: 114–122.
- Bultema, J.B., Braun, H.P., Boekema, E.J., and Kouril, R. (2009). Megacomplex organization of the oxidative phosphorylation system by structural analysis of respiratory supercomplexes from potato. *Biochim. Biophys. Acta* **1787**: 60–67.
- Cardol, P., Vanrobaeys, F., Devreese, B., Van Beeumen, J., Matagne, R.F., and Remacle, C. (2004). Higher plant-like subunit composition of mitochondrial complex I from *Chlamydomonas reinhardtii*: 31 conserved components among eukaryotes. *Biochim. Biophys. Acta* **1658**: 212–224.
- Carroll, J., Fearnley, I.M., Shannon, R.J., Hirst, J., and Walker, J.E. (2003). Analysis of the subunit composition of complex I from bovine heart mitochondria. *Mol. Cell. Proteomics* **2**: 117–126.
- Carroll, J., Fearnley, I.M., Skehel, J.M., Shannon, R.J., Hirst, J., and Walker, J.E. (2006). Bovine complex I is a complex of 45 different subunits. *J. Biol. Chem.* **281**: 32724–32727.
- Clason, T., Ruiz, T., Schägger, H., Peng, G., Zickermann, V., Brandt, U., Michel, H., and Radermacher, M. (2010). The structure of eukaryotic and prokaryotic complex I. *J. Struct. Biol.* **169**: 81–88.
- Clason, T., Zickermann, V., Ruiz, T., Brandt, U., and Radermacher, M. (2007). Direct localization of the 51 and 24 kDa subunits of mitochondrial complex I by three-dimensional difference imaging. *J. Struct. Biol.* **159**: 433–442.
- Combettes, B., and Grienemberger, J.M. (1999). Analysis of wheat mitochondrial complex I purified by a one-step immunoaffinity chromatography. *Biochimie* **81**: 645–653.
- Dudkina, N.V., Eubel, H., Keegstra, W., Boekema, E.J., and Braun, H.P. (2005). Structure of a mitochondrial supercomplex formed by respiratory chain complexes I and III. *Proc. Natl. Acad. Sci. USA* **102**: 3225–3229.
- Dutilleul, C., Garmier, M., Noctor, G., Mathieu, C., Chétrit, P., Foyer, C.H., and De Paepe, R. (2003). Leaf mitochondria modulate whole cell redox homeostasis, set antioxidant capacity, and determine stress resistance through altered signaling and diurnal regulation. *Plant Cell* **15**: 1212–1226.
- Eubel, H., Jansch, L., and Braun, H.P. (2003). New insights into the respiratory chain of plant mitochondria. Supercomplexes and a unique composition of complex II. *Plant Physiol.* **133**: 274–286.
- Finel, M., Skehel, J.M., Albracht, S.P., Fearnley, I.M., and Walker, J.E. (1992). Resolution of NADH:ubiquinone oxidoreductase from bovine heart mitochondria into two subcomplexes, one of which contains the redox centers of the enzyme. *Biochemistry* **31**: 11425–11434.
- Friedrich, T., and Böttcher, B. (2004). The gross structure of the respiratory complex I: A Lego system. *Biochim. Biophys. Acta* **1608**: 1–9.
- Glaser, E., Sjöling, S., Tanudji, M., and Whelan, J. (1998). Mitochondrial protein import in plants. Signals, sorting, targeting, processing and regulation. *Plant Mol. Biol.* **38**: 311–338.
- Grigorieff, N. (1998). Three-dimensional structure of bovine NADH:ubiquinone oxidoreductase (complex I) at 22 Å in ice. *J. Mol. Biol.* **277**: 1033–1046.
- Guénébaut, V., Schlitt, A., Weiss, H., Leonard, K., and Friedrich, T. (1998). Consistent structure between bacterial and mitochondrial NADH:ubiquinone oxidoreductase (complex I). *J. Mol. Biol.* **276**: 105–112.
- Guénébaut, V., Vincentelli, R., Mills, D., Weiss, H., and Leonard, K.R. (1997). Three-dimensional structure of NADH-dehydrogenase from *Neurospora crassa* by electron microscopy and conical tilt reconstruction. *J. Mol. Biol.* **265**: 409–418.
- Heazlewood, J.L., Howell, K.A., and Millar, A.H. (2003). Mitochondrial complex I from *Arabidopsis* and rice: Orthologs of mammalian and fungal components coupled with plant-specific subunits. *Biochim. Biophys. Acta* **1604**: 159–169.
- Herz, U., Schröder, W., Liddell, A., Leaver, C.J., Brennicke, A., and Grohmann, L. (1994). Purification of the NADH:ubiquinone oxidoreductase (complex I) of the respiratory chain from the inner mitochondrial membrane of *Solanum tuberosum*. *J. Biol. Chem.* **269**: 2263–2269.
- Hinchliffe, P., and Sazanov, L.A. (2005). Organization of iron-sulfur clusters in respiratory complex I. *Science* **309**: 771–774.
- Hirst, J., Carroll, J., Fearnley, I.M., Shannon, R.J., and Walker, J.E. (2003). The nuclear encoded subunits of complex I from bovine heart mitochondria. *Biochim. Biophys. Acta* **1604**: 135–150.
- Holt, P.J., Morgan, D.J., and Sazanov, L.A. (2003). The location of NuoL and NuoM subunits in the membrane domain of the *Escherichia coli* complex I: Implications for the mechanism of proton pumping. *J. Biol. Chem.* **278**: 43114–43120.
- Huang, S., Taylor, N.L., Whelan, J., and Millar, A.H. (2009). Refining the definition of plant mitochondrial presequences through analysis of sorting signals, N-terminal modifications, and cleavage motifs. *Plant Physiol.* **150**: 1272–1285.
- Jansch, L., Kruff, V., Schmitz, U.K., and Braun, H.P. (1995). Cytochrome c reductase from potato does not comprise three core proteins but contains an additional low-molecular-mass subunit. *Eur. J. Biochem.* **228**: 878–885.

- Laemmli, U.K.** (1970). Cleavage of structural proteins during the assembly of the head of bacteriophage T4. *Nature* **227**: 680–685.
- Lazarou, M., Thorburn, D.R., Ryan, M.T., and McKenzie, M.** (2009). Assembly of mitochondrial complex I and defects in disease. *Biochim. Biophys. Acta* **1793**: 78–88.
- Leif, H., Sled, V.D., Ohnishi, T., Weiss, H., and Friedrich, T.** (1995). Isolation and characterization of the proton-translocating NADH: ubiquinone oxidoreductase from *Escherichia coli*. *Eur. J. Biochem.* **230**: 538–548.
- Leterme, S., and Boutry, M.** (1993). Purification and preliminary characterization of mitochondrial complex I (NADH: ubiquinone reductase) from broad bean (*Vicia faba* L.). *Plant Physiol.* **102**: 435–443.
- Martin, V., Villarreal, F., Miras, A., Navaza, A., Haouz, A., González-Lebrero, R.M., Kaufman, S.B., and Zabaleta, E.** (2009). Recombinant plant gamma carbonic anhydrase homotrimers bind inorganic carbon. *FEBS Lett.* **583**: 3425–3430.
- May, M.J., and Leaver, C.J.** (1993). Oxidative stimulation of glutathione synthesis in *Arabidopsis thaliana* suspension cultures. *Plant Physiol.* **103**: 621–627.
- Meyer, E.H., Taylor, N.L., and Millar, A.H.** (2008). Resolving and identifying protein components of plant mitochondrial respiratory complexes using three dimensions of gel electrophoresis. *J. Proteome Res.* **2**: 786–794.
- Millar, A.H., Mittova, V., Kiddle, G., Heazlewood, J.L., Bartoli, C.G., Theodoulou, F.L., and Foyer, C.H.** (2003). Control of ascorbate synthesis by respiration and its implications for stress responses. *Plant Physiol.* **133**: 443–447.
- Morgan, D.J., and Sazanov, L.A.** (2008). Three-dimensional structure of respiratory complex I from *Escherichia coli* in ice in the presence of nucleotides. *Biochim. Biophys. Acta* **1777**: 711–718.
- Morgner, N., Zickermann, V., Kerscher, S., Wittig, I., Abdrakhmanova, A., Barth, H.D., Brutschy, B., and Brandt, U.** (2008). Subunit mass fingerprinting of mitochondrial complex I. *Biochim. Biophys. Acta* **1777**: 1384–1391.
- Neuhoff, V., Arold, N., Taube, D., and Ehrhardt, W.** (1988). Improved staining of proteins in polyacrylamide gels including isoelectric focusing gels with clear background at nanogram sensitivity using Coomassie Brilliant Blue G-250 and R-250. *Electrophoresis* **6**: 255–262.
- Peng, G., Fritsch, G., Zickermann, V., Schagger, H., Mentel, R., Lottspeich, F., Bostina, M., Radermacher, M., Huber, R., Stetter, K.O., and Michel, H.** (2003). Isolation, characterization and electron microscopic single particle analysis of the NADH:ubiquinone oxidoreductase (complex I) from the hyperthermophilic eubacterium *Aquifex aeolicus*. *Biochemistry* **42**: 3032–3039.
- Perales, M., Eubel, H., Heinemeyer, J., Colaneri, A., Zabaleta, E., and Braun, H.P.** (2005). Disruption of a nuclear gene encoding a mitochondrial gamma carbonic anhydrase reduces complex I and supercomplex I+III<sub>2</sub> levels and alters mitochondrial physiology in *Arabidopsis*. *J. Mol. Biol.* **350**: 263–277.
- Perales, M., Parisi, G., Fornasari, M.S., Colaneri, A., Villarreal, F., Gonzalez-Schain, N., Echave, J., Gomez-Casati, D., Braun, H.P., Araya, A., and Zabaleta, E.** (2004). Gamma carbonic anhydrase like complex interact with plant mitochondrial complex I. *Plant Mol. Biol.* **56**: 947–995.
- Peters, K., Dukina, N.V., Jansch, L., Braun, H.P., and Boekema, E.J.** (2008). A structural investigation of complex I and I+III<sub>2</sub> supercomplex from *Zea mays* at 11–13 Å resolution: Assignment of the carbonic anhydrase domain and evidence for structural heterogeneity within complex I. *Biochim. Biophys. Acta* **1777**: 84–93.
- Pineau, B., Layoune, O., Danon, A., and De Paepe, R.** (2008). L-galactono-1,4-lactone dehydrogenase is required for the accumulation of plant respiratory complex I. *J. Biol. Chem.* **283**: 32500–32505.
- Radermacher, M., Ruiz, T., Clason, T., Benjamin, S., Brandt, U., and Zickermann, V.** (2006). The three-dimensional structure of complex I from *Yarrowia lipolytica*: A highly dynamic enzyme. *J. Struct. Biol.* **154**: 269–279.
- Rasmusson, A.G., Geisler, D.A., and Möller, I.M.** (2008). The multiplicity of dehydrogenases in the electron transport chain of plant mitochondria. *Mitochondrion* **8**: 47–60.
- Rasmusson, A.G., Mendel-Hartvig, J., Möller, I.M., and Wiskich, J.T.** (1994). Isolation of the rotenone-sensitive NADH-ubiquinone reductase (Complex I) from red beet mitochondria. *Physiol. Plant.* **90**: 607–615.
- Remacle, C., Barbieri, M.R., Cardol, P., and Hamel, P.P.** (2008). Eukaryotic complex I: Functional diversity and experimental systems to unravel the assembly process. *Mol. Genet. Genomics* **280**: 93–110.
- Sazanov, L.A.** (2007). Respiratory complex I: Mechanistic and structural insights provided by the crystal structure of the hydrophilic domain. *Biochemistry* **46**: 2275–2288.
- Sazanov, L.A., and Hinchliffe, P.** (2006). Structure of the hydrophilic domain of respiratory complex I from *Thermus thermophilus*. *Science* **311**: 1430–1436.
- Sazanov, L.A., Peak-Chew, S.Y., Fearnley, I.M., and Walker, J.E.** (2000). Resolution of the membrane domain of bovine complex I into subcomplexes: Implications for the structural organization of the enzyme. *Biochemistry* **39**: 7229–7235.
- Schagger, H., and von Jagow, G.** (1987). Tricine-sodium dodecyl sulfate-polyacrylamide gel electrophoresis for the separation of proteins in the range from 1 to 100 kDa. *Anal. Biochem.* **166**: 368–379.
- Sunderhaus, S., Dudkina, N., Jansch, L., Klodmann, J., Heinemeyer, J., Perales, M., Zabaleta, E., Boekema, E., and Braun, H.P.** (2006). Carbonic anhydrase subunits form a matrix-exposed domain attached to the membrane arm of mitochondrial complex I in plants. *J. Biol. Chem.* **281**: 6482–6488.
- Thorner, J.P.** (1986). Biochemical characterization and structure of pigment-proteins of photosynthetic organisms. In *Encyclopedia of Plant Physiology* 19 (New Series), L.A. Stachelin and J.C.J. Arnetzen, eds (Berlin: Springer Verlag), pp. 95–142.
- Trost, P., Bonora, P., Scagliarini, S., and Pupillo, P.** (1995). Purification and properties of NAD(P)H: (quinone-acceptor) oxidoreductase of sugarbeet cells. *Eur. J. Biochem.* **234**: 452–458.
- Vogel, R.O., Smeitink, J.A., and Nijtmans, L.G.** (2007). Human mitochondrial complex I assembly: A dynamic and versatile process. *Biochim. Biophys. Acta* **1767**: 1215–1227.
- Weiss, H., and Juchs, B.** (1978). Isolation of a multiprotein complex containing cytochrome b and c<sub>1</sub> from *Neurospora crassa* mitochondria by affinity chromatography on immobilized cytochrome c. Difference in the binding between ferricytochrome c and ferrocyanochrome c to the multiprotein complex. *Eur. J. Biochem.* **88**: 17–28.
- Werhahn, W.H., Niemeyer, A., Jansch, L., Kruff, V., Schmitz, U.K., and Braun, H.P.** (2001). Purification and characterization of the preprotein translocase of the outer mitochondrial membrane from *Arabidopsis thaliana*: Identification of multiple forms of TOM20. *Plant Physiol.* **125**: 943–954.
- Wittig, I., Braun, H.P., and Schagger, H.** (2006). Blue-native PAGE. *Nat. Protoc.* **1**: 418–428.
- Zerbetto, E., Vergani, L., and Dabbeni-Sala, F.** (1997). Quantification of muscle mitochondrial oxidative phosphorylation enzymes via histochemical staining of blue native polyacrylamide gels. *Electrophoresis* **18**: 2059–2064.
- Zickermann, V., Dröse, S., Tocilescu, M.A., Zwicker, K., Kerscher, S., and Brandt, U.** (2008). Challenges in elucidating structure and mechanism of proton pumping NADH:ubiquinone oxidoreductase (complex I). *J. Bioenerg. Biomembr.* **40**: 475–483.
- Zickermann, V., Kerscher, S., Zwicker, K., Tocilescu, M.A., Radermacher, M., and Brandt, U.** (2009). Architecture of complex I and its implications for electron transfer and proton pumping. *Biochim. Biophys. Acta* **1787**: 574–583.

**Internal Architecture of Mitochondrial Complex I from *Arabidopsis thaliana***  
Jennifer Klodmann, Stephanie Sunderhaus, Manfred Nimtz, Lothar Jansch and Hans-Peter Braun  
*Plant Cell* 2010;22;797-810; originally published online March 2, 2010;  
DOI 10.1105/tpc.109.073726

This information is current as of June 28, 2012

<b>Supplemental Data</b>	<a href="http://www.plantcell.org/content/suppl/2010/02/23/tpc.109.073726.DC1.html">http://www.plantcell.org/content/suppl/2010/02/23/tpc.109.073726.DC1.html</a>
<b>References</b>	This article cites 66 articles, 18 of which can be accessed free at: <a href="http://www.plantcell.org/content/22/3/797.full.html#ref-list-1">http://www.plantcell.org/content/22/3/797.full.html#ref-list-1</a>
<b>Permissions</b>	<a href="https://www.copyright.com/ccc/openurl.do?sid=pd_hw1532298X&amp;issn=1532298X&amp;WT.mc_id=pd_hw1532298X">https://www.copyright.com/ccc/openurl.do?sid=pd_hw1532298X&amp;issn=1532298X&amp;WT.mc_id=pd_hw1532298X</a>
<b>eTOCs</b>	Sign up for eTOCs at: <a href="http://www.plantcell.org/cgi/alerts/ctmain">http://www.plantcell.org/cgi/alerts/ctmain</a>
<b>CiteTrack Alerts</b>	Sign up for CiteTrack Alerts at: <a href="http://www.plantcell.org/cgi/alerts/ctmain">http://www.plantcell.org/cgi/alerts/ctmain</a>
<b>Subscription Information</b>	Subscription Information for <i>The Plant Cell</i> and <i>Plant Physiology</i> is available at: <a href="http://www.aspb.org/publications/subscriptions.cfm">http://www.aspb.org/publications/subscriptions.cfm</a>





Contents lists available at ScienceDirect

## Phytochemistry

journal homepage: [www.elsevier.com/locate/phytochem](http://www.elsevier.com/locate/phytochem)

## Proteomic approach to characterize mitochondrial complex I from plants

Jennifer Klodmann\*, Hans-Peter Braun\*

Institute for Plant Genetics, Faculty of Natural Sciences, Leibniz Universität Hannover, Herrenhäuser Str. 2, D-30419 Hannover, Germany

## ARTICLE INFO

Article history:  
Available online 15 December 2010

Keywords:  
NADH dehydrogenase  
Complex I  
Respiratory chain  
Mitochondria  
Carbonic anhydrase  
*Arabidopsis thaliana*

## ABSTRACT

Mitochondrial NADH dehydrogenase complex (complex I) is by far the largest protein complex of the respiratory chain. It is best characterized for bovine mitochondria and known to consist of 45 different subunits in this species. Proteomic analyses recently allowed for the first time to systematically explore complex I from plants. The enzyme is especially large and includes numerous extra subunits. Upon subunit separation by various gel electrophoresis procedures and protein identifications by mass spectrometry, overall 47 distinct types of proteins were found to form part of *Arabidopsis* complex I. An additional subunit, ND4L, is present but could not be detected by the procedures employed due to its extreme biochemical properties. Seven of the 48 subunits occur in pairs of isoforms, six of which were experimentally proven. Fifteen subunits of complex I from *Arabidopsis* are specific for plants. Some of these resemble enzymes of known functions, e.g. carbonic anhydrases and L-galactono-1,4-lactone dehydrogenase (GLDH), which catalyzes the last step of ascorbate biosynthesis. This article aims to review proteomic data on the protein composition of complex I in plants. Furthermore, a proteomic re-evaluation on its protein constituents is presented.

© 2010 Elsevier Ltd. All rights reserved.

## 1. Introduction

In mitochondria, ATP formation is coupled to oxygen consumption. Prerequisite for this process is the so-called oxidative phosphorylation (OXPHOS) system, which consists of five multi-protein complexes (termed complexes I–V), cytochrome *c* and the lipid ubiquinone (Hatefi, 1985). The complexes I–IV form part of an electron transfer chain (also called the respiratory chain), which catalyzes NADH oxidation by reduction of oxygen to water. Complex V catalyzes phosphorylation of ADP. This endergonic reaction is driven by a proton gradient across the inner mitochondrial membrane which is generated by the exergonic electron transfer reactions of the respiratory chain.

## 1.1. Size and function of complex I

With an approximate mass of 1000 kDa, complex I (NADH:ubiquinone oxidoreductase, EC 1.6.5.3) is the largest protein complex of the mitochondrial OXPHOS system. Its major function is the transfer of two electrons from NADH (matrix side) to ubiquinone (inner mitochondrial membrane). Coupled to this reaction four protons are translocated from the mitochondrial matrix into the intermembrane space (reviewed in Brandt, 2006; Friedrich and Böttcher, 2004; Lazarou et al., 2009; Remacle et al., 2008; Vogel

et al., 2007; Zickermann et al., 2008, 2009). Complex I was first purified from bovine heart mitochondria about 50 years ago by Hatefi et al. (1962). Since then, it has been studied in different eukaryotes including mammals (*bos taurus* (Carroll et al., 2003; Hirst et al., 2003), *homo sapiens* (Murray et al., 2003)), fungi (*Neurospora crassa* (Marques et al., 2005), *Yarrowia lipolytica* (Abdrakhmanova et al., 2004), and *Pichia Pastoris* (Bridges et al., 2010)), the green algae *Chlamydomonas reinhardtii* (Cardol et al., 2004) and in higher plants (Heazlewood et al., 2003; Klodmann et al., 2010; Meyer et al., 2008; Sunderhaus et al., 2006). In bacteria, a more simple form of complex I is present in the cytoplasmic membrane (Weidner et al., 1993) designated NADH dehydrogenase-1 (NDH-1). It only has half of the size of the eukaryotic complex I (550 kDa) (Yagi et al., 1998) and often is considered to represent a “minimal model” of complex I because it contains all subunits necessary to perform its major functions. The NDH-1 complex has been extensively studied in *Escherichia coli* and *Thermus thermophilus* resulting in the recent elucidation of its structure by X-ray crystallography (Berrisford and Sazanov, 2009; Efremov et al., 2010; Hinchliffe and Sazanov, 2005; Sazanov and Hinchliffe, 2006; Sazanov, 2007). Currently available information on complex I in various species is summarized on “Complex I home page” (<http://www.scripps.edu/mem/ci/>).

## 1.2. Shape of complex I

Complex I has an L-like shape with a peripheral arm protruding into the mitochondrial matrix and a membrane arm embedded in

\* Corresponding authors. Tel.: +49 511 7622674; fax: +49 511 7623608.

E-mail addresses: [klodmann@genetik.uni-hannover.de](mailto:klodmann@genetik.uni-hannover.de) (J. Klodmann), [braun@genetik.uni-hannover.de](mailto:braun@genetik.uni-hannover.de) (H.-P. Braun).



the inner membrane (Fig. 1). Each arm consists of at least seven “core subunits” also found in the bacterial enzyme. For a long time, crystallization of the complex did not succeed due to its size and hydrophobicity. Instead, analyses by electron microscopy allowed elucidating its overall structure (Böttcher et al., 2002; Clason et al., 2010; Dudkina et al., 2005; Grigorieff 1998; Guénebaut et al., 1997, 1998; Morgan and Sazanov, 2008; Peng et al., 2003; Radermacher et al., 2006). Insights into the internal subunit arrangement within complex I were obtained by controlled destabilization of the purified enzyme using chaotropes or different detergents and the subsequent characterization of the generated subcomplexes. Based on these experiments, first topological models have been presented (Brandt, 2006 and references within, Lazarou et al., 2009; Radermacher et al., 2006; Zickermann et al., 2008, 2009).

### 1.3. Subunit composition of complex I

Besides the 14 core subunits, eukaryotic complex I contains about 30 extra subunits, several of which are conserved in different groups of species. Overall, 18 of these subunits of the especially well characterized bovine complex (Carroll et al., 2002, 2003, 2006; Hirst et al., 2003) likewise are present in most other eukaryotic model systems like *N. crassa*, *Y. lipolytica*, *C. reinhardtii*, and *A. thaliana* (Cardol et al., 2004; Gawryluk and Gray, 2010; Morgner et al., 2008). The function of the eukaryotic extra subunits is largely unclear so far. Some of them were suggested to be important for assembly of the mitochondrial enzyme, which has to be built up by proteins encoded by two different genomes localized in the nucleus and the mitochondria (Brandt, 2006). Other subunits exhibit structural similarity to proteins of known function, e.g. the apoptosis factor GRIM19 (bovine complex I subunit B16.6 (Lazarou et al., 2009; Remacle et al., 2008) and subunit NDUFA13 in human complex I (Fearnley et al., 2001; Lu and Cao, 2008; Murray et al., 2003; Zhang et al., 2003)) and the mitochondrial preprotein translocase protein TIM17/22 (bovine complex I subunit B14.7). The remaining 10–15 extra subunits seem to be specific for subdomains of the eukaryotic kingdom. Only for some of them a biological function was proposed: complex I of mammals and fungi includes an acyl

carrier protein which indeed was shown to be involved in mitochondrial fatty acid biosynthesis (Carroll et al., 2003; Sackmann et al., 1991; Zensen et al., 1992). Furthermore, an extra subunit in fungi resembles rhodanese which are involved in FeS cluster biosynthesis (Cipollone et al., 2007; Mueller, 2006). Finally, complex I of plant mitochondria includes additional subunits as discussed below.

Different nomenclatures are used for complex I subunits in different organisms. In this review, we use the bovine names (Carroll et al., 2003, 2006; Hirst et al., 2003). For plant specific subunits, names are taken from the literature or represent accession numbers of the corresponding *Arabidopsis* genes taken from the TAIR database ([www.arabidopsis.org](http://www.arabidopsis.org)).

### 1.4. The two complex I arms

The structure of the peripheral arm of bacterial complex I has been analyzed by X-ray crystallography. In *E. coli*, it consists of seven subunits which are also present in all eukaryotic complexes analyzed so far, namely the 75, 51, 49, 30, 24 kDa, PSST, and TYKY subunits. In *Thermus thermophilus* an additional frataxin-like subunit occurs (Nqo15) which is specific for this organism and its closest relatives (Hinchliffe et al., 2006). These “core” subunits of the peripheral arm comprise all redox prosthetic groups for electron transfer from NADH to ubiquinone: a flavin mononucleotide (FMN) and eight to nine iron–sulfur (FeS) clusters (Berrisford and Sazanov, 2009; Ohnishi, 1998; Hinchliffe and Sazanov, 2005; Hinchliffe et al., 2006; Sazanov and Hinchliffe, 2006; Sazanov, 2007; Yagi and Matsuno-Yagi, 2003).

Until recently, structural characterization of the hydrophobic membrane arm of complex I was entirely based on electron and immune-electron microscopy analyses (Abdrakhmanova et al., 2004; Baranova et al., 2007a,b; Clason et al., 2007). Like the peripheral arm, the membrane arm of bacterial complex I contains seven subunits termed ND1, ND2, ND3, ND4, ND4L, ND5 and ND6. They are extremely hydrophobic and in eukaryotes are encoded by the mitochondrial genome. Three subunits of the membrane arm (ND2, ND4 and ND5) show homology to a special type of Na<sup>+</sup>/H<sup>+</sup> antiporters (Fearnley and Walker, 1992; Mathiesen and Hägerhäll,

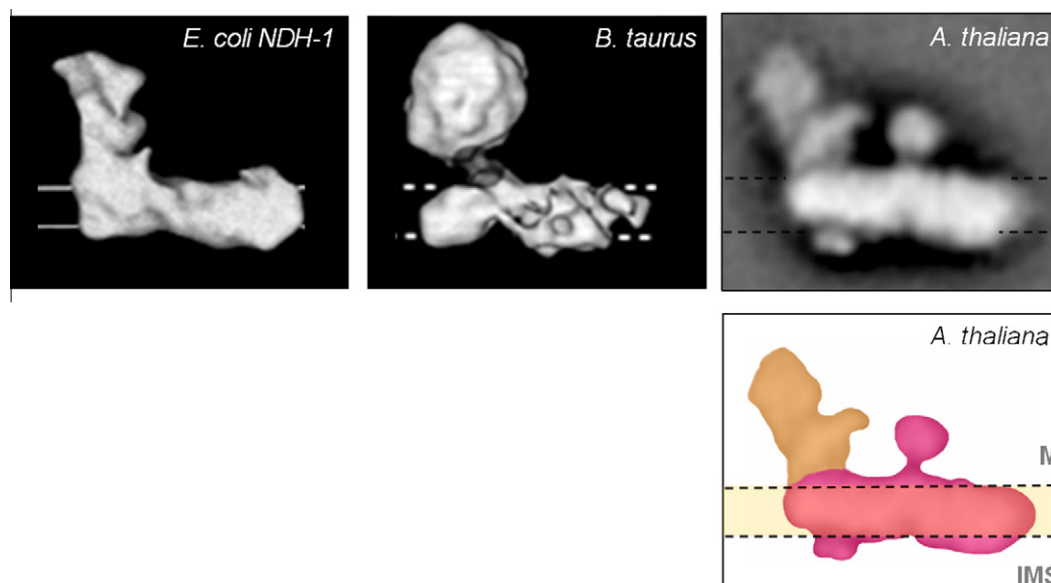


**Fig. 1.** Structure of complex I from *E. coli*, *B. taurus* and *A. thaliana* as revealed by single particle electron microscopy. A model of plant complex I from *A. thaliana* is given to the right. The position of the inner mitochondrial membrane is indicated in yellow. M: matrix; IMS: inter membrane space. Images were taken from Guénebaut et al. (1998) (*E. coli*), Grigorieff (1998) (*B. taurus*), and Sunderhaus et al. (2006) (*A. thaliana*), with permission.



2002) and therefore are supposed to be involved in proton translocation. The arrangement of the hydrophobic subunits was very recently revealed at higher resolution by X-ray crystallography (Efremov et al., 2010). ND5 is arranged at the distal end of the membrane arm. The second subunit (counted from the distal end to the connection with the peripheral arm) is ND4, followed by ND2. Subunits ND3, ND4L and ND6 are located next to the peripheral arm. In the crystal structure of the membrane arm of *E. coli* subunit ND1 was missing. This implies a more external position of ND1, for instance close to the point of attachment of the two complex I arms. The crystal structure of the complex I membrane arm from *T. thermophilus* confirms this conclusion.

### 1.5. Functional modules of complex I

The complex I core enzyme as found in bacteria is evolutionary related to different kinds of hydrogenases. Hydrogenase modules within complex I nicely correspond to functional modules of the enzyme complex. Three modules are defined: the NADH oxidizing module (N-module), the quinone reducing module (Q-module), and the proton translocating module (P-module) (reviewed in Brandt, 2006; Friedrich and Scheide, 2000). The N- and Q-modules form part of the peripheral arm; the P-module represents the membrane arm.

Within the N-module, the 75, 51 and 24 kDa subunits are in close proximity. They all are related to the subunits of bacterial NAD<sup>+</sup> reducing hydrogenases. The 51 kDa subunit comprises the FMN as well as the NADH binding site and therefore, is the entrance site for electrons into the complex. It also contains a FeS-cluster (N3) which is likely to constitute the starting point for electron transfer through the complex. The 24 kDa subunit contains the FeS-cluster N1a which seems not to be involved in electron channeling due to its distance to the other clusters. A role in two-to-one electron conversion at the FMN has been proposed (Brandt, 2006). The 75 kDa subunit coordinates three FeS clusters (N1b, N5 and N4) involved in electron transfer from the 51 kDa subunits to the Q-module.

The Q-module comprises four core subunits, 49, 30 kDa, TYKY and PSST, which are homologous to the subunits of bacterial NiFe hydrogenases. Within the TYKY subunit, the FeS clusters N6a and N6b transfer electrons from the 75 kDa subunit of the N module to the final FeS-cluster N2 which is attached to the PSST subunit. The mechanism of ubiquinone reduction is currently not completely understood. A ubiquinone binding pocket has been predicted next to cluster N2 between the PSST and 49 kDa subunits (reviewed in Tocilescu et al., in press) but it is distant to the membrane and therefore, difficult to access for the lipid ubiquinone. The presence of a so-called “hydrophobic ramp” through the complex has been suggested as well as docking of ubiquinone on the basis of conformational changes in the complex which transfer the binding pocket close to the membrane (reviewed in Zickermann et al., 2008).

The P-module is represented by the membrane arm and its seven central subunits ND1, ND2, ND3, ND4, ND4L, ND5 and ND6. Subunits ND1, ND2, ND4 and ND5 show homology to NiFe Hydrogenases from *E. coli*. ND2, ND4 and ND5 are homologous to each other and evolutionary related to Na<sup>+</sup>/H<sup>+</sup> antiporters (Fearnley and Walker, 1992; Mathiesen and Hägerhäll, 2002). They are considered to be involved in proton translocation.

### 1.6. Coupling of oxido-reduction and proton translocation

X-ray structure analysis of the bacterial membrane arm (Efremov et al., 2010) gave new insights into the interaction of cluster N2 and ubiquinone. Subunit ND1 seems to bind the isoprenoid tail of ubiquinone at its interface with a subunit bundle formed by the

ND3, ND4L and ND6 subunits. Based on this proposed interaction, the transfer distance for the ubiquinone head group from the membrane to the location of the N2 cluster is about 10 Å. This would imply that the hydrophobic tail of ubiquinone remains mainly within the membrane during the binding process (Efremov et al., 2010).

NADH-ubiquinone oxidoreduction and proton translocation from the mitochondrial matrix to the intermembrane space are coupled within complex I. A direct redox-driven coupling as well as an indirect mechanism due to conformational changes have been extensively discussed (reviewed in Zickermann et al., 2009). Recent evidence for conformational coupling is supported by the crystal structures of the membrane arm. Most strikingly, the membrane arm includes a 110 Å amphiphilic helix which horizontally spans the entire domain. Discontinuous membrane-spanning helices of the antiporter-like ND2, ND4 and ND5 subunits directly interact with this horizontal helix. Lateral movement of the horizontal helix, which represents an N-terminal extension of ND5 with respect to the homologous ND2 and ND4 subunits, is supposed to simultaneously open and close proton translocating pores within the three putative antiporters (Efremov et al., 2010). The horizontal amphiphilic helix also was found in the crystal structure of the holo-complex from *Y. lipolytica*. It is shorter but also postulated to form the basis for a conformational coupling mechanism (Hunte et al., 2010).

## 2. Complex I in plants

The OXPHOS system in plants is more complex than in mammals because it includes an additional so-called alternative oxidase (AOX) and several distinct alternative NADH or NADPH dehydrogenases (for review see Rasmusson et al., 2008). These extra components directly interact with the ubiquinone pool and, as a consequence, respiratory electron transfer in plants is branched and very flexible. Furthermore, the “classical” OXPHOS complexes also have special features in plants with the presence of additional subunits which can introduce extra activities into the respiratory enzyme complexes. For instance, complex III of the respiratory chain includes both subunits of the mitochondrial processing peptidase (MPP) in plants (Braun et al., 1992). Complex I has been biochemically characterized for several different plant species (Combettes and Grienberger, 1999; Herz et al., 1994; Jansch et al., 1996; Leterme and Boutry, 1993; Rasmusson et al., 1994; Trost et al., 1995). Electron microscopic (EM) studies recently revealed a very special shape of *Arabidopsis* complex I because it includes a second matrix-exposed domain which is attached to the membrane arm at a central position (Dudkina et al., 2005). This domain is absent in the bacterial, fungal or mammalian complex (Fig. 1). The extra domain, which has a spherical shape, likely presents a general feature of plant complex I because it was described for all other complex I particles characterized by EM so far, e.g. in maize, potato and the alga *Polytomella* (Bultema et al., 2009; Peters et al., 2008; Sunderhaus et al., 2006). Biochemical investigations revealed that it includes carbonic anhydrase-like subunits which are unique to plant complex I (Sunderhaus et al., 2006). Several further plant-specific complex I subunits have been described and will be discussed below.

### 2.1. Proteomic investigations to characterize complex I subunits in plants

For about 20 years, subunit composition of plant complex I was systematically investigated to understand its special features. Initially, plant complex I was prepared by column chromatography and N-terminal sequences of subunits were determined by cyclic

Edman degradation to characterize its subunits (Herz et al., 1994; Leterme and Boutry, 1993). Based on this strategy, partial sequences for up to 17 distinct subunits were obtained. In parallel, the mitochondrial genomes of several plants were characterized. Interestingly, the 49 and 30 kDa subunits of the peripheral arm of complex I are encoded on the mitochondrial genome in plants. These subunits are therefore named ND7 and ND9 in plants. In consequence, the mitochondrial genome of *Arabidopsis* and other plants encodes nine complex I subunits termed ND1, ND2, ND3, ND4, ND4L, ND5, ND6, ND7 and ND9 (Unsel et al., 1997).

Broad-range characterization of complex I subunits was much facilitated by the introduction of mass spectrometry in protein analysis. The first proteomic investigation on complex I subunits in plants was carried out by Heazlewood and colleagues (Heazlewood et al., 2003): Mitochondrial proteins from *Arabidopsis* and rice were separated by two dimensional blue native/SDS polyacrylamide gel electrophoresis (2D BN/SDS–PAGE) and complex I subunits were systematically identified by quadrupole time-of-flight mass spectrometry (Q-ToF MS). For *Arabidopsis*, two forms of complex I were visible on the gels, one running at about 1000 kDa and the other slightly below. The smaller version of complex I includes an additional 60 kDa protein and probably lacks some other subunits. Overall, 22 protein spots could be resolved on the second gel dimension, which contain 29 distinct proteins. Among these, four represent mitochondrial encoded subunits (ND1, ND5, ND7 and ND9) and 17 are orthologs of known nuclear encoded subunits of complex I from other groups of organisms. Interestingly, the 9 remaining proteins are specific for plants. The study was complemented by systematic database searches for further complex I subunits in *Arabidopsis* using the protein sequences of human complex I. Besides the 6 missing mitochondrial-encoded subunits, which are difficult to detect by mass spectrometry due to their hydrophobicity, some further nuclear-encoded complex I subunits could be predicted for *Arabidopsis*.

Five of the 9 plant specific complex I subunits described in Heazlewood et al. (2003) resemble known enzymes which are not related to complex I in other groups of organisms. Four subunits in the 30 kDa range are similar to archaeobacterial  $\gamma$ -type carbonic anhydrases and later were shown to form part of the second matrix exposed domain of plant complex I (Sunderhaus et al., 2006) (based on a falsely annotated database entry, these subunits originally were designated “ferripyochelin-binding proteins” in Heazlewood et al., 2003). Furthermore, the 60 kDa protein forming part of the slightly smaller version of *Arabidopsis* complex I represents L-galactono-1,4-lactone dehydrogenase (GLDH). This enzyme catalyzes the final step of ascorbate biosynthesis. The remaining 4 plant specific subunits, which all have a low molecular mass (9–13 kDa), do not resemble known proteins of any organism investigated so far.

In a similar approach, subunits of complex I from *Chlamydomonas reinhardtii* were systematically characterized (Cardol et al., 2004). Interestingly, most of the plant specific subunits found in *Arabidopsis* also are present in *Chlamydomonas* complex I, e.g. four  $\gamma$ -type carbonic anhydrase proteins. This underlines a high degree of homology between complex I from green algae and higher plants.

Based on a direct MS analysis of the entire membrane arm of complex I from *Arabidopsis*, 19 subunits were identified at once, 5 of which were described for the first time: the B12 and B22 subunits (At1g14450 and At4g34700), a fifth subunit resembling archaeobacterial  $\gamma$ -type carbonic anhydrases (At1g19580), and two further plant specific subunits of low molecular mass (At4g00585 and At1g67350) (Sunderhaus et al., 2006). The number of plant specific complex I subunits thereby increased to 12.

An extended proteomic investigation on complex I subunits in *Arabidopsis* was presented by Meyer et al. (2008). For the first time, a three-dimensional electrophoretic system was employed to char-

acterize plant complex I, which is based on blue native/SDS/SDS–PAGE. Using this experimental system, *Arabidopsis* complex I is resolved into 37 spots. Systematic MS analysis allowed identifying 42 different complex I subunits, including 7 of the 9 mitochondrial encoded subunits and 33 nuclear encoded subunits. Two newly identified subunits of low molecular mass (At1g68680 and At1g67785) increased the overall number of plant specific complex I proteins to 14.

Most recently, the internal subunit arrangement of plant complex I was investigated by its defined dissection into subcomplexes using low concentrations of SDS (Klodmann et al., 2010). Subunits of 10 distinct subcomplexes were resolved by 2D blue native/SDS–PAGE and systematically identified by mass spectrometry. The set of 40 identified subunits included 3 new subunits not identified in complex I from plants before: the 13 kDa subunit (At3g03070), ND3 (AtMg00990), and the plant specific subunit At1g14105). At the same time, eight subunits described by previous studies (Sunderhaus et al., 2006; Meyer et al., 2008) were not found. Since subunit identifications were entirely based on the characterization of complex I subcomplexes, the missing subunits were interpreted to be detached from complex I as monomers during SDS-mediated destabilization. Indeed, 6 protein spots of the holo-complex were shown not to form part of any of the 10 subcomplexes (Klodmann et al., 2010, supplementary material), but were not identified by MS.

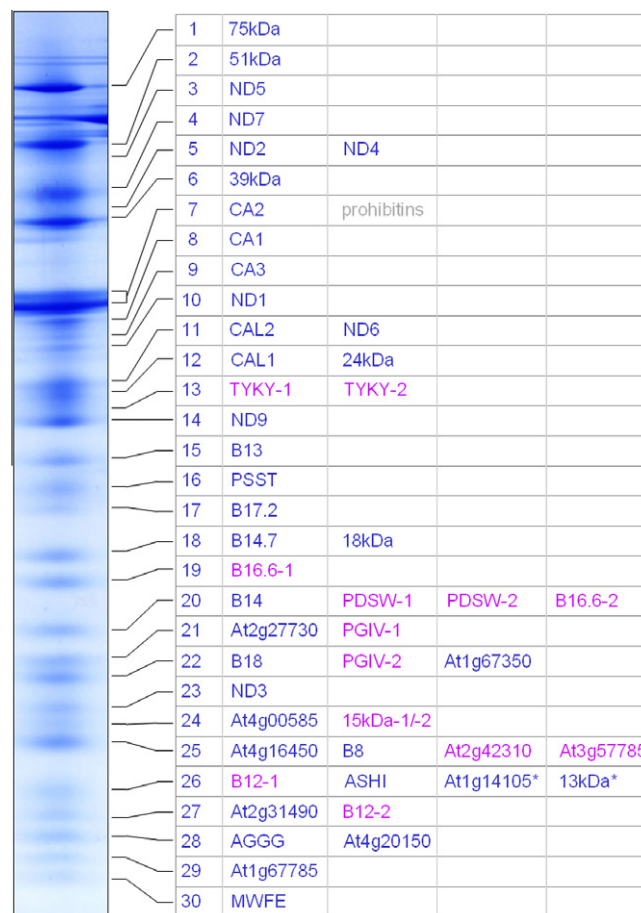


**Fig. 2.** Subunits of plant complex I. *Arabidopsis* complex I was separated by 2D blue native/SDS–PAGE. Protein spots were cut out, digested with trypsin and analyzed by mass spectrometry (Table 1). Identities of complex I subunits are given to the right of the gel. Subunits occurring as pairs of isoforms are given in purple. Spot 7 additionally includes prohibition proteins (given in gray), which are known to form part of a separate prohibition complex co-migrating with complex I on the blue native gel dimension.

**Table 1**Subunits of *Arabidopsis* complex I. Complex I subunits identified by mass spectrometry (this study).

Spot <sup>a</sup>	Identity in <i>Arabidopsis</i>		Homologs in			Mass [kDa] <sup>d</sup>	GRAVY <sup>e</sup>	Score <sup>f</sup>	No MP <sup>g</sup>	Coverage [%] <sup>h</sup>
	Accession Nos. <sup>b</sup>	Name <sup>c</sup>	<i>E. coli</i>	<i>B. taurus</i>	<i>Y. lipolytica</i>					
1	At5g37510	75 kDa	NUOG	75 kDa	NUAM	81.18	−0.150	2083	33	43
2	At5g08530	51 kDa	NUOF	51 kDa	NUBM	53.35	−0.303	1166	21	34
3	AtMg00060/ AtMg00513/ AtMg00665	ND5	NUOL	ND5	NU5M	73.91	0.585	105	2	3
4	AtMg00510	ND7	NUOD	49 kDa	NUCM	44.58	−0.408	577	9	21
5	AtMg00285/ AtMg01320	ND2	NUON	ND2	NU2M	54.88	0.727	116	2	4
5	AtMg00580	ND4	NUOM	ND4	NU4M	55.23	0.687	46	1	2
6	At2g20360	39 kDa	–	39 kDa	NUEM	43.94	−0.059	1050	18	40
7	At1g47260 ■	CA2	–	–	–	30.07	−0.157	1086	17	65
8	At1g19580 ■	CA1	–	–	–	29.97	−0.223	402	9	41
9	At5g66510 ■	CA3	–	–	–	27.84	−0.293	356	7	24
10	AtMg00516/ AtMg01120/ AtMg01275	ND1	NUOH	ND1	NU1M	35.68	0.773	74	2	10
11	At3g48680 ■	CAL2	–	–	–	27.96	0.041	707	11	41
11	AtMg00270	ND6	NUOJ	ND6	NU6M	23.50	0.677	37	1	6
12	At5g63510 ■	CAL1	–	–	–	27.57	0.060	612	11	48
12	At4g02580	24 kDa	NUOE	24 kDa	NUHM	28.39	−0.360	377	7	22
13	At1g79010	TYKY-1	NUOI	TYKY	NUKM	25.49	−0.559	488	11	37
13	At1g16700	TYKY-2	NUOI	TYKY	NUKM	25.36	−0.559	463	11	37
14	AtMg00070	ND9	NUOC	30 kDa	NUGM	22.69	−0.676	531	9	38
15	At5g52840	B13	–	B13	NUFM	19.17	−0.478	539	10	57
16	At5g11770	PSST	NUOB	PSST	NUKM	24.04	−0.123	537	9	39
17	At3g03100	B17.2	–	B17.2	N7BM	18.32	−0.775	482	10	47
18	At2g42210	B14.7	–	B14.7	NUJM	17.00	−0.050	329	8	28
18	At1g04630	B16.6-1	–	B16.6	NB6M	16.13	−0.487	67	1	7
18	At5g67590	18 kDa	–	18 kDa	NUYM	17.14	−0.607	260	6	39
19	At2g33220	B16.6-2	–	B16.6	NB6M	16.12	−0.472	598	10	62
20	At3g12260	B14	–	B14	NB4M	15.08	−0.238	319	6	38
20	At3g18410	PDSW-1	–	PDSW	NIDM	12.44	−0.956	276	7	40
20	At1g49140	PDSW-2	–	PDSW	NIDM	12.52	−0.88	195	5	37
21	At2g27730 ■	At2g27730	–	–	–	11.95	−0.467	576	6	41
21	At3g06310	PGIV-1	–	PGIV	NUPM	12.16	−0.456	30	1	9
22	At1g67350 ■	At1g67350	–	–	–	11.78	0.615	483	8	76
22	At2g02050	B18	–	B18	NB8M	11.74	−0.428	329	7	64
22	At5g18800	PGIV-2	–	PGIV	NUPM	12.00	−0.492	51	1	9
23	AtMg00990	ND3	NuoA	ND3	NU3M	13.66	0.590	96	2	18
24	At4g00585 ■	At4g00585	–	–	–	9.86	−0.592	165	2	32
24	At3g62790/ At2g47690	15 kDa-1/ 15 kDa-2	–	15 kDa	–	9.89/ 9.88	−1.249/ −1.253	159	2	15
25	At4g16450	At4g16450	–	–	NUXM	11.35	0.024	552	6	71
25	At5g47890	B8	–	B8	NI8M	10.85	−0.289	359	6	61
25	At2g42310 ■	At2g42310/ At3g57785-1 At2g42310/ At3g57785-2	–	–	–	12.63	−0.539	221	4	33
25	At3g57785 ■	At3g57785	–	–	–	12.66	−0.521	109	3	25
26	At1g14450	B12-1	–	B12	NB2M	8.30	−0.578	44	1	12
26	At5g47570	ASHI	–	ASHI	NIAM	13.21	0.061	172	4	26
26	At5g14105 ■	At5g14105	–	–	–	8.44	−0.247	36	1	17
26	At3g03070	13 kDa	–	13 kDa	NUMM	12.23	−0.246	268	4	43
27	At2g31490 ■	At2g31490	–	–	–	8.29	−0.500	116	2	24
27	At2g02510	B12-2	–	B12	NB2M	8.05	−0.503	136	3	42
28	At1g76200	AGGG	–	AGGG	–	7.57	−0.536	145	3	55
28	At4g20150 ■	At4g20150	–	–	–	9.21	−0.200	167	3	30
29	At1g67785 ■	At1g67785	–	–	–	7.53	−0.417	149	4	43
30	At3g08610	MWFE	–	MWFE	NIMM	7.34	−0.189	98	2	22
Further <i>Arabidopsis</i> complex I subunits identified by previous mass spectrometry studies <sup>i</sup>										
–	At3g47930 ■	GLDH	–	–	–	68.56	−0.479	91	11	30
–	At4g34700	B22	–	B22	NI2M	13.62	−0.726	73	3	27
–	At1g68680 ■	At1g68680	–	–	–	8.34	0.176	63	4	26
Further complex I subunit so far not identified by mass spectrometry										
–	AtMg00650	ND4L	ND4L	ND4L	NULM	10.91	−0.976	–	–	–

■ Subunit specific for complex I of plants.

<sup>a</sup> Spot number in accordance with Fig. 2. Several spots include more than one complex I subunit.<sup>b</sup> Accession numbers as given by TAIR (<http://www.arabidopsis.org/>). Six subunits are present in isoforms (TYKY-1 and TYKY-2, B16.6-1 and B16.6-2, PDSW-1 and PDSW-2, PGIV-1 and PGIV-2, At2g42310 and At3g57785, B12-1 and B12-2). Additionally, isoforms are predicted for the 15 kDa subunit (15 kDa-1 and 15 kDa-2) because it is encoded by two different nuclear genes. However, the only peptide identified for this subunit is identical for both isoforms. For details on isoforms see Table 2. Furthermore, some of the mitochondrial encoded subunits are encoded by more than one gene. However, the corresponding protein sequences are identical.<sup>c</sup> Subunits of complex I from *Arabidopsis* are named according to the bovine nomenclature. Subunits specific to complex I of plant mitochondria are named according to the corresponding genes annotated by TAIR ([www.arabidopsis.org](http://www.arabidopsis.org/)). Exceptions: (i) the plant specific carbonic anhydrase subunits are named CA1, CA2, CA3, CAL1 and CAL2 in



**Table 1** (continued)

accordance with the literature, (ii) *Arabidopsis* homologues to the 30 and 49 kDa subunits of bovine complex I are designated ND9 and ND7, because the corresponding proteins are encoded by the mitochondrial genome in plants, (iii) the L-galactono-1,4-lactone dehydrogenase subunit is named GLDH.

<sup>d</sup> Calculated molecular mass of the identified protein as deduced from the corresponding gene. Note that in some cases mitochondrial targeting peptides (~2–5 kDa) are removed from the proteins after import into mitochondria.

<sup>e</sup> GRAVY (grand average of hydropathy) score of the protein.

<sup>f</sup> Probability score for the protein identification based on mass spectrometry analysis and MASCOT search.

<sup>g</sup> Number of matching peptides.

<sup>h</sup> Sequence coverage of a protein by identified peptides.

<sup>i</sup> MS data taken from Klodmann et al. (2010), Meyer et al. (2008), and Sunderhaus et al. (2006).

Proteomic investigations also were employed to analyze the mechanism of protein transport into mitochondria. Using a mass spectrometry based approach, four nuclear encoded complex I subunits were shown to have cleavable mitochondrial targeting sequences in *Arabidopsis*: the carbonic anhydrase like subunits CAL1 and CAL2, the 18 kDa subunit and the PSST subunit (Huang et al., 2009). Interestingly, other nuclear encoded mitochondrial complex I subunits are imported into the organelle without a cleavable pre-sequence, e.g. the B14 subunit and the carbonic anhydrase subunits CA1, CA2 and CA3 (Huang et al., 2009; Klodmann et al., 2010). For the remaining complex I subunits of *Arabidopsis*, presence or absence of targeting sequences so far is not known. Furthermore, proteomic investigations were used to systematically search for phosphorylation of mitochondrial proteins (Ito et al., 2009). So far, phosphorylation of any complex I subunit has not been proven in *Arabidopsis*.

## 2.2. Proteomic re-investigation of complex I subunits in *Arabidopsis*

To further define plant complex I and identify all its components, the subunit composition of complex I from *Arabidopsis* was carefully re-investigated based on high-resolution blue native/SDS-PAGE in combination with Q-ToF mass spectrometry (Fig. 2, Table 1). Complex I was resolved into 30 spots. Fifty distinct proteins were identified by MS, including 8 of the 9 mitochondrial encoded subunits and 42 nuclear encoded subunits. This is the largest set of plant complex I proteins so-far experimentally identified by a single proteomic study. Twelve of the identified proteins represent pairs of isoforms, reducing the total number of distinct types of detected plant complex I subunits to 44. Only three previously identified *Arabidopsis* complex I subunits were not found: GLDH, which was absent because we did not analyze the smaller version of complex I, the B22 subunit found in Sunderhaus et al. (2006) and the At1g68680 subunit described in Meyer et al. (2008). Together with the mitochondrial encoded ND4L subunit, which is small and extremely hydrophobic (predicted GRAVY score of 0.976) and which never has been detected by any proteomic investigation in plants but certainly forms part of complex I, the total number of distinct types of subunits is 48 in *Arabidopsis*. For bovine complex I, 45 subunits have been reported (Carroll et al., 2006) and complex I of the non-fermenting yeast *Yarrowia lipolytica* has been shown to contain 40 subunits (Morgner et al., 2008). Therefore, complex I of plants includes the highest number of distinct components. Indeed, potato complex I has been shown to have a slightly larger molecular mass than the bovine complex by direct comparison using one-dimensional blue native PAGE (Jansch et al., 1995).

Altogether, 15 complex I subunits are unique to plants (Table 1). Seventeen plant specific subunits were reported in Klodmann et al. (2010) but one subunit designated unique to plants in Sunderhaus et al. (2006) (At1g14450) was in fact identified as an ortholog of the bovine B12 subunit and has to be subtracted and another subunit (At4g16450) turned out to be homologous to the 20.9 kDa complex I subunit of *Neurospora crassa* and *Yarrowia lipolytica*. Five of the 15 special subunits represent proteins resembling  $\gamma$ -type carbonic anhydrases, one represents GLDH and all the remaining 9 subunits are rather small (7–12 kDa) and of so far unknown func-

tion. Complementary, 13 bovine complex I subunits do not have counterparts in *Arabidopsis*. It currently can not be excluded that some of the specific subunits of bovine and *Arabidopsis* complex I represent orthologs but could not be assigned to each other due to low sequence conservation. However, some bovine complex I subunits clearly are absent in plants. For instance, the acyl carrier subunit of complex I from fungi and mammals is not attached to complex I in plants (Meyer et al., 2007). Instead, soluble forms of the acyl carrier protein are present in the matrix of plant mitochondria (At1g65290, At2g44620 and At5g47630).

Overall, 25 complex I subunits in *Arabidopsis* represent orthologs of nuclear encoded subunits of bovine complex I. Two of them, the ND7 and ND9 proteins, are encoded by the mitochondrial genome in plants, the remaining 23 being encoded by the nuclear genome like in mammals and/or fungi.

Pairs of isoforms were detected by mass spectrometry for 6 complex I subunits in *Arabidopsis*. Additionally, the 15 kDa subunit is encoded by two genes in *Arabidopsis* (At3g62790 and At2g47690). However, the only peptide of this subunit identified by MS completely matches to both genes. All pairs of isoforms are highly expressed in *Arabidopsis* (currently between 59 and 259 matching ESTs per gene; TAIR, <http://www.arabidopsis.org/>). Sequence identity lies in the range of 84–98% (Table 2). In addition, it currently can not be excluded that the 5 subunits resembling  $\gamma$ -type carbonic anhydrases represent isoforms. Three of them, termed CA1, CA2 and CA3, have a largely conserved active site if compared to the archaeobacterial prototype of this enzyme, the  $\gamma$ -carbonic anhydrase of *Methanosarcina thermophila* (CAM), whereas the two other complex I subunits are more derived and therefore have been termed “carbonic anhydrase-like” proteins (CAL1 and CAL2; Perales et al., 2004). However, it is unlikely that these proteins represent alternative isoforms for several reasons: (i) the prototype carbonic anhydrase of *M. thermophila* represents a trimer. This nicely corresponds to the size of the extra matrix-exposed domain of plant complex I (Peters et al., 2008); (ii) two-hybrid experiments have revealed direct interaction of CA2 with CAL1 and CAL2 (Perales et al., 2004) which only is possible if these subunits simultaneously are present in individual complex I particles; and (iii) sequence identity between the five members of the *Arabidopsis* CA/CAL protein family is low in comparison to the sequence identities of the above described 7 pairs of isoforms (65–75% between the CA1, CA2 and CA3 proteins; only about 30% between one or the other CAL subunit and CA1, CA2 or CA3; 90% between CAL1 and CAL2).

The localization of many complex I subunits within *Arabidopsis* complex I has been elucidated based on the subunit compositions of its subcomplexes generated by low-SDS treatment (Klodmann et al., 2010). An updated version of the presented topological model of plant complex I, which includes all its 48 subunits, is presented in Fig. 3.

## 2.3. Biochemical function and physiological role of plant specific complex I subunits

Despite large efforts, the physiological role of the extra subunits in plants is not completely understood. So far, direct evidence for

**Table 2**Properties of isoforms of complex I subunits in *Arabidopsis*.

Name <sup>a</sup>	Accession <sup>a</sup>	MW <sup>b</sup>	GRAVY <sup>c</sup>	EST <sup>d</sup>	Sequence identity (%) <sup>e</sup>
TYKY-1	At1g79010	25.49	−0.559	163	94.1
TYKY-2	At1g16700	25.36	−0.559	81	
B16.6-1	At1g04630	16.13	−0.487	74	97.2
B16.6-2	At2g33220	16.12	−0.472	259	
PDSW-1	At3g18410	12.44	−0.956	168	96.3
PDSW-2	At1g49140	12.52	−0.880	132	
PGIV-1	At3g06310	12.16	−0.456	60	88.0
PGIV-2	At5g18800	12.00	−0.492	75	
15 kDa-1	At3g62790	9.89	−1.249	76	97.6
15 kDa-2	At2g47690	9.88	−1.253	103	
At2g42310/At3g57785-1	At2g42310	12.63	−0.539	206	91.2
At2g42310/At3g57785-2	At3g57785	12.66	−0.521	72	
B12-1	At1g14450	8.30	−0.578	112	84.9
B12-2	At2g02510	8.05	−0.503	59	

<sup>a</sup> Subunit name and accession number in correspondence with Table 1.<sup>b</sup> Molecular mass (kDa). Note: the molecular mass of the 15 kDa-2 (At2g47690) subunit was corrected because its annotation at TAIR (<http://www.arabidopsis.org/>) probably is not correct (compared to the 15 kDa-1 isoform the sequence comprises an N-terminal extension which most likely does not form part of the protein).<sup>c</sup> GRAVY (grand average of hydropathy) score of the protein.<sup>d</sup> Number of matching ESTs at TAIR (<http://www.arabidopsis.org/>) on August 31st, 2010.<sup>e</sup> Percent sequence identity upon pair-wise comparison.

carbonic anhydrase activity of complex I is absent. However, several lines of evidence suggest that the CA and CAL subunits are involved in CO<sub>2</sub>/HCO<sub>3</sub><sup>−</sup> metabolism:

- Sequences of the subunits are clearly related to the proto-type  $\gamma$ -type carbonic anhydrase from *M. thermophila* (CAM). This is especially clear for the CA1, CA2 and CA3 proteins. The sequences of the CAL1 and CAL2 proteins are less similar.
- Structural modeling reveals a high degree of conservation of amino acids in CAM and the CA1, CA2 and CA3 proteins at the active site.

- The genes encoding CA2 and CA3 are down-regulated if *Arabidopsis* is cultivated at elevated CO<sub>2</sub> (Perales et al., 2005).
- CA2 over-expressed in *E. coli* can efficiently bind CO<sub>2</sub>/HCO<sub>3</sub><sup>−</sup> (Martin et al., 2009).
- By analogy, CO<sub>2</sub>–HCO<sub>3</sub><sup>−</sup> conversion in cyanobacteria, which is essential in the context of the cyanobacterial CO<sub>2</sub> concentrating mechanism, was shown to depend on cyanobacterial complex I. Attachment of carbonic anhydrases at the inner surface of the membrane arm of complex I might be advantageous for CO<sub>2</sub>–HCO<sub>3</sub><sup>−</sup> conversion because of the basic pH at this micro-location (the reaction equilibrium of this conversion is very much on the HCO<sub>3</sub><sup>−</sup> side at basic pH).

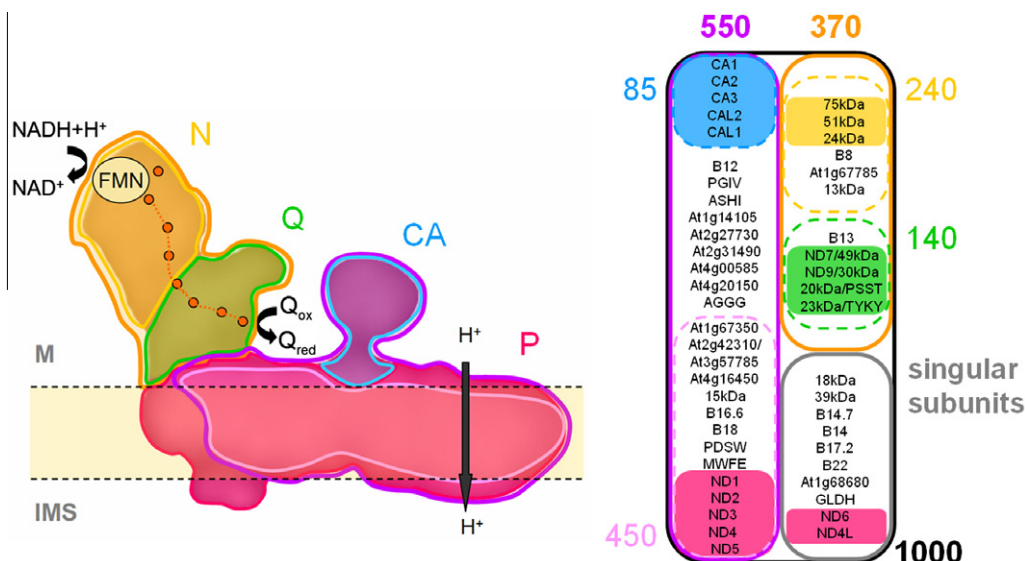


**Fig. 3.** Modular subunit arrangement within *Arabidopsis* complex I. Left: Functional modules of plant complex I (N: N-module [yellow]; Q: Q-module [green]; P: P-module [red]; CA: carbonic anhydrase domain [blue]). NADH oxidation takes place at FMN. Electrons are subsequently transferred via seven FeS clusters (orange dots) to the Q-reduction site. Proton translocation takes place at the P-module. The inner mitochondrial membrane is indicated in light yellow. M = matrix, IMS = Inter membrane space. Right: Assignment of subunits to the functional modules. The assignment is based on defined fragmentation of isolated complex I by low-SDS treatment (Klodmann et al., 2010). Generated subcomplexes were separated by blue native PAGE and their subunits by SDS–PAGE. Using this procedure, the holo-complex (1000 kDa) can be dissected into up to 10 subcomplexes. In a first step, the membrane arm (purple, 550 kDa) and the peripheral arm (orange, 370 kDa) are separated. Next, the peripheral arm can be dissected into the N-module subcomplex (yellow, 240 kDa) and the Q-module subcomplex (green, 140 kDa). At the same time, the membrane arm is dissected into a smaller version (pink, 450 kDa) which lacks the carbonic anhydrase domain (blue, 85 kDa) and most likely some further subunits. Subunits not forming part of any of the complex I subcomplexes most likely are detached from the complex at an initial stage and therefore are assumed to be localized in the periphery of the complex or at the interface of the two complex I arms. Subunits highlighted in red, yellow and green represent the 14 core subunits present in the *E. coli* complex. The CA subunits in plants are highlighted in blue.

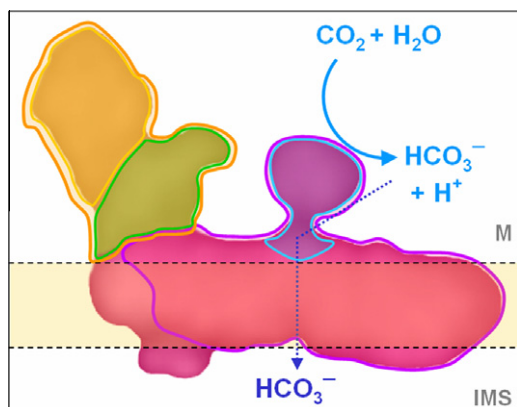


**Fig. 4.** Supposed function of the carbonic anhydrase domain. A model of plant complex I is shown with the carbonic anhydrase domain highlighted in blue. The position of the inner mitochondrial membrane is indicated in yellow. M = matrix, IMS = inter membrane space,  $\text{CO}_2$  = carbon dioxide,  $\text{H}_2\text{O}$  = water,  $\text{HCO}_3^-$  = bicarbonate.

Recently some further bacterial  $\gamma$ -type carbonic anhydrases were functionally characterized and shown to represent highly active enzymes. These proteins exhibit an even higher degree of sequence similarity with the CA1, CA2 and CA3 proteins than CAM (Jeyakanthan et al., 2008; Peña et al., 2010; Zimmerman et al., 2010).

What could be the physiological role of the complex I integrated carbonic anhydrases? Characterization of an *Arabidopsis* knock out mutant deficient in CA2 did not reveal an altered developmental phenotype if compared to wild-type plants. However, complex I assembly was very much reduced in the mutant line. Therefore, complex I biogenesis seems to depend on the CA subunits. Since the CA proteins are specific to plants, a role of them during photosynthesis has been postulated (Braun and Zabaleta, 2007). In contrast to animal cells, mitochondrial  $\text{CO}_2$  in plants is an essential substrate for photosynthesis which under many conditions is rate limiting for plant growth. This especially is true for plants grown at hot or dry location due to stomata closure. An active  $\text{CO}_2$  transport system from mitochondria to chloroplasts has been suggested, which is based on  $\text{CO}_2$ – $\text{HCO}_3^-$  conversion at mitochondrial complex I, bicarbonate transport across the mitochondrial and the chloroplast membranes and  $\text{HCO}_3^-$ – $\text{CO}_2$  re-conversion by carbonic anhydrases localized in chloroplasts. The suggested mechanism is analogous to the well characterized  $\text{CO}_2$  concentration mechanism described for cyanobacteria. Possibly, complex I itself could be involved in  $\text{HCO}_3^-$  transfer across the inner mitochondrial membrane (Fig. 4). Indeed, a small cavity is visible within the intermembrane-space exposed side of the membrane arm exactly in opposite to the site of attachment of the CA domain on the matrix-exposed side (Figs. 1 and 4), which could represent the opening of a transport channel. However, so far the postulated physiological role of the CA/CAL subunits largely is speculative and has to be further investigated. Furthermore, it recently was reported that complex I from some protist mitochondria also includes carbonic anhydrase subunits (Gawryluk and Gray, 2010). This implies that CA function might be important beyond photosynthesis.

The physiological role of another plant specific subunit, the L-galactono-1,4-lactone dehydrogenase (GLDH), also is not clear so far. GLDH does not form part of the holo-complex I, but of a slightly smaller version which runs at about 850 kDa on blue native gels (Heazlewood et al., 2003; Millar et al., 2003). Rotenone, a specific electron transport inhibitor of complex I, also inhibits

ascorbate formation, indicating functional involvement of complex I in this metabolic pathway. However, characterization of an *Arabidopsis* knock out line deficient in GLDH (Pineau et al., 2008) rather points to a role of GLDH during the assembly process of complex I. It remains to be established if GLDH is a bifunctional protein which is indeed involved in both, ascorbate formation and assembly of this respiratory enzyme.

### 3. Conclusion

Proteomic investigations have greatly contributed for comprehensive characterization of plant complex I (Cardol et al., 2004; Heazlewood et al., 2003; Klodmann et al., 2010; Meyer et al., 2008; Sunderhaus et al., 2006). By employing this experimental approach it became clear that complex I of plants has an especially sophisticated configuration: it includes 48 distinct types of subunits, some of which occur in isoforms. Furthermore, it includes 15 subunits specific for plants. The postulated functions of some of these extra subunits remain to be further investigated, e.g. by the characterization of *Arabidopsis* knock out plants deficient of the proteins of interest. Comparative proteome analyses of mutant and wild-type plants will further help to obtain in depth insights into the multiple functions of complex I in plants.

### Acknowledgments

This work was supported by the Deutsche Forschungsgemeinschaft (DFG), Grants Br1829/8-1 and Br1829/10-1.

### References

- Abdrakhmanova, A., Zickermann, V., Bostina, M., Radermacher, M., Schagger, H., Kerscher, S., Brandt, U., 2004. Subunit composition of mitochondrial complex I from the yeast *Yarrowia lipolytica*. *Biochim. Biophys. Acta* 1658, 148–156.
- Baranova, E.A., Morgan, D.J., Sazanov, L.A., 2007a. Single particle analysis confirms distal location of subunits NuoL and NuoM in *Escherichia coli* complex I. *J. Struct. Biol.* 159, 238–242.
- Baranova, E.A., Holt, P.J., Sazanov, L.A., 2007b. Projection structure of the membrane domain of *Escherichia coli* respiratory complex I at 8 Å resolution. *J. Mol. Biol.* 366, 140–154.
- Berrisford, J.M., Sazanov, L.A., 2009. Structural basis for the mechanism of respiratory complex I. *J. Biol. Chem.* 284, 29773–29783.
- Böttcher, B., Scheide, D., Hesterberg, M., Nagel-Steger, L., Friedrich, T., 2002. A novel, enzymatically active conformation of the *Escherichia coli* NADH:ubiquinone oxidoreductase (complex I). *J. Biol. Chem.* 277, 17970–17977.
- Brandt, U., 2006. Energy converting NADH:quinone oxidoreductase (complex I). *Annu. Rev. Biochem.* 75, 69–92.
- Braun, H.P., Emmermann, M., Kruff, V., Schmitz, U.K., 1992. The general mitochondrial processing peptidase from potato is an integral part of cytochrome c reductase of the respiratory chain. *EMBO J.* 11, 3219–3227.
- Braun, H.P., Zabaleta, E., 2007. Carbonic anhydrase subunits of the mitochondrial NADH dehydrogenase complex (complex I) in plants. *Physiol. Plantarum* 129, 114–122.
- Bridges, H.R., Fearnley, I.M., Hirst, J., 2010. The subunit composition of mitochondrial NADH:ubiquinone oxidoreductase (complex I) from *Pichia pastoris*. *Mol. Cell. Proteomics* 9, 2318–2326.
- Bultema, J.B., Braun, H.P., Boekema, E.J., Kouril, R., 2009. Megacomplex organization of the oxidative phosphorylation system by structural analysis of respiratory supercomplexes from potato. *Biochim. Biophys. Acta* 1787, 60–67.
- Cardol, P., Vanrobaeys, F., Devreese, B., Van Beeumen, J., Matagne, R.F., Remacle, C., 2004. Higher plant-like subunit composition of mitochondrial complex I from *Chlamydomonas reinhardtii*: 31 conserved components among eukaryotes. *Biochim. Biophys. Acta* 1658, 212–224.
- Carroll, J., Shannon, R.J., Fearnley, I.M., Walker, J.E., Hirst, J., 2002. Definition of the nuclear encoded protein composition of bovine heart mitochondrial complex I. Identification of two new subunits. *J. Biol. Chem.* 277, 50311–50317.
- Carroll, J., Fearnley, I.M., Shannon, R.J., Hirst, J., Walker, J.E., 2003. Analysis of the subunit composition of complex I from bovine heart mitochondria. *Mol. Cell. Proteomics* 2, 117–126.
- Carroll, J., Fearnley, I.M., Skehel, J.M., Shannon, R.J., Hirst, J., Walker, J.E., 2006. Bovine complex I is a complex of 45 different subunits. *J. Biol. Chem.* 281, 32724–32727.
- Cipollone, R., Ascenzi, P., Visca, P., 2007. Common themes and variations in the rhodanese superfamily. *IUBMB Life* 59, 51–59.

- Clason, T., Zickermann, V., Ruiz, T., Brandt, U., Radermacher, M., 2007. Direct localization of the 51 and 24 kDa subunits of mitochondrial complex I by three-dimensional difference imaging. *J. Struct. Biol.* 159, 433–442.
- Clason, T., Ruiz, T., Schägger, H., Peng, G., Zickermann, V., Brandt, U., Michel, H., Radermacher, M., 2010. The structure of eukaryotic and prokaryotic complex I. *J. Struct. Biol.* 169, 81–88.
- Combettes, B., Grienberger, J.M., 1999. Analysis of wheat mitochondrial complex I purified by a one-step immunoaffinity chromatography. *Biochimie* 81, 645–653.
- Dudkina, N.V., Eubel, H., Keegstra, W., Boekema, E.J., Braun, H.P., 2005. Structure of a mitochondrial supercomplex formed by respiratory chain complexes I and III. *Proc. Natl. Acad. Sci. USA* 102, 3225–3229.
- Efremov, R.G., Baradaran, R., Sazanov, L.A., 2010. The architecture of respiratory complex I. *Nature* 465, 441–445.
- Fearnley, I.M., Walker, J.E., 1992. Conservation of sequences of subunits of mitochondrial complex I and their relationships with other proteins. *Biochim. Biophys. Acta* 1140, 105–134.
- Fearnley, I.M., Carroll, J., Shannon, R.J., Runswick, M.J., Walker, J.E., Hirst, J., 2001. GRIM-19, a cell death regulatory gene product, is a subunit of bovine mitochondrial NADH:ubiquinone oxidoreductase (complex I). *J. Biol. Chem.* 276, 38345–38348.
- Friedrich, T., Scheide, D., 2000. The respiratory complex I of bacteria, archaea and eukarya and its module common with membrane-bound multisubunit hydrogenases. *FEBS Lett.* 479, 1–5.
- Friedrich, T., Böttcher, B., 2004. The gross structure of the respiratory complex I: a Lego System. *Biochim. Biophys. Acta* 1608, 1–9.
- Gawryluk, R.M., Gray, M.W., 2010. Evidence for an early evolutionary emergence of gamma-type carbonic anhydrases as components of mitochondrial respiratory complex I. *BMC Evol. Biol.* 10, 176.
- Grigorieff, N., 1998. Three-dimensional structure of bovine NADH:ubiquinone oxidoreductase (complex I) at 2.2 Å in ice. *J. Mol. Biol.* 277, 1033–1046.
- Guénébaut, V., Vincentelli, R., Mills, D., Weiss, H., Leonard, K.R., 1997. Three-dimensional structure of NADH-dehydrogenase from *Neurospora crassa* by electron microscopy and conical tilt reconstruction. *J. Mol. Biol.* 265, 409–418.
- Guénébaut, V., Schlitt, A., Weiss, H., Leonard, K., Friedrich, T., 1998. Consistent structure between bacterial and mitochondrial NADH:ubiquinone oxidoreductase (complex I). *J. Mol. Biol.* 276, 105–112.
- Hatefi, Y., 1985. The mitochondrial electron transport and oxidative phosphorylation system. *Ann. Rev. Biochem.* 54, 1015–1069.
- Hatefi, Y., Haavik, A.G., Griffiths, D.E., 1962. Studies on the electron transfer system: XL. Preparation and properties of mitochondrial DPNH-Coenzyme Q reductase. *J. Biol. Chem.* 237, 1676–1680.
- Heazlewood, J.L., Howell, K.A., Millar, A.H., 2003. Mitochondrial complex I from *Arabidopsis* and rice: orthologs of mammalian and fungal components coupled with plant-specific subunits. *Biochim. Biophys. Acta* 1604, 159–169.
- Herz, U., Schröder, W., Liddell, A., Leaver, C.J., Brennicke, A., Grohmann, L., 1994. Purification of the NADH:ubiquinone oxidoreductase (complex I) of the respiratory chain from the inner mitochondrial membrane of *Solanum tuberosum*. *J. Biol. Chem.* 269, 2263–2269.
- Hinchliffe, P., Sazanov, L.A., 2005. Organization of iron–sulfur clusters in respiratory complex I. *Science* 309, 771–774.
- Hinchliffe, P., Carroll, J., Sazanov, L.A., 2006. Identification of a novel subunit of respiratory complex I from *Thermus thermophilus*. *Biochemistry* 45, 4413–4420.
- Hirst, J., Carroll, J., Fearnley, I.M., Shannon, R.J., Walker, J.E., 2003. The nuclear encoded subunits of complex I from bovine heart mitochondria. *Biochim. Biophys. Acta* 1604, 135–150.
- Huang, S., Taylor, N.L., Whelan, J., Millar, A.H., 2009. Refining the definition of plant mitochondrial presequences through analysis of sorting signals, N-terminal modifications, and cleavage motifs. *Plant Physiol.* 150, 1272–1285.
- Hunte, C., Zickermann, V., Brandt, U., 2010. Functional modules and structural basis of conformational coupling in mitochondrial complex I. *Science* 329, 448–451.
- Ito, J., Taylor, N.L., Castleden, I., Weckwerth, W., Millar, A.H., Heazlewood, J.L., 2009. A survey of the *Arabidopsis thaliana* mitochondrial phosphoproteome. *Proteomics* 9, 4229–4240.
- Jansch, L., Kruff, V., Schmitz, U.K., Braun, H.P., 1995. Cytochrome c reductase from potato does not comprise three core proteins but contains an additional low-molecular-mass subunit. *Eur. J. Biochem.* 228, 878–885.
- Jansch, L., Kruff, V., Schmitz, U.K., Braun, H.P., 1996. New insights into the composition, molecular mass and stoichiometry of the protein complexes of plant mitochondria. *Plant J.* 9, 357–368.
- Jeyakanthan, J., Rangarajan, S., Mridula, P., Kanauija, S.P., Shiro, Y., Kuramitsu, S., Yokoyama, S., Sekar, K., 2008. Observation of a calcium-binding site in the gamma-class carbonic anhydrase from *Pyrococcus horikoshii*. *Acta Crystallogr. D. Biol. Crystallogr.* 64, 1012–1019.
- Klodmann, J., Sunderhaus, S., Nimtz, M., Jansch, L., Braun, H.P., 2010. Internal architecture of mitochondrial complex I from *Arabidopsis thaliana*. *Plant Cell* 22, 797–810.
- Lazarou, M., Thorburn, D.R., Ryan, M.T., McKenzie, M., 2009. Assembly of mitochondrial complex I and defects in disease. *Biochim. Biophys. Acta* 1793, 78–88.
- Leterme, S., Boutry, M., 1993. Purification and preliminary characterization of mitochondrial complex I (NADH: ubiquinone reductase) from broad bean (*Vicia faba* L.). *Plant Physiol.* 102, 435–443.
- Lu, H., Cao, X., 2008. GRIM-19 is essential for maintenance of mitochondrial membrane potential. *Mol. Biol. Cell* 19, 1893–1902.
- Marques, I., Duarte, M., Assuncao, J., Ushakova, A.V., Videira, A., 2005. *Biochim. Biophys. Acta* 1707, 211–220.
- Martin, V., Villarreal, F., Miras, I., Navaza, A., Haouz, A., González-Lebrero, R.M., Kaufman, S.B., Zabaleta, E., 2009. Recombinant plant gamma carbonic anhydrase homotrimers bind inorganic carbon. *FEBS Lett.* 583, 3425–3430.
- Mathiesen, C., Hägerhäll, C., 2002. Transmembrane topology of the Nuol, M and N subunits of NADH:quinone oxidoreductase and their homologues among membrane-bound hydrogenases and bona fide antiporters. *Biochim. Biophys. Acta* 1556, 121–132.
- Meyer, E.H., Heazlewood, J.L., Millar, A.H., 2007. Mitochondrial acyl carrier proteins in *Arabidopsis thaliana* are predominantly soluble matrix proteins and none can be confirmed as subunits of respiratory Complex I. *Plant Mol. Biol.* 64, 319–327.
- Meyer, E.H., Taylor, N.L., Millar, A.H., 2008. Resolving and identifying protein components of plant mitochondrial respiratory complexes using three dimensions of gel electrophoresis. *J. Proteome Res.* 2, 786–794.
- Millar, A.H., Mittova, V., Kiddle, G., Heazlewood, J.L., Bartoli, C.G., Theodoulou, F.L., Foyer, C.H., 2003. Control of ascorbate synthesis by respiration and its implications for stress responses. *Plant Physiol.* 133, 443–447.
- Morgan, D.J., Sazanov, L.A., 2008. Three-dimensional structure of respiratory complex I from *Escherichia coli* in ice in the presence of nucleotides. *Biochim. Biophys. Acta* 1777, 711–718.
- Morgner, N., Zickermann, V., Kersch, S., Wittig, I., Abdrakhmanova, A., Barth, H.D., Brutschy, B., Brandt, U., 2008. Subunit mass fingerprinting of mitochondrial complex I. *Biochim. Biophys. Acta* 1777, 1384–1391.
- Mueller, E.G., 2006. Trafficking in persulfides: delivering sulfur in biosynthetic pathways. *Nat. Chem. Biol.* 2, 185–194.
- Murray, J., Zhang, B., Taylor, S.W., Oglesbee, D., Fahy, E., Marusich, M.F., Ghosh, S.S., Capaldi, R.A., 2003. The subunit composition of the human NADH dehydrogenase obtained by rapid one-step immunopurification. *J. Biol. Chem.* 278, 13619–13622.
- Ohnishi, T., 1998. Iron-sulfur clusters/semiquinones in complex I. *Biochim. Biophys. Acta* 1364, 186–206.
- Peña, K.L., Castel, S.E., de Araujo, C., Espie, G.S., Kimber, M.S., 2010. Structural basis of the oxidative activation of the carboxysomal gamma-carbonic anhydrase. *Cnm Proc. Natl. Acad. Sci. USA* 107, 2455–2460.
- Peng, G., Fritzsche, G., Zickermann, V., Schägger, H., Mentele, R., Lottspeich, F., Bostina, M., Radermacher, M., Huber, R., Stetter, K.O., Michel, H., 2003. Isolation, characterization and electron microscopic single particle analysis of the NADH:ubiquinone oxidoreductase (complex I) from the hyperthermophilic eubacterium *Aquifex aeolicus*. *Biochemistry* 42, 3032–3039.
- Perales, M., Parisi, G., Fornasari, M.S., Colaneri, A., Villarreal, F., Gonzalez-Schain, N., Echave, J., Gomez-Casati, D., Braun, H.P., Araya, A., Zabaleta, E., 2004. Gamma carbonic anhydrase like complex interact with plant mitochondrial complex I. *Plant Mol. Biol.* 56, 947–957.
- Perales, M., Eubel, H., Heinemeyer, J., Colaneri, A., Zabaleta, E., Braun, H.P., 2005. Disruption of a nuclear gene encoding a mitochondrial gamma carbonic anhydrase reduces complex I and supercomplex I+III<sub>2</sub> levels and alters mitochondrial physiology in *Arabidopsis*. *J. Mol. Biol.* 350, 263–277.
- Peters, K., Dudkina, N.V., Jansch, L., Braun, H.P., Boekema, E.J., 2008. A structural investigation of complex I and I+III<sub>2</sub> supercomplex from *Zea mays* at 11–13 Å resolution: assignment of the carbonic anhydrase domain and evidence for structural heterogeneity within complex I. *Biochim. Biophys. Acta* 1777, 84–93.
- Pineau, B., Layoune, O., Danon, A., De Paepe, R., 2008. L-Galactono-1,4-lactone dehydrogenase is required for the accumulation of plant respiratory complex I. *J. Biol. Chem.* 283, 32500–32505.
- Radermacher, M., Ruiz, T., Clason, T., Benjamin, S., Brandt, U., Zickermann, V., 2006. The three-dimensional structure of complex I from *Yarrowia lipolytica*: a highly dynamic enzyme. *J. Struct. Biol.* 154, 269–279.
- Rasmuson, A.G., Mendel-Hartvig, J., Möller, I.M., Wiskich, J.T., 1994. Isolation of the rotenone-sensitive NADH-ubiquinone reductase (Complex I) from red beet mitochondria. *Physiol. Plantarum* 90, 607–615.
- Rasmuson, A.G., Geisler, D.A., Möller, I.M., 2008. The multiplicity of dehydrogenases in the electron transport chain of plant mitochondria. *Mitochondrion* 8, 47–60.
- Remacle, C., Barbieri, M.R., Cardol, P., Hamel, P.P., 2008. Eukaryotic complex I: functional diversity and experimental systems to unravel the assembly process. *Mol. Genet. Genomics* 280, 93–110.
- Sackmann, U., Zensen, R., Rohlen, D., Jahnke, U., Weiss, H., 1991. The acyl-carrier protein in *Neurospora crassa* mitochondria is a subunit of NADH:ubiquinone reductase (complex I). *Eur. J. Biochem.* 200, 463–469.
- Sazanov, L.A., Hinchliffe, P., 2006. Structure of the hydrophilic domain of respiratory complex I from *Thermus thermophilus*. *Science* 311, 1430–1436.
- Sazanov, L.A., 2007. Respiratory complex I: mechanistic and structural insights provided by the crystal structure of the hydrophilic domain. *Biochemistry* 46, 2275–2288.
- Sunderhaus, S., Dudkina, N., Jansch, L., Klodmann, J., Heinemeyer, J., Perales, M., Zabaleta, E., Boekema, E., Braun, H.P., 2006. Carbonic anhydrase subunits form a matrix-exposed domain attached to the membrane arm of mitochondrial complex I in plants. *J. Biol. Chem.* 281, 6482–6488.
- Tocilescu, M.A., Zickermann, V., Zwicker, K., Brandt, U., in press. Quinone binding and reduction by respiratory complex I. *Biochim. Biophys. Acta*.
- Unsel, M., Marienfeld, J.R., Brandt, P., Brennicke, A., 1997. The mitochondrial genome of *Arabidopsis thaliana* contains 57 genes in 366,924 nucleotides. *Nat. Genet.* 15, 57–61.

- Trost, P., Bonora, P., Scagliarini, S., Pupillo, P., 1995. Purification and properties of NAD(P)H: (quinone-acceptor) oxidoreductase of sugarbeet cells. *Eur. J. Biochem.* 234, 452–458.
- Vogel, R.O., Smeitink, J.A., Nijtmans, L.G., 2007. Human mitochondrial complex I assembly: a dynamic and versatile process. *Biochim. Biophys. Acta* 1767, 1215–1227.
- Weidner, U., Geier, S., Ptock, A., Friedrich, T., Leif, H., Weiss, H., 1993. The gene locus of the proton-translocating NADH: ubiquinone oxidoreductase in *Escherichia coli*. Organization of the 14 genes and relationship between the derived proteins and subunits of mitochondrial complex I. *J. Mol. Biol.* 233, 109–122.
- Yagi, T., Yano, T., Di Bernardo, S., Matsuno-Yagi, A., 1998. Prokaryotic complex I (NDH-1), an overview. *Biochim. Biophys. Acta* 1364, 125–133.
- Yagi, T., Matsuno-Yagi, A., 2003. The proton-translocating NADH-quinone oxidoreductase in the respiratory chain: the secret unlocked. *Biochemistry* 42, 2266–2274.
- Zensen, R., Husmann, H., Schneider, R., Peine, T., Weiss, H., 1992. De novo synthesis and desaturation of fatty acids at the mitochondrial acyl-carrier protein, a subunit of NADH:ubiquinone oxidoreductase in *Neurospora crassa*. *FEBS Lett.* 310, 179–181.
- Zhang, J., Yang, J., Roy, S.K., Tininini, S., Hu, J., Bromberg, J.F., Poli, V., Stark, G.R., Kalvakolanu, D.V., 2003. The cell death regulator GRIM-19 is an inhibitor of signal transducer and activator of transcription 3. *Proc. Natl. Acad. Sci. USA* 100, 9342–9347.
- Zickermann, V., Dröse, S., Tocilescu, M.A., Zwicker, K., Kerscher, S., Brandt, U., 2008. Challenges in elucidating structure and mechanism of proton pumping NADH:ubiquinone oxidoreductase (complex I). *J. Bioenerg. Biomembr.* 40, 475–483.
- Zickermann, V., Kerscher, S., Zwicker, K., Tocilescu, M.A., Radermacher, M., Brandt, U., 2009. Architecture of complex I and its implications for electron transfer and proton pumping. *Biochim. Biophys. Acta* 1787, 574–583.
- Zimmerman, S.A., Tomb, J.F., Ferry, J.G., 2010. Characterization of CamH from *Methanosarcina thermophila*, founding member of a subclass of the gamma class of carbonic anhydrases. *J. Bacteriol.* 192, 1353–1360.



## RESEARCH ARTICLE

# Low-SDS Blue native PAGE

*Jennifer Klodmann, Dagmar Lewejohann and Hans-Peter Braun*

Institute for Plant Genetics, Faculty of Natural Sciences, Leibniz Universität Hannover, Hannover, Germany

SDS normally is strictly avoided during Blue native (BN) PAGE because it leads to disassembly of protein complexes and unfolding of proteins. Here, we report a modified BN-PAGE procedure, which is based on low-SDS treatment of biological samples prior to native gel electrophoresis. Using mitochondrial OXPHOS complexes from Arabidopsis as a model system, low SDS concentrations are shown to partially dissect protein complexes in a very defined and reproducible way. If combined with 2-D BN/SDS-PAGE, generated subcomplexes and their subunits can be systematically investigated, allowing insights into the internal architecture of protein complexes. Furthermore, a 3-D BN/low-SDS BN/SDS-PAGE system is introduced to facilitate structural analysis of individual protein complexes without their previous purification.

Received: October 6, 2010

Revised: November 26, 2010

Accepted: December 13, 2010

**Keywords:**

2-D Blue native/SDS-PAGE / Blue native PAGE / Destabilization / Plant proteomics / Protein complex / SDS

## 1 Introduction

SDS is a highly efficient anionic detergent that is extensively used in protein biochemistry. Upon incubation with SDS, biomembranes are solubilized, protein complexes are dissolved into their individual subunits, and proteins are denatured. SDS binds to polypeptides at a constant weight ratio of approximately 1.4 g/g protein. Since SDS is an anionic compound, negative charge is introduced into proteins and conceals their intrinsic charge, which under native conditions very much varies depending on the ratio of acidic and basic amino acid residues. SDS therefore was found to be an ideal compound for the preparation of protein mixtures for gel electrophoresis [1–4]. However, SDS is not compatible with physiological analyses of proteins because most enzymes become inactive in its presence.

For a long time, “native” protein gel electrophoresis in the absence of SDS did not allow satisfactory results. This situation changed when Coomassie-blue was introduced as a substitute for SDS during gel electrophoresis [5]. Coomassie blue is a wool dye which was introduced into protein

biochemistry to visualize proteins on gels in 1963 [6]. It tightly binds to proteins and at the same time introduces negative charge into proteins because it is a negatively charged compound. However, in contrast to SDS, it does not dissolve protein complexes or denature and thereby inactivate proteins. If Coomassie-pretreated protein fractions are separated on polyacrylamide gradient gels, intact protein complexes are resolved, which can be separated into their subunits upon combination of the so-called “Blue native” gel dimension with a second SDS gel dimension in orthogonal direction [5]. However, native analysis of membrane-bound protein complexes still requires the usage of detergents for membrane solubilization. For Blue native (BN) PAGE, mild nonionic detergents were introduced to allow the separation of enzymatically active membrane protein complexes such as dodecylmaltoside, Triton X-100, and digitonin [6, 7]. Also, less known detergents were successfully combined with BN-PAGE, such as octylglucoside, Brij 96, and saponin [8–10]. As a general rule, SDS is never combined with Blue native gel electrophoresis except for the second gel dimension to separate subunits of protein complexes.

Here, we report the usage of low concentrations of SDS during BN-PAGE to carefully destabilize protein complexes and thereby analyze their internal structure. It was found that defined concentrations of SDS below its critical micellar concentration (CMC) very specifically dissect protein complexes into subcomplexes and that separation of subunits of the generated subcomplexes on a second gel

**Correspondence:** Professor Hans-Peter Braun, Institute for Plant Genetics, Leibniz Universität Hannover, Herrenhäuser Straße 2, D-30419 Hannover, Germany

**E-mail:** braun@genetik.uni-hannover.de

**Fax:** +49-511-7623608

**Abbreviation:** BN, Blue native

dimension gives insights into the internal structure of large protein particles. This recently was shown for complex I of the respiratory chain of *Arabidopsis thaliana* [11] and here is applied to analyze further complexes of the mitochondrial oxidative phosphorylation (OXPHOS) system. Finally, a 2-D BN/BN gel system employing low SDS concentrations for the second Blue native gel dimension is introduced as a tool to efficiently allow the analysis of the internal subunit arrangement of individual protein complexes without their previous biochemical isolation.

## 2 Materials and methods

### 2.1 Isolation of mitochondria from Arabidopsis

Mitochondria were isolated from an *Arabidopsis* suspension cell culture as described previously [12]. Purified mitochondrial fractions were divided into aliquots à 1 mg mitochondrial protein, shock frozen by liquid nitrogen, and stored at  $-80^{\circ}\text{C}$ .

### 2.2 Purification of complex I from Arabidopsis

*Arabidopsis* complex I was enriched by sucrose gradient ultracentrifugation and remaining contaminants of complex III were removed by a cytochrome *c*-mediated depletion procedure [11].

### 2.3 SDS pretreatment of isolated mitochondria and purified complex I

Mitochondria (1 mg mitochondrial protein) were sedimented by centrifugation for 10 min at  $14\,263 \times g$

(Eppendorf centrifuge Sigma 2K15) and  $4^{\circ}\text{C}$ . Pellets were resuspended in 100  $\mu\text{L}$  “digitonin solubilization buffer” (30 mM HEPES, 150 mM potassium acetate, 10% v/v glycerol, and 5% w/v digitonin, pH 7.4). After incubation (10 min on ice), the solubilized mitochondria were centrifuged at  $18\,320 \times g$  (same centrifuge, full speed) to remove membrane particles. Subsequently, a 1 or 10% SDS solution was added to the supernatant to adjust the desired final concentration of 0.05–1.0% SDS. Incubation was for 5 min at  $0^{\circ}\text{C}$  or higher temperatures as indicated. *Arabidopsis* complex I fractions (about 20  $\mu\text{g}$  in 20  $\mu\text{L}$  “washing buffer” (20 mM Tris-acetate, pH 7.0, 5% w/v sucrose, 0.04% w/v digitonin, and 0.2 mM PMSF)) were supplemented with a 1% SDS solution to adjust the desired final concentration of 0.015–0.08% SDS. Incubation was 5 min on ice.

### 2.4 Gel electrophoresis procedures

SDS-pretreated mitochondrial fractions were supplemented with 5  $\mu\text{L}$  “Coomassie blue solution” (5% w/v Coomassie and 750 mM aminocaproic acid), SDS-pretreated complex I fractions with 1  $\mu\text{L}$  “Coomassie blue solution”. Fractions were directly loaded onto a Blue native gel. Blue native PAGE was carried out as described earlier [13] using the Protean II electrophoresis system (BioRad, München, Germany). Electrophoresis took place at constant voltage of 100 V for 45 min and subsequently at a constant current flow of 15 mA for another 11 h. Temperature during the electrophoretic run was  $4^{\circ}\text{C}$ .

Vertical strips of the gels of the first gel dimension were used to carry out another electrophoresis dimension in orthogonal direction. Either SDS-PAGE or BN-PAGE was used for this second gel dimension as indicated. Second-dimension SDS-PAGE followed standard BN/SDS-PAGE

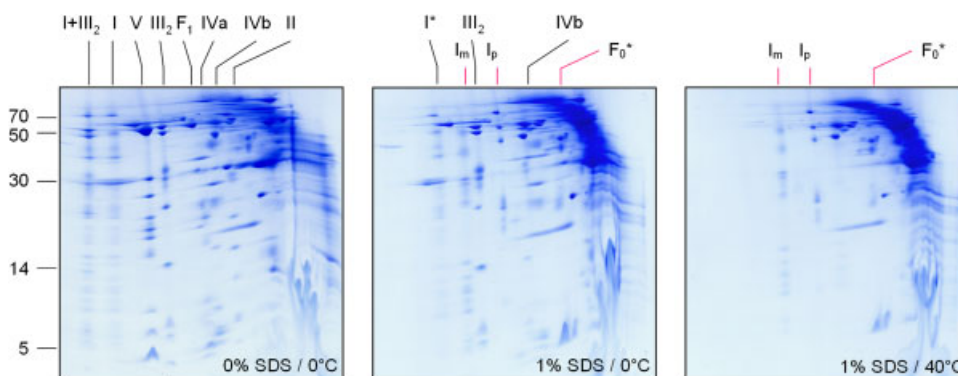


**Figure 1.** Effect of SDS and temperature on the stability of mitochondrial protein complexes in *Arabidopsis*. Isolated mitochondria (1 mg) were resolved in solubilization buffer (Section 2) supplemented/not supplemented by 1% SDS. Samples were incubated for 5 min on ice or at  $40^{\circ}\text{C}$  as indicated. Finally, the samples were supplemented with Coomassie blue and proteins were resolved by 2-D BN/SDS-PAGE. The gels were stained by Coomassie blue. The protein complexes were identified on the basis of their known subunit compositions as revealed by previous publications, e.g. documented by Eubel et al. [17]. Identities of the protein complexes are given above the gels: I+III<sub>2</sub>: supercomplex composed of complex I and dimeric complex III; I: complex I; I\* slightly smaller version of complex I; V: complex V; III<sub>2</sub>: dimeric complex III; IVa, IVb: large and small versions of complex IV; II: complex II, F<sub>1</sub>: F<sub>1</sub>-part of complex V; I<sub>m</sub>: membrane arm of complex I; I<sub>p</sub>: peripheral arm of complex I, F<sub>0</sub>\* subcomplex of the F<sub>0</sub> part of complex V.

procedures [13]. For BN/BN-PAGE, the vertical strip of the first-dimension gel was incubated for 10 min in “cathode buffer” (50 mM Tricine, 15 mM BisTris, 0.02% w/v Coomassie G250, pH 7.0) supplemented by a 1% SDS solution to reach the desired final concentration (0.05–0.1% SDS). Second-dimension BN-PAGE was carried out as described previously [14]. All gels were either stained by Coomassie colloidal [15] or silver [16].

### 3 Results

In protein biochemistry, SDS normally is used at above 1%, e.g. at 5% in the sample buffer for SDS-PAGE according to Laemmli [4]. Here, we investigate the effects of SDS on mitochondrial protein complexes at low or very low concentrations using BN-PAGE. Isolated mitochondria from *Arabidopsis* (corresponding 1 mg mitochondrial protein) were solubilized in a standard buffer for BN-PAGE including 5% digitonin. Before loading onto a Blue native gel, SDS was added to a final concentration of 1%. After incubation at 0°C for 5 min, the fraction was analyzed by a standard BN/SDS-PAGE [13]. As expected, SDS treatment caused dissection of mitochondrial protein complexes (Fig. 1). In the absence of SDS during sample preparation, the known separation pattern of the five OXPHOS complexes becomes visible on the gels: The I+III<sub>2</sub> supercomplex, complex V, dimeric complex III, the F<sub>1</sub> subdomain of complex V (which partly gets dissected from the holo-complex), a larger and a smaller version of complex IV and complex II, which in plants is composed of eight subunits. This pattern is well known from previous studies (e.g. documented by Eubel et al. [17]). At 1% SDS and 0°C during sample preparation, all the OXPHOS protein complexes get dissected. However, several defined subcomplexes of the OXPHOS complexes turned out to be stable under the conditions applied, e.g. a smaller version of complex I and dimeric complex III partially lacking the 23 kDa FeS subunit. If sample preparation is carried out at 1% SDS and 40°C, all subcomplexes are dissected except the membrane and the peripheral arm of complex I, which turned out to be surprisingly stable. If sample preparation is carried out at even higher temperatures, the two complex I arms also completely disassemble (data not shown).

The defined destabilizing effects of SDS on protein complexes during BN-PAGE prompted us to more carefully investigate this process at seven distinct low-percentage SDS concentrations (Fig. 2 and Supporting Information Figs. 1 and 2). In Fig. 2, the OXPHOS complexes are shown in distinct colors and the subcomplexes in slightly lighter colors corresponding to the colors of the holo-complex, respectively. The I+III<sub>2</sub> supercomplex (purple) already gets dissected into complex I and dimeric complex III at 0.05% SDS. Complex I (red) is converted into a slightly smaller version at 0.1% SDS, most likely because a few subunits get detached from the holo-enzyme [11]. Starting at 0.4% SDS,

it gets dissected into its two arms, the membrane arm and the peripheral arm (given in light red and dark orange on the figures), which was reported previously. These arms get dissected into further subcomplexes at higher SDS concentrations as discussed below. Complex V (given in black in Fig. 2) is very sensitive to SDS treatment. At 0.2% SDS during sample preparation, it largely gets dissected into its F<sub>1</sub> and F<sub>0</sub> subdomains (gray), which both are visible in the central region of the 2-D gels. At 0.3% SDS, the F<sub>0</sub> subdomain is further dissected into a subcomplex composed of the subunit c-oligomer and subunit 6. Dimeric complex III (blue) is the most stable complex of the OXPHOS system in *Arabidopsis*. Until 0.3% SDS, the complex is not affected. At 0.4% SDS, it partially loses its 23 kDa FeS subunit. At the same time, Complex III monomers become visible on the gels. Complexes IV and II (green and brown) are affected by SDS pretreatment starting at 0.3%. Already at 0.4% SDS, both complexes are completely dissected. No subcomplexes are visible for these two complexes on the 2-D BN/SDS gels.

SDS treatment of mitochondrial fractions leads to the simultaneous dissection of several protein complexes into subcomplexes. This makes gel evaluation complicated. In an alternative approach, isolated protein complexes are pretreated with SDS and resulting subcomplexes are resolved by 2-D BN/SDS-PAGE. This was previously shown for isolated complex I of *Arabidopsis* [11]. Under the conditions applied, complex I nearly completely becomes dissected into its two arms at 0.015% SDS (Fig. 3). Both arms are perfectly stable. However, upon increase of the SDS concentration they both are dissected into numerous smaller subcomplexes. Analysis of subunit identities of the generated subcomplexes by mass spectrometry gave insights into the inner architecture of mitochondrial complex I from *Arabidopsis* [11].

Finally, SDS can also be used to analyze the protein complexes in combination with 2-D BN/BN-PAGE. This gel system originally was suggested by Schagger and Pfeiffer [7]. It is based on a first native gel dimension carried out under most gentle conditions which is combined with a second native gel dimension carried out under slightly less gentle conditions. This differential mildness can be achieved by using two different detergents (e.g. digitonin for the first gel dimension, dodecylmaltoside for the second), temperature (0 versus 25°C), salt, etc. [14]. Here, we report BN/BN-PAGE in the presence of digitonin for the first and low-SDS for the second native gel dimension. Treatment of a first dimension gel strip with 0.05% SDS already causes dissection of complex I into its two arms and dissociation of complex V into its F<sub>0</sub> and F<sub>1</sub> subdomains (Fig. 4). Treatment by 0.1% SDS leads to further dissection of the two complex I arms into defined subcomplexes. Vertical strips of the 2-D BN/BN gel can be transferred onto a third-dimension SDS-PAGE to separate the subunits of subcomplexes, which in the case of complex I allows results very similar to the ones shown on the gel to the right-hand side in Fig. 3. This

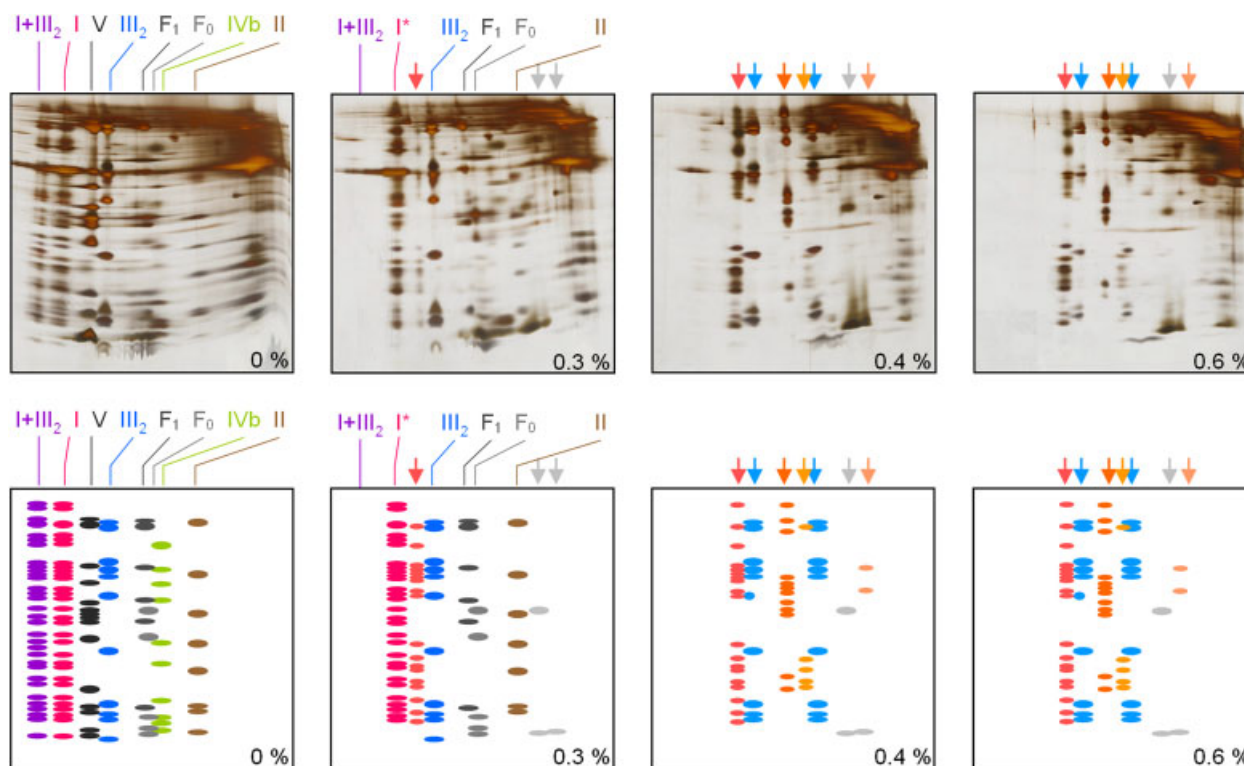


**Figure 2.** Effect of low-SDS pretreatment on the stability of mitochondrial protein complexes in Arabidopsis. Isolated mitochondria (1 mg) were resolved in solubilization buffer supplemented with 0, 0.3, 0.4, or 0.6% SDS as indicated and incubated for 5 min on ice. Subsequently, samples were supplemented with Coomassie blue and proteins were resolved by 2-D BN/SDS-PAGE. Gels were silver stained. The identities of protein complexes are given above the gels (for abbreviations, see Fig. 1) in different colors (I+III<sub>2</sub> supercomplex: purple; complex I: red; complex V: black; complex IV: green; complex II: brown). Generated subcomplexes are indicated by arrows and in lighter colors which correspond to the color of the respective holo-complex (complex I subcomplexes: orange to light red; complex V subcomplexes: light to dark gray; complex III<sub>2</sub> subcomplexes; middle blue). The results of further SDS pretreatment experiments are shown in Supporting Information Figs. 1 and 2.

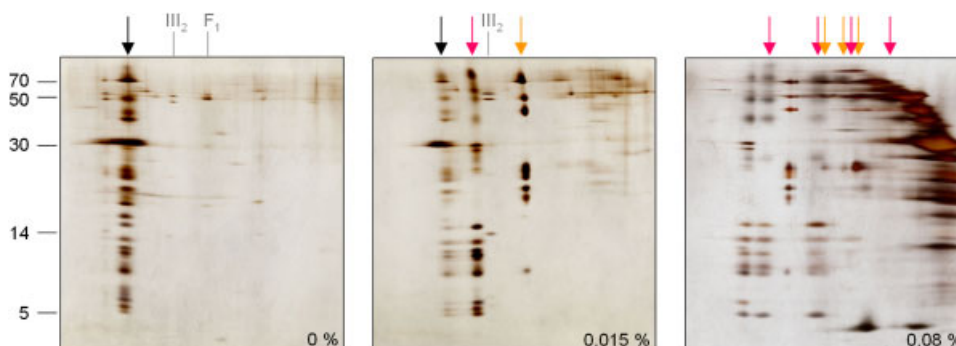


**Figure 3.** Effect of low-SDS on isolated complex I from Arabidopsis. Complex I was isolated as described under Section 2 and incubated for 5 min with 0, 0.015, and 0.08% SDS as indicated. Fractions were subsequently supplemented with Coomassie blue and the proteins resolved by 2-D BN-PAGE. The gels were stained with silver. The black arrow indicates subunits of intact complex I (left and central gel), the red arrow the membrane arm of complex I (central gel) and its subcomplexes (gel to the right), and the orange arrow the peripheral arm of complex I (central gel) and its subcomplexes (gel to the right). Identities of contaminating protein complexes are given in gray.

3-D BN (digitonin)/BN (low SDS)/SDS-PAGE system allows analyzing dissection products of individual protein complexes out of the protein mixtures without their previous purification.

## 4 Discussion

Here, we report the usage of SDS during BN-PAGE. Remarkably, pretreatment of protein fractions with low SDS

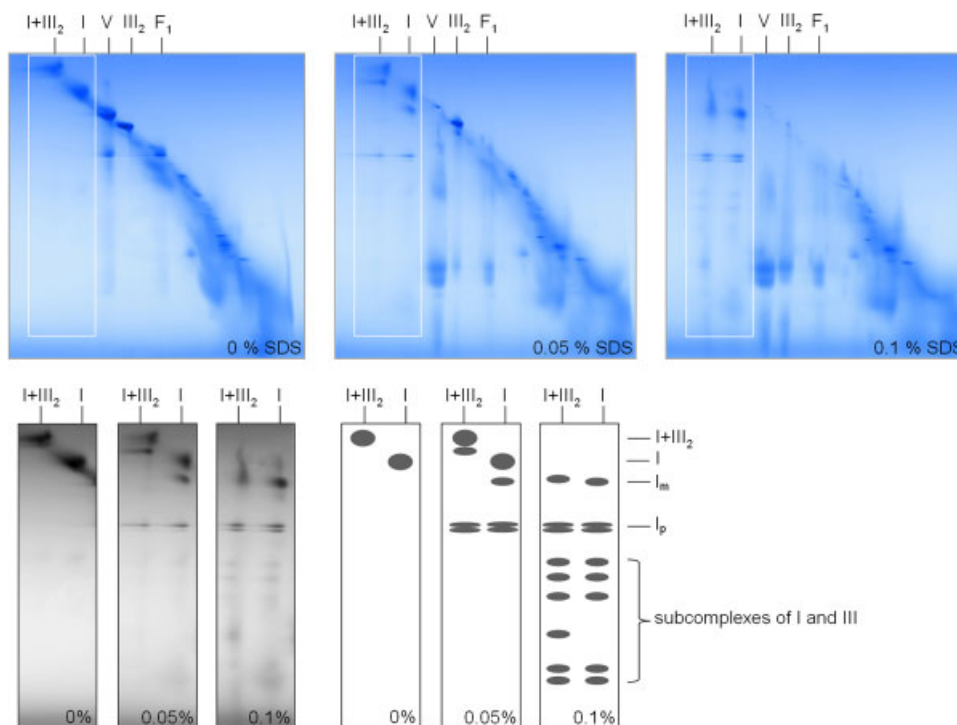


**Figure 4.** Separation of mitochondrial protein complexes by 2-D BN/PAGE in the presence of low-SDS during the run of the second gel dimension. Isolated mitochondria from Arabidopsis were prepared by standard treatment for the first dimension BN-PAGE (Section 2). After the gel electrophoresis run, a gel strip with separated protein complexes is incubated with 0, 0.05, or 0.1% SDS for 30 min. Finally, the gel strip is transferred horizontally onto another BN gel dimension. Insets of the resulting 2-D gels and corresponding schemes are given in the lower part of the figure. The identities of the protein complexes and subcomplexes are given above the gels and to the right of the schemes (for abbreviations, see Fig. 1).

concentrations leads to very distinct effects. Many protein complexes get dissected into subcomplexes at very defined SDS concentrations. Analysis of the subunit composition of these subcomplexes gives insights into the inner structure of large protein particles. This approach is not only applicable to mitochondrial protein complexes, but also to complexes from all subcellular compartments. Indeed, evaluation of subcomplex formation by BN-PAGE was used before for structural investigations, e.g. in proteasome research [18]. However, dissection of the proteasome occurred due to usage of the standard buffer conditions applied during BN-PAGE and rather reflects general instability of the proteasome. We suggest generating subcomplexes of protein particles by defined destabilizations using low concentrations of SDS. The concentrations used in our method are below the CMC of the detergent, which lies in the range of 0.5–8.0 mM depending on the salt concentration (0.5 mM at 500 mM NaCl, 8.0 mM in ddH<sub>2</sub>O [0.1% SDS, which is the highest SDS concentration used in the experiments shown in Figs. 2–4, corresponds to 3.5 mM SDS]). However, the suitable SDS concentrations for dissection of protein complexes should be empirically determined because they very much depend on protein and lipid concentration of a biological sample. For instance, under the conditions applied, 0.04% SDS was necessary to dissect complex I into its two arms in mitochondrial fractions but only 0.015% SDS in fractions containing purified complex I. If optimized carefully, low-SDS BN/SDS-PAGE should become a suitable tool for the analyses of protein complexes from various cellular fractions.

This work was supported by the Deutsche Forschungsgemeinschaft (DFG), grants Br1829/8-1 and Br1829/10-1.

The authors have declared no conflict of interest.

## 5 References

- [1] De Vito, E., Santomé, J. A., Disc electrophoresis of proteins in the presence of sodium dodecyl sulphate. *Experientia* 1966, 22, 124–125.
- [2] Shapiro, A. L., Viñuela, E., Maizel Jr J. V., Molecular weight estimation of polypeptide chains by electrophoresis in SDS-polyacrylamide gels. *Biochem. Biophys. Res. Commun.* 1967, 28, 815–820.
- [3] Weber, K., Osborn, M., The reliability of molecular weight determinations by dodecyl sulfate-polyacrylamide gel electrophoresis. *J. Biol. Chem.* 1969, 244, 4406–4412.
- [4] Laemmli, U. K., Cleavage of structural proteins during the assembly of the head of bacteriophage T4. *Nature* 1970, 227, 680–685.
- [5] Schägger H, von Jagow G., Blue native electrophoresis for isolation of membrane protein complexes in enzymatically active form. *Anal. Biochem.* 1991, 199, 223–231.
- [6] Fazekas de St Groth, S., Webster, R. G., Dwyer, A., Two new staining procedures for quantitative estimation of proteins on electrophoretic strips. *Biochim. Biophys. Acta* 1963, 71, 377–391.
- [7] Schägger, H., Pfeiffer, K., Supercomplexes in the respiratory chains of yeast and mammalian mitochondria. *EMBO J.* 2000, 19, 1777–1783.

- [8] Eubel, H., Braun, H. P., Millar, A. H., Blue-native PAGE in plants: a tool in analysis of protein-protein interactions. *Plant Methods* 2005, 1, 11.
- [9] Rivas, S., Romeis, T., Jones, J. D. G., The cf-9 disease resistance protein is present in an similar to 420-kilodalton heteromultimeric membrane-associated complex at one molecule per complex. *Plant Cell* 2002, 14, 689–702.
- [10] Camacho-Carvajal, M. M., Wollscheid, B., Aebersold, R., Steimle, V., Schamel, W. W. A., Two-dimensional blue native/SDS gel electrophoresis of multi-protein complexes from whole cellular lysates – a proteomics approach. *Mol. Cell. Proteomics* 2004, 3, 176–182.
- [11] Klodmann, J., Sunderhaus, S., Nimtz, M., Jansch, L., Braun, H. P., Internal architecture of mitochondrial complex I from *Arabidopsis thaliana*. *Plant Cell* 2010, 22, 797–810.
- [12] Werhahn, W., Niemeyer, A., Jansch, L., Kruf, V. et al., Purification and characterization of the preprotein translocase of the outer mitochondrial membrane from *Arabidopsis*. Identification of multiple forms of TOM20. *Plant Physiol.* 2001, 125, 943–954.
- [13] Wittig, I., Braun, H. P., Schägger, H., Blue-Native PAGE. *Nat. Protoc.* 2006, 1, 418–428.
- [14] Sunderhaus, S., Eubel, H., Braun, H. P., Two-dimensional blue native/blue native polyacrylamide gel electrophoresis for the characterization of mitochondrial protein complexes and supercomplexes. *Methods Mol. Biol.* 2007, 372, 315–324.
- [15] Neuhoff, V., Arold, N., Taube, D., Ehrhardt, W., Improved staining of proteins in polyacrylamide gels including isoelectric focusing gels with clear background at nanogram sensitivity using Coomassie Brilliant Blue G-250 and R-250. *Electrophoresis* 1988, 9, 255–262.
- [16] Heukeshoven, J., Dernick, R., Improved silver staining procedure for fast staining in PhastSystem Development Unit. I. Staining of sodium dodecyl sulfate gels. *Electrophoresis* 1988, 9, 28–32.
- [17] Eubel, H., Jansch, L., Braun, H. P., New insights into the respiratory chain of plant mitochondria. Supercomplexes and a unique composition of complex II. *Plant Physiol.* 2003, 133, 274–286.
- [18] Shibatani, T., Carlson, E. J., Larabee, F., McCormack, A. L. et al., Global organization and function of mammalian cytosolic proteasome pools: Implications for PA28 and 19S regulatory complexes. *Mol. Biol. Cell.* 2006, 17, 4962–4971.



# Defining the *Protein Complex Proteome* of Plant Mitochondria<sup>1[W]</sup>

Jennifer Klodmann, Michael Senkler, Christina Rode, and Hans-Peter Braun\*

Institute for Plant Genetics, Faculty of Natural Sciences, Leibniz Universität Hannover, D-30419 Hannover, Germany

A classical approach, protein separation by two-dimensional blue native/sodium dodecyl sulfate-polyacrylamide gel electrophoresis, was combined with tandem mass spectrometry and up-to-date computer technology to characterize the mitochondrial “protein complex proteome” of *Arabidopsis* (*Arabidopsis thaliana*) in so far unrivaled depth. We further developed the novel GelMap software package to annotate and evaluate two-dimensional blue native/sodium dodecyl sulfate gels. The software allows (1) annotation of proteins according to functional and structural correlations (e.g. subunits of a distinct protein complex), (2) assignment of comprehensive protein identification lists to individual gel spots, and thereby (3) selective display of protein complexes of low abundance. In total, 471 distinct proteins were identified by mass spectrometry, several of which form part of at least 35 different mitochondrial protein complexes. To our knowledge, numerous protein complexes were described for the first time (e.g. complexes including pentatricopeptide repeat proteins involved in nucleic acid metabolism). Discovery of further protein complexes within our data set is open to everybody via the public GelMap portal at [www.gelmap.de/arabidopsis\\_mito](http://www.gelmap.de/arabidopsis_mito).

The proteome of *Arabidopsis* (*Arabidopsis thaliana*) mitochondria has been extensively characterized by gel-based and gel-free strategies (Kruft et al., 2001; Millar et al., 2001; Heazlewood et al., 2004, 2007; Lee et al., 2011; Taylor et al., 2011). Based on these projects, more than 500 proteins were assigned to mitochondria in *Arabidopsis*. However, targeting prediction software tools assign more than 1,500 proteins encoded by the *Arabidopsis* genome to this subcellular compartment. Therefore, it is concluded that most mitochondrial proteins, especially those of low abundance and/or high hydrophobicity, remain to be discovered. Many mitochondrial proteins form part of protein complexes (e.g. the complexes of the respiratory chain). However, again, only the complexes of high abundance could be characterized, while the ones of low abundance so far are not known.

Two-dimensional (2D) blue native (BN)/SDS-PAGE represents an alternative gel-based approach to analyze the mitochondrial proteome. Native gel electrophoresis is used for the first gel dimension to separate protein complexes, which are resolved into their subunits on a second gel dimension in the presence of SDS (Schägger and von Jagow, 1991). BN/SDS-PAGE is an

ideal gel system for the analysis of protein complexes. At the same time and in contrast to the conventional 2D isoelectric focusing/SDS-PAGE system, detection of hydrophobic proteins is facilitated. The only disadvantage of BN/SDS-PAGE is a slightly reduced resolution of the resulting gels. Therefore, BN/SDS-PAGE was not used for broad-scale identification of proteins from plant mitochondria so far. The BN/SDS-PAGE analyses published to date allowed the identification of limited sets of proteins forming part of the mitochondrial proteome of potato (*Solanum tuberosum*; Jänsch et al., 1996 [16 proteins]; Bykova et al., 2003a [eight proteins]), *Arabidopsis* (Werhahn and Braun, 2002 [14 proteins]; Giegé et al., 2003 [26 proteins]), rice (*Oryza sativa*; Heazlewood et al., 2003b [57 proteins]; Millar et al., 2004b [18 proteins]), and *Arum maculatum* (Sunderhaus et al., 2010 [nine proteins]). Furthermore, 2D BN/SDS-PAGE was extensively used to systematically analyze subunits of individual protein complexes of plant mitochondria, like complex I (Heazlewood et al., 2003a; Millar et al., 2003; Sunderhaus et al., 2006; Meyer et al., 2007, 2008; Klodmann et al., 2010; Klodmann and Braun, 2011), complexes II and IV (Eubel et al., 2003; Millar et al., 2004a; Huang et al., 2010), complex III (Meyer et al., 2008), complex V (Heazlewood et al., 2003c; Meyer et al., 2008), the I+III<sub>2</sub> supercomplex (Peters et al., 2008), the formate dehydrogenase complex (Bykova et al., 2003b), and the TOM complex (Jänsch et al., 1998; Werhahn et al., 2001, 2003).

Meanwhile, mass spectrometry (MS) and appendant software tools have much improved. Therefore, we decided to reuse BN/SDS-PAGE for a first broad-scale proteomic analysis of plant mitochondria based on this experimental system. Overall, 471 unique proteins

<sup>1</sup> This work was supported by the Deutsche Forschungsgemeinschaft (grant no. Br 1829/10–1).

\* Corresponding author; e-mail [braun@genetik.uni-hannover.de](mailto:braun@genetik.uni-hannover.de).

The author responsible for distribution of materials integral to the findings presented in this article in accordance with the policy described in the Instructions for Authors ([www.plantphysiol.org](http://www.plantphysiol.org)) is: Hans-Peter Braun ([braun@genetik.uni-hannover.de](mailto:braun@genetik.uni-hannover.de)).

<sup>[W]</sup> The online version of this article contains Web-only data.

[www.plantphysiol.org/cgi/doi/10.1104/pp.111.182352](http://www.plantphysiol.org/cgi/doi/10.1104/pp.111.182352)

were identified in 200 gel spots excised from a single BN gel. The new 2D gel presentation software tool GelMap was further developed to allow a systematic exploration of the “protein complex proteome” of plant mitochondria. Evidence for the occurrence of at least 35 different protein complexes in Arabidopsis mitochondria is presented, several of which are described, to our knowledge, for the first time (e.g. protein complexes including the plant-specific pentatricopeptide repeat (PPR) proteins). The protein complex proteome of Arabidopsis mitochondria as defined by our study so far consists of more than 200 distinct proteins. Results of our investigation are presented at [www.gelmap.de/arabidopsis\\_mito](http://www.gelmap.de/arabidopsis_mito).

## RESULTS AND DISCUSSION

### Separation of Mitochondrial Proteins from Arabidopsis by 2D BN/SDS-PAGE

Mitochondrial fractions of 10 independent mitochondrial isolations from Arabidopsis cell suspension cultures were separated by 2D BN/SDS-PAGE as described in “Materials and Methods.” The resulting gels were highly reproducible, as revealed by gel comparisons using the Delta 2D 4.2 software package (data not shown). A typical gel (Fig. 1) was selected for further analyses. The most prominent 200 spots were excised and analyzed by electrospray tandem MS. On average, six different proteins were identified per spot. Identifications were accepted if supported by MS reliability scores (Mascot) and by at least two matching peptides per protein (for details, see Supplemental Table S1). However, in some cases, single peptide hits were accepted for identification if other lines of evidence were present (e.g. data from previous publications). Primary data of all MS identifications are available in Supplemental Table S1 and at [www.gelmap.de/arabidopsis\\_mito](http://www.gelmap.de/arabidopsis_mito) (at this site, tables are accessible directly by clicking the table symbol in the top right corner of the digital reference map). Overall, 1,160 proteins were identified within the 200 spots that represent 471 unique proteins. For all spots, values for apparent molecular mass were determined based on a precise scaling of the 2D BN/SDS gel as given in Figure 2.

### Evaluation of Organelle Purity

To assess the purity of mitochondrial fractions, the subcellular localizations of all identified proteins were evaluated using the Arabidopsis SubCellular Proteomic Database (SUBA II; <http://suba.plantenergy.uwa.edu.au/>). This database summarizes all experimental and computer prediction data for subcellular localizations of proteins in Arabidopsis (Heazlewood et al., 2005, 2007). Of the overall 200 analyzed gel spots, 194 of the “first hit” identifications (97%) represent mitochondrial proteins according to experimental evidence given in the SUBA II database (Supplemental Table S2.1). Evaluation of all 471 unique proteins by the

SUBA II database is more complicated. Many proteins of this data set are of very low abundance and consequently have not been assigned to a subcellular localization by experimental data yet. Overall, experimental evidence for the subcellular localization of 23% of the unique proteins has not been obtained according to SUBA II (Supplemental Table S2.2). A total of 57% of the identified unique proteins represent known mitochondrial proteins, and another 20% are assigned to other cellular compartments like plastids (9%), peroxisomes (2%), or the plasma membrane (8%). However, most of the unassigned proteins are localized in mitochondria according to targeting prediction computer programs and therefore represent candidates for new constituents of this subcellular compartment. Furthermore, identifications of proteins assigned to other subcellular compartments in most cases are based on only a few peptides (resulting in a comparatively low MS reliability score), which indicates that these proteins are of rather low abundance in our fraction. Therefore, evaluation of our MS data set using SUBA II was repeated based on the identified peptides of all proteins (Supplemental Table S2.3). Of the overall 6,992 peptides, 6,204 peptides belong to known mitochondrial proteins (89%). A comparatively low number of 346 peptides (5%) are assigned to known nonmitochondrial proteins. Another 442 peptides (6%) are of unknown subcellular localization

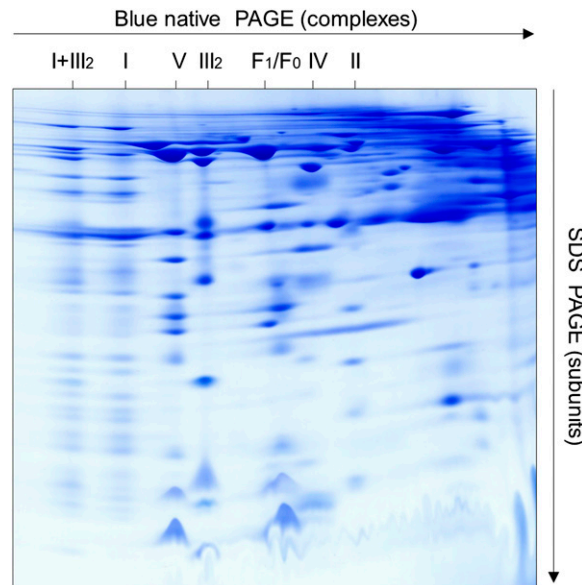


**Figure 1.** Analysis of the mitochondrial proteome of Arabidopsis by 2D BN/SDS-PAGE. Freshly isolated mitochondria (1 mg of mitochondrial protein) were solubilized by digitonin (5 g detergent g<sup>-1</sup> protein), supplemented with Coomassie blue and loaded onto the 2D gel system. After electrophoresis, the gel was stained by Coomassie blue-colloidal. The identity of the OXPHOS complexes is given above the gel. I+III<sub>2</sub>, Supercomplex composed of complex I and dimeric complex III; I, complex I; V, complex V (ATP synthase); III<sub>2</sub>, dimeric complex III; F<sub>1</sub>, F<sub>1</sub> part of ATP synthase; F<sub>0</sub>, F<sub>0</sub> part of ATP synthase; IV, complex IV; II, complex II.



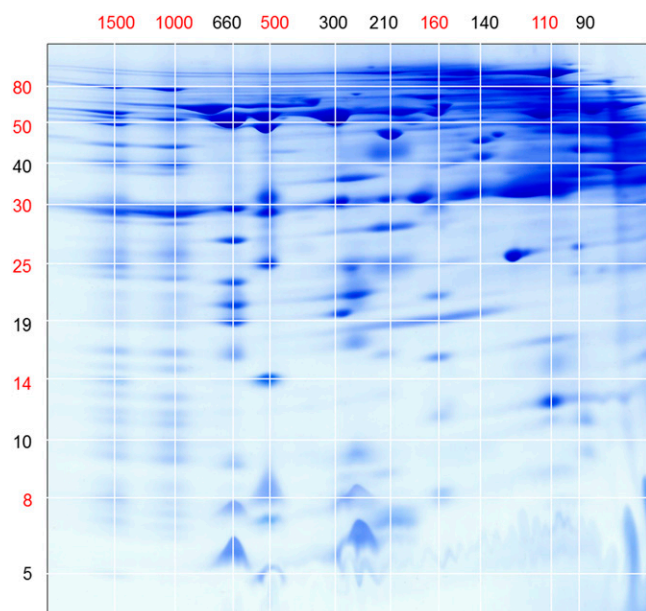


**Figure 2.** Molecular mass scale for the gel shown in Figure 1. The numbers refer to molecular masses (in kD). Masses used for calibration are given in red. BN gel dimension (horizontal) is as follows: I+III<sub>2</sub> supercomplex (1,500 kD), complex I (1,000 kD), dimeric complex III (500 kD), complex II (160 kD), and aconitate hydratase (110 kD). SDS gel dimension (vertical) is as follows: 75-kD subunit of complex I (spot 171),  $\alpha$ -MPP (52 kD; spot 47), prohibitin (30 kD; spot 175), FeS subunit of complex III (23 kD; spot 53), QCR7 subunit of complex III (14 kD; spot 54), and the QCR8 subunit of complex III (8 kD; spot 56). Masses between those used for calibration were calculated with Eureka software (version 0.83  $\beta$ ; [www.eureka.com](http://www.eureka.com)).

because experimental data are lacking so far. However, most of the corresponding proteins are predicted to be localized in mitochondria (Supplemental Table S3). Therefore, the unassigned peptides/proteins represent candidates for newly identified mitochondrial proteins. Based on the different evaluation results, we finally concluded that our organellar fraction has a purity in the range of 93% to 95%.

### Annotation of the Protein Complex Proteome of Arabidopsis Mitochondria

The novel GelMap annotation software package was used for online data presentation. GelMap was recently developed to functionally annotate 2D isoelectric focusing/SDS gels (Rode et al., 2011). The original software proved not to be suitable for the annotation of 2D BN/SDS gels because spots in general include several different proteins. Therefore, we upgraded the application range of GelMap for the assignment of lists of proteins to individual spots. Since all proteins are annotated according to distinct functions and protein complexes, the software now allows one to selectively display unknown protein complexes based on the vertical positioning of their subunits on a 2D BN gel.

For GelMap annotation, the image file of the 2D BN/SDS gel (Fig. 1) was loaded into the Delta 2D 4.2

software package for automated spot detection. A spot coordination (coord) file was generated by Delta 2D and exported into Excel. This Excel coord table was extended by several columns to add further details for all 1,160 identified proteins, like statistical values (Mascot score, number of peptides, coverage), biological values (calculated molecular mass, apparent molecular mass on the first gel dimension [native conditions] and the second gel dimension [denaturing conditions]), protein accession number, protein name, assignment to a protein complex and to a physiological process and to a subcellular compartment (Table I; Supplemental Table S1). The image file and coord table were both loaded into GelMap at [www.gelmap.de](http://www.gelmap.de). The how-to area of the GelMap Web site provides all information necessary to prepare and upload a data set (<http://gelmap.de/howto>). Based on the GelMap software package, the content of the columns of the coord table is automatically displayed on the map in pop-ups linked to the spots or in a menu to the right of the gel image, which includes information concerning the assignment of the proteins to protein complexes or functional categories (Fig. 3; Supplemental Fig. S2). By clicking on a spot, names of all included proteins and their MS reliability scores are listed in a pop-up window (Fig. 4), and by clicking on a protein name, further information is displayed, including a “more protein details” link at the bottom, which gives access to the coord table, including all information available for the protein of interest. A “more peptide details” link leads to a second table indicating peptide-specific information (e.g. ion score of a peptide, its amino acid sequence, and its modifications). In case a spot only includes a single protein, the additional information pop-up is displayed directly. Features best can be followed if directly tested on the Internet ([www.gelmap.de/arabidopsis\\_mito](http://www.gelmap.de/arabidopsis_mito)). Proteins detected within the same spot are sorted according to their Mascot scores (column 2 in Supplemental Table S1). In general, we interpret that high scores (resulting from high scores for the identified peptides and/or many identified unique peptides) reflect high abundance of a protein. However, this assumption is not always correct, because the Mascot scores also depend on the biochemical properties of proteins.

### The Protein Complex Proteome of Arabidopsis Mitochondria

The annotation of the Arabidopsis mitochondrial proteome as generated by GelMap offers several advantages. First of all, it allows easy access to protein identification data of large proteome data sets based on functional categorization. But more importantly, it specifically allows searching for protein complexes of low abundance, which are positioned at the same location on the gels as protein complexes of high abundance, like the complexes of the oxidative phosphorylation system. The low-abundance protein complexes in most cases have comparatively low MS

**Table I.** Column content of the results table presented in Supplemental Table S1

Column (from Left to Right)	Content	Comment
1	Spot number	Spot number on the 2D BN/SDS gel (Figure 3)
2	Mascot score	Probability score for the protein identification ( <a href="http://www.matrixscience.com">www.matrixscience.com</a> )
3	No. of peptides	No. of unique peptides matching to a protein hit
4	Coverage	Sequence coverage of a protein by the identified peptides
5	Calculated molecular mass	Calculated molecular mass of the protein (note that in many cases, presequences are cleaved off from nucleus-encoded mitochondrial proteins after their transfer into mitochondria is completed; as a consequence, the apparent molecular mass is 1–8 kD smaller than predicted)
6	Apparent molecular mass, second dimension	Apparent molecular mass as determined on the second gel dimension (for mass determination, see Fig. 2)
7	Apparent molecular mass, first dimension	Apparent molecular mass as determined on the first gel dimension (for mass determination, see Fig. 2)
8	Accession number, Arabidopsis Genome Initiative	Accession numbers according to the TAIR database ( <a href="http://www.arabidopsis.org/">http://www.arabidopsis.org/</a> ); numbers are linked to protein entries of the TAIR database
9	Name of protein	Assigned mitochondrial protein complex (in many cases according to precise location on the same vertical line on the 2D BN/SDS gel)
10	Protein complex	
11	Physiological category	Seven categories were defined: (a) oxidative phosphorylation; (b) pyruvate metabolism and TCA cycle; (c) transport; (d) protein folding and processing; (e) processing of nucleic acids; (f) other metabolic pathways; and (g) uncharacterized
12	Subcellular localization	Subcellular localization according to the SUBA II database ( <a href="http://suba.plantenergy.uwa.edu.au/">http://suba.plantenergy.uwa.edu.au/</a> )
13	Database	Database used for protein identification (T = TAIR [ <a href="http://www.arabidopsis.org/">http://www.arabidopsis.org/</a> ], database release 10)
14	Coordinate on the x axis	Generated by Delta 2D
15	Coordinate on the y axis	Generated by Delta 2D
16	Spot number	Copy of column 1 for better readability of the table

reliability scores, which nevertheless are clearly above the threshold. Using the categorization tools offered by GelMap, their positioning along a vertical line becomes visible, allowing one to deduce new protein-protein interactions. The following 35 protein complexes were found in the course of the project (for summary, see Table II).

#### The I+III<sub>2</sub> Supercomplex (1,500 kD) and Complex I (1,000 kD)

Subunits present within plant complex I recently were systematically characterized (Klodmann et al., 2010; Klodmann and Braun, 2011). Currently, 48 different subunits are known, seven of which occur in pairs of isoforms. In the frame of our study, 44 subunits were detected in monomeric complex I. Four subunits were not found (ND4L [AtMg00650], 13-kD subunit [At3g03070], and the plant-specific subunits At5g14105 and At1g68680). Subunit ND4L was never identified in any proteomic study, probably due to its extreme hydrophobicity. The plant-specific subunit At1g68680 (8.3-kD protein), which was described by Meyer et al. (2008), is present on our 2D gel map but at a position far away from complex I (spot 168; 60-kD range with respect to the native gel dimension). It could have been detached from complex I during

solubilization, or it may represent an erroneously identified complex I subunit. Most of the identified subunits of complex I also were found in the 1,500-kD I+III<sub>2</sub> supercomplex.

Four additional proteins were discovered in our study, which represent candidates for newly identified complex I subunits: At3g10110 (spot 17), At1g18320 (spot 186), At1g72170 (spots 149 and 151), and At2g28430 (spot 154). The first two subunits represent isoforms and resemble proteins of the TIM preprotein translocase family. Interestingly, another complex I subunit, the so-called “B14.7” protein, exhibits similarity to the proteins of the TIM family (Carroll et al., 2002). Three of the four new subunits were found both in the 1,500-kD supercomplex and in monomeric complex I, supporting their assignment as complex I subunits (one new subunit, At2g28430, was detected only in the supercomplex).

Complex I subunits were additionally detected in 27 spots not forming part of the vertical rows of spots representing the I+III<sub>2</sub> supercomplex or monomeric complex I. All these subunits migrate on the second gel dimension at a lower molecular mass than on the first gel dimension. At the same time, their MS reliability scores are low, most likely indicating their comparatively low abundance. Interestingly, several of these complex I subunits form part of vertical rows of

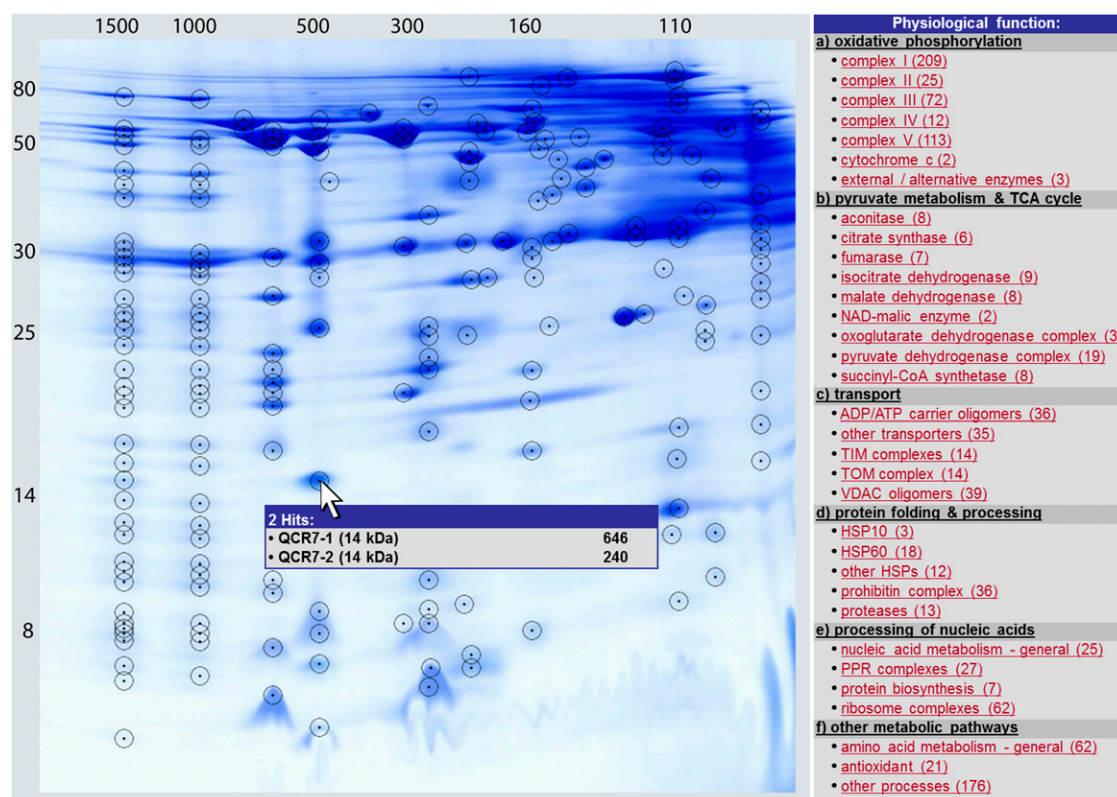


**Figure 3.** Reference map of the protein complex proteome of Arabidopsis mitochondria as presented in GelMap ([www.gelmap.de/arabidopsis\\_mito](http://www.gelmap.de/arabidopsis_mito)). Protein spots identified by MS are circled. Most spots include multiple proteins. The menu to the right offers functional classifications of subunits according to physiological functions and protein complexes. The numbers in parentheses refer to the number of identified proteins per individual complex. Upon clicking on a protein complex, names of all its subunits become available (Supplemental Fig. S2). Detailed information on spots is given upon clicking on the encircled spots on the 2D image (see Fig. 4). The GelMap software package also has different search options (e.g. for a distinct protein by name or accession number). The search options are located beneath the menu to the right of the gel image (not shown here). For further features of GelMap, see [www.gelmap.de/arabidopsis\\_mito](http://www.gelmap.de/arabidopsis_mito).

spots on the 2D gel, indicating the presence of complex I breakdown products or assembly intermediates in our mitochondrial fraction. For instance, four complex I subunits of the membrane arm of complex I (Klodmann et al., 2010) were identified in vertical alignment close to the ATP synthase complex (650 kD). Also, in most other cases, the positions of complex I subunits separated from the holoenzyme nicely correlate with the positions of known complex I subcomplexes (Klodmann et al., 2010). This illustrates the suitability of the GelMap software tool to identify protein complexes of low abundance (e.g. assembly intermediates of OXPHOS complexes).

### The ATP Synthase Complex (Complex V)

Based on our molecular mass calibration (Fig. 2), complex V runs at 660 kD on the native gel dimension. Fourteen subunits have been reported for Arabidopsis (Heazlewood et al., 2003c; Meyer et al., 2008), all of which are included in our map except for subunit c, which is small and very hydrophobic. Additionally, a homolog of subunit g from other groups of eukaryotes

was detected in the low native mass range (14-kD protein; present in three isoforms: At4g29480, At2g19680, and At4g26210; spots 164 and 165). In yeast, this subunit only is associated with ATP synthase within the dimeric ATP synthase supercomplex (Arnold et al., 1998). Under the conditions applied during our investigation, ATP synthase dimers are not stabilized. Since subunit g is completely detached from the ATP synthase monomer on our 2D gel, it probably also represents a dimer-specific protein in Arabidopsis.

The more hydrophobic subunits of complex V, especially subunits a and b, were identified in several neighboring spots and therefore are difficult to precisely localize on our map. Our interpretation of the assignment of these subunits to the spots on the 2D gel is given in Supplemental Figure S1.

On our 2D gel (Fig. 1), the known  $F_1$  and  $F_0$  subcomplexes run at 300 and 260 kD. The relatively high abundances of these subcomplexes indicate that they represent breakdown products rather than assembly intermediates.  $F_1$  includes subunits  $\alpha$ ,  $\beta$ ,  $\gamma$ ,  $\delta$ , and  $\epsilon$ , and  $F_0$  includes subunits a, d, 8, OSCP, ATP17 (plant specific), and 6 (plant specific). The FAD subunit



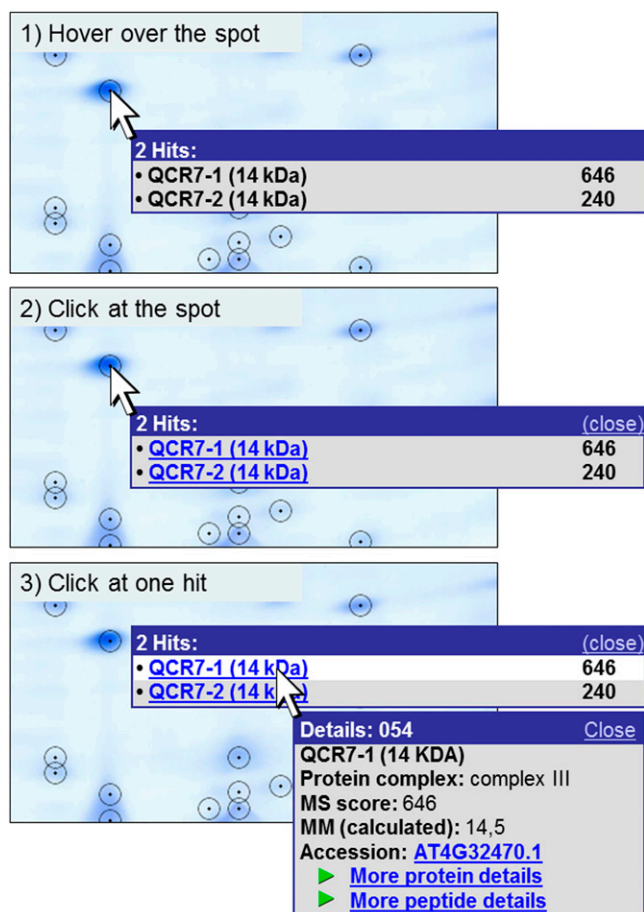


**Figure 4.** Pop-up function on the gel map. Information about the proteins identified in a spot can be viewed directly on the gel image. The user can hover over a spot (1) that opens a tooltip containing the names of all included proteins (left) as well as their MS reliability scores (right). By clicking on the spot (2), the window is fixed, and protein names are hyperlinked to more detailed information. Protein details become visible in a new window by clicking on the protein of interest (3). If only one protein is identified in a spot, the first click on the spot already opens the details window shown in 3. This window contains (from top to bottom): spot number (in the blue frame), protein name, dedicated protein complex, MS reliability score, the calculated molecular mass, and the Accession number (according to TAIR), which is linked to the respective entry on the TAIR homepage ([www.arabidopsis.org](http://www.arabidopsis.org)). The “more protein details” link at the bottom of the details window is linked to a table showing all proteins identified in the respective spot (Supplemental Table S1). Besides the characteristics already given in the pop-up window, it contains further information about spot characteristics (such as coordinates and apparent masses), MS analysis, and the physiological context of the proteins (Table I). The “more peptide details” link leads to a table that includes details of the peptides identified by MS.

does not form part of the two subcomplexes but was only detectable within the holocomplex or as a singular protein (spots 132 and 133).

Subunits of complex V additionally were detected within several other spots not forming part of the vertical rows of spots representing the holocomplex or the  $F_1$  and  $F_0$  subcomplexes, especially in the low

native mass range. These proteins may form part of smaller complex V subcomplexes or assembly intermediates.

### Cytochrome *c* Reductase (Complex III; 500 kD)

This central complex of the OXPHOS system has 10 subunits in plants (Braun and Schmitz, 1995; Meyer et al., 2008), all of which are included in our map. For the first time to our knowledge, the so-called “hinge” subunit (QCR6) was detected for Arabidopsis. Six of the subunits are present in pairs of isoforms ( $\alpha$ -MPP, cytochrome  $c_1$ , FeS protein, QCR6, QCR7, and QCR8). All 10 subunits also form part of the I+III<sub>2</sub> supercomplex. No subcomplexes of complex III were detected, further supporting its extraordinary stability (Heinemeyer et al., 2009).

### Cytochrome *c* Oxidase (Complex IV)

On BN/SDS gels, complex IV usually is found in a larger (230 kD) and a smaller (200 kD) form. The smaller form lacks Cox VIb and possibly other subunits (Eubel et al., 2003). On our BN/SDS reference gel, complex IV is present in the smaller form. Its apparent molecular mass was determined to be 207 kD. For Arabidopsis, 14 different subunits were described, until now termed Cox I, Cox II, Cox III, Cox Vb, Cox Vc, Cox VIa, Cox VIb, Cox VIc, and Cox X1 to Cox X6 (Millar et al., 2004a). The Cox X1 to X6 subunits are plant specific. The map includes Cox II, Cox Vc, Cox X2, and Cox X4. The Cox I, Cox III, and Cox Vb subunits are visible on the gel but peptides could not be detected, most likely due to the extreme hydrophobicity of these proteins. Currently, further efforts are being made to identify these subunits and include them in the online version of GelMap. The Cox X6 subunit was found in gel regions representing larger native masses and therefore might only be included in the larger form of complex IV. Some of the complex IV subunits occur in two or more isoforms (Millar et al., 2004a), several of which were detected in the frame of our project.

### Succinate Dehydrogenase (Complex II)

The holocomplex has a size of 160 kD and consists of eight subunits termed SDH1 to SDH8, four of which are plant specific (SDH5–SDH8; Eubel et al., 2003; Millar et al., 2004a). All these proteins except SDH8 are included in our map (SDH8 migrates at the dye front on the 2D BN/SDS gel). Some proteins occur in isoforms. All subunits except SDH5 also are present in a smaller form of complex II, which runs at about 100 kD. Analyses by BN PAGE revealed that complex II gets dissected into two subcomplexes that comigrate at this position on the native gel dimension (S. Sunderhaus and H.P. Braun, unpublished data).

**Table II.** *The protein complex proteome of Arabidopsis mitochondria*

Protein Complex	Apparent Molecular Mass <sup>a</sup>	Composition	No. of Different Subunits Included in the Map <sup>b</sup> (+No. of Additional Subunits Not Found in This Study)		Additional Isoforms <sup>c</sup>
	kD				
I+III <sub>2</sub> supercomplex	1,500	Heterooligomer	All subunits of complex I and III		–
Complex I	1,000	Heterooligomer	44 + 3 <sup>d</sup>	(+4)	8
Prohibitin	1,000	Homooligomer	1		6
HSP60 complex	783	Homo-14-mer	1		5
Membrane arm, complex I	660	Heterooligomer	Approximately 35 subunits of complex I		–
Complex V	660	heterooligomer	14	(+1)	2
Complex III	500	Heterooligomer	10		6
PPR2 complex	369	Homooligomer (?)	1 + X		1
NAD malic enzyme	369	Heterohexamer	2		0
F <sub>1</sub> part of complex V	300	Heterooligomer	Five subunits of complex V		–
TOM complex	260	Heterooligomer	4	(+2)	6
F <sub>0</sub> part of complex V	260	Heterooligomer	Seven subunits of complex V		–
Clp protease complex	260	Homo-14-mer	1		0
Oxoglutarate DH-E1	210	Homodimer	1		1
PPR3 complex	209	Homooligomer (?)	1 + X		0
Lon protease	209	Homodimer	1		3
Glu dehydrogenase	209	Homo-hexamer	1		2
Complex IV	207	Heterooligomer	6	(+8)	8
Fumarase	200	Homotetramer	1		1
Complex II	160	Heterooligomer	7	(+1)	5
PPR1 complex	160	Homooligomer (?)	1 + X		0
Isocitrate DH	160	Homotetramer	1		3
Malate DH	160	Homotetramer	1		2
Alternative ND (NDA + NDB)	160	Heterotrimer	2		4
PPR5 complex	156	Homooligomer (?)	1 + X		1
Metaxin/SAM complex (?)	150	Heterooligomer	1		0
Arginase	150	Homotrimer	1		1
Pyruvate DH-E1	138	Heterotetramer	2		1
Isovaleryl-CoA dehydrogenase	132	Homotetramer (?)	1		0
TIM23 complex	115	Heterooligomer	2	(+4)	2
Citrate synthase	110	Homodimer	1		1
HSP10 complex	108	Homoheptamer	1		1
Voltage-dependent anion channel complexes	90/180	Homotri/hexamers	1		4
ADP/ATP translocase	60/120	Homodi/tetramers	1		2
TIM9-10 complex	86	Heterohexamer	2		0
Σ <sup>e</sup> (35 complexes)	86–1,500		118	(+20)	76

<sup>a</sup>Apparent molecular mass as determined in this study. <sup>b</sup>Without isoforms. <sup>c</sup>Based on the genome sequence. Note that not all isoforms were detected in the frame of this project. <sup>d</sup>Three new complex I subunits were discovered in the frame of this project. <sup>e</sup>Subunits detected in a holocomplex and in subcomplexes only were counted once.

### Cytochrome *c*

The intermembrane space protein cytochrome *c*, which translocates electrons from complex III to complex IV, occurs as a monomer of 12 kD but also was detected in the native range of about 100 kD. It is positioned on a vertical line together with the cytochrome *c*-binding enzyme L-galactono-1,4-lactone dehydrogenase. We speculate that these two proteins form a protein complex of about 100 kD.

### Alternative NAD(P)H Dehydrogenases

Alternative NAD(P)H dehydrogenases are encoded by two gene families in *Arabidopsis* termed NDA (two genes) and NDB (four genes; Michalecka et al., 2003).

On our map, we found the NDA2, NDB2, and NDB4 proteins (spots 96 and 94). Molecular masses of the monomeric precursor proteins are in the range of 56 to 65 kD. All proteins were detected in the 160-kD range of the native gel dimension. Similar results were previously reported for NDA2 (Rasmusson and Agius, 2001). We postulate that the NDA and NDB proteins might form a protein complex that probably has a heterotrimeric structure.

### Protein Complexes of Tricarboxylic Acid Cycle Enzymes

All enzymes of the tricarboxylic acid (TCA) cycle are included in our map. Due to horizontal and vertical smearing effects of the BN/SDS gel, most proteins

were identified within several spots. However, based on their Mascot scores, conclusions can be drawn concerning their main locations on the map. In accordance with reports in the literature, three enzymes, fumarase, isocitrate dehydrogenase, and malate dehydrogenase, have a homotetrameric structure (Table II). Citrate synthase most likely represents a homodimer (spot 118). Furthermore, the E1 subunit of the 2-oxoglutarate dehydrogenase complex forms a homodimer (spot 77). In contrast, aconitase can only be found as a monomer on the gel (spots 114 and 201). Succinyl-CoA synthetase consists of an  $\alpha$ -subunit (spot 130) and a  $\beta$ -subunit (spots 119 and 202), but evidence for the interaction of these two subunits is not obvious in our map. Finally, as reported above, succinate dehydrogenase (complex II of the respiratory chain) is a heterooligomer composed of eight distinct subunits in plants. Most TCA cycle enzymes are present in multiple isoforms. It currently cannot be decided if the homooligomeric TCA cycle protein complexes are composed of multiple copies of identical or distinct isoforms. Further biochemical analyses are necessary to validate and characterize the new protein complexes identified by this approach.

### Pyruvate Dehydrogenase Complex

Pyruvate dehydrogenase probably is the largest protein complex of the mitochondrial matrix. It is composed of numerous copies of the E1- $\alpha$ , E1- $\beta$ , E2, and E3 subunits and has an overall molecular mass of about 9.5 MD (Zhou et al., 2001). The holoenzyme was outside of the molecular mass limit of our BN/SDS gel. However, subcomplexes were found. A tetramer composed of two E1- $\alpha$  (spot 110) and two E1- $\beta$  (spot 104) subunits runs at about 140 kD on the native gel dimension (Table II). Furthermore, much larger protein associations were detected that include the E3 subunit (spots 3, 31, 96, and 172).

### NAD Malic Enzyme

NAD malic enzyme forms a protein complex of about 370 kD (spot 59). It is composed of two distinct subunits of about 60 kD each. The protein complex, therefore, probably has a hexameric structure. In the literature, different oligomeric structures were reported for this enzyme complex that range from dimeric to octameric (Jenner et al., 2001).

### The Preprotein Translocase of the Outer Mitochondrial Membrane (the TOM Complex)

The core of the TOM complex consists of six distinct subunits: TOM40, TOM20, TOM22 (TOM9), TOM7, TOM6, and TOM5 (Werhahn et al., 2001, 2003). Its native molecular mass is 260 kD on our 2D gel, slightly smaller than reported before. All subunits are included in our map, except for the very small TOM5 and TOM6 proteins, which migrate within the dye

front of the second dimension gel. The preprotein receptor TOM20 occurs in several isoforms. One protein of unknown function comigrates with the TOM complex on the 2D gel (At3g49240; spot 62). It has a size of 70.2 kD and contains a tetratricopeptide motif like the TOM70 preprotein receptor, which was characterized for fungal and mammalian mitochondria. It currently cannot be decided if this protein physically interacts with the TOM complex in Arabidopsis. Metaxin (36 kD), another outer membrane protein involved in protein translocation, runs at 150 kD on the native gel dimension.

### Preprotein Translocases of the Inner Mitochondrial Membrane (the TIM Complexes)

Four distinct TIM complexes are known, which are designated TIM22, TIM23, TIM9/10, and TIM9/13 complexes according to the protein components included (Lister et al., 2005, 2007). Only two of these complexes clearly were identified on our map: (1) the TIM 9/10 complex, which has a hexameric structure (three TIM9 and three TIM10 proteins; Baker et al., 2009), is located in the mitochondrial intermembrane space and runs at about 86 kD on the BN gel dimension; and (2) the TIM23 complex, which runs at about 110 kD and includes at least the TIM17 and TIM44 subunits. Another TIM complex, which includes the TIM21 protein, runs at about 150 kD. TIM21 represents a nonessential subunit of the TIM23 complex. Its binding partners were not identified in the course of our study. As already mentioned above, two subunits resembling TIM proteins form part of complex I and the I+III<sub>2</sub> supercomplex in plants (At3g10110/At1g18320 and At2g42210; spots 17, 186, 147, and 148).

### The ADP/ATP Translocase and Other Members of the Mitochondrial Metabolite Carrier Family

The ADP/ATP translocase runs at 30 kD on the second gel dimension. On the native gel dimension, it smears from 30 kD to about 1,500 kD. However, highest Mascot scores clearly are in the 60- to 120-kD range, indicating dimeric to tetrameric structures. Several isoforms occur that may be combined or separated within the oligomers. The ADP/ATP translocase is known to have a large N-terminal extension that is removed upon import but dispensable for protein targeting (Emmermann et al., 1991; Winning et al., 1992; Mozo et al., 1995). Possibly, this precursor protein should be considered to represent a polyprotein that is cleaved into two separate polypeptides, the smaller of which is of unknown function. Similar to the results obtained for the ADP/ATP translocase, other members of the mitochondrial metabolite carrier family were predominantly found in the 60- to 120-kD region (e.g. members of the dicarboxylate and tricarboxylate carrier subfamilies, the phosphate translocase, and the plant uncoupling protein).

### Porin Complexes

“Porin” of the outer mitochondrial membrane, which is designated the “voltage-dependent anion channel” of mitochondria, runs at 30 kD on the second gel dimension and is widely distributed on the native gel dimension between 30 and 1,500 kD. Spots with highest Mascot scores are at about 100 and 180 kD, indicating that porins most likely form trimers that might associate to form hexamers.

### Heat Stress Protein Complexes

The HSP60 complex is composed of two heptameric rings of HSP60 monomers. Its native molecular mass is close to 800 kD. In the presence of ATP, two heptameric HSP10 rings bind to the HSP60 complex. Since 2D BN/SDS-PAGE was carried out in the absence of ATP, the HSP10 heptamers are dissociated and form an extra protein complex of about 100 kD.

### Prohibitin Complex

Prohibitin forms large ring-like protein complexes that are assumed to have functional importance as chaperones for the protein complexes of the oxidative phosphorylation system (Van Aken et al., 2010). The main form of this protein complex migrates between 900 and 1,100 kD on the native gel dimension. Five different isoforms (prohibitin 1, 2, 3, 4, and 6) were detected in our 2D map.

### Protease Complexes

In plants, the heterodimeric mitochondrial processing peptidase forms part of complex III (Braun et al., 1992; see above). Two further protease complexes were detected in our 2D map: the clp protease complex at 260 kD (spot 194), which is composed of 14 clp monomers (Halperin et al., 2001; Peltier et al., 2004), and a putative homodimeric Lon protease complex at 209 kD (spot 77).

### Protein Complexes of Mitochondrial Amino Acid Metabolism

The Glu dehydrogenase complex (spots 80 and 81) runs at 209 kD and probably has a homotetrameric structure. An arginase complex runs at 150 kD (spot 103) and probably is represented by a homotrimer. The 40-kD isovaleryl-CoA dehydrogenase (spot 101) runs at 132 kD and probably forms a trimer or tetramer. The Gly dehydrogenase complex is of high abundance in mitochondria isolated from green tissue but of low abundance in nongreen cell cultures. It consists of the T, P, L, and H subunits (Douce et al., 2001). The P and L proteins are part of our map but do not form a protein complex. Hence, the complex seems to be destabilized under the conditions applied.

### PPR Protein Complexes

PPR proteins represent a large protein family that especially occurs in plant organelles. They are involved in RNA maturation processes like RNA splicing or editing (Delannoy et al., 2007). Twenty-seven PPR proteins were detected in our map, several of which obviously form part of protein complexes because they run on the native gel dimension much higher than explainable by their monomeric molecular mass. For instance, (1) PPR1 (spot 94, Mascot score 855, 70 kD) runs at 160 kD; (2) PPR2-1 and PPR2-2 (spot 95, Mascot scores 129 and 106, 67 kD) both run at 396 kD; (3) PPR3 (spot 80, Mascot score 447, 50 kD) runs at 209 kD; and (4) PPR5-1 (spot 98, Mascot score 114, 46 kD) runs at 156 kD. Further experimental evidence is necessary to determine the exact composition of these PPR protein complexes. It currently cannot be decided whether these complexes have homooligomeric or heterooligomeric subunit composition.

### Further Proteins and Protein Complexes

Many further enzymes listed under “other metabolic pathways” similarly migrate at a much higher position on the native gel dimension than on the denaturing gel dimension, indicating the presence of further protein complexes. It is beyond the scope of this publication to list all these discrepancies. However, our database is publicly accessible via the GelMap platform at [www.gelmap.de/arabidopsis\\_mito](http://www.gelmap.de/arabidopsis_mito) and can be queried for any protein accession of interest. The database also includes several proteins that so far could not be experimentally assigned to a subcellular compartment. These proteins represent candidates for new mitochondrial components, but their subcellular localization should be evaluated by further studies.

The presented reference map allows, to our knowledge for the first time, a systematic definition of the mitochondrial protein complex proteome. The protein complexes described in this study refer to Arabidopsis mitochondria isolated from dark-grown suspension culture cells. Analyses of other tissues of this model plant as well as analyses of Arabidopsis plants cultivated in varying conditions surely will reveal differing results. Changes in the abundance of protein complexes will be analyzed in the future, and the results will be implemented into the GelMap project.

The identification of protein complexes by the combination of 2D BN/SDS-PAGE, tandem MS, and GelMap provides comprehensive insights into the plant mitochondrial protein complex proteome. Many protein complexes could be identified for the first time. Biochemical studies will follow to validate the presence and composition of these protein complexes in the future.

### CONCLUSION

Our study allowed us to identify 471 distinct proteins on a 2D BN/SDS gel and to assign more than 150



of these proteins to 35 different mitochondrial protein complexes. Due to the application of BN/SDS-PAGE, hydrophobic proteins are not discriminated. Therefore, broad-range insights into the protein complex proteome of plant mitochondria have been possible. Several protein complexes were described for the first time (e.g. complexes including the plant-specific PPR proteins). Nevertheless, our experimental strategy to identify protein complexes has to be considered to represent a biased approach, because the 200 most abundant spots were selected for MS analysis, and thereby protein complexes of low abundance only were detected if positioned at a gel region of a protein complex of high abundance. If the protein complex proteome of plant mitochondria is completely analyzed, it would be necessary to systematically scan a 2D BN/SDS gel by MS (e.g. within 100 horizontal gel stripes by 100 spots each [=10,000 spots]). In principle, such an analysis would be feasible, and annotation by GelMap would allow visualizing all protein complexes above the detection limit for MS-based protein identifications. Already for the study presented here, the GelMap software package proved to be very helpful for the exploration of a 2D BN/SDS gel. Its option to differentially display protein complexes should be of increased value for evaluating BN/SDS gels of nonmitochondrial fractions, because resolution of the resulting gels often is of lower quality. We believe that GelMap in general will prove to be a valuable tool for gel-based proteomics.

## MATERIALS AND METHODS

### Preparation of Mitochondria and 2D BN/SDS-PAGE

Mitochondria were isolated from *Arabidopsis thaliana* cell suspension cultures as described by Werhahn et al. (2001). Organelle fractions were divided into aliquots of 100  $\mu\text{L}$  (10  $\mu\text{g}$  mitochondrial protein  $\mu\text{L}^{-1}$ ). For sample preparation prior to BN PAGE, freshly prepared organelles of one aliquot were sedimented by centrifugation for 10 min at full speed (Eppendorf centrifuge) and resuspended in 100  $\mu\text{L}$  of digitonin solubilization buffer (30 mM HEPES, 150 mM potassium acetate, 10% [v/v] glycerol, and 5% [w/v] digitonin). After incubation for 10 min on ice, insoluble material was discarded by another centrifugation step (10 min, full speed, Eppendorf centrifuge), and the supernatant was supplemented with 5  $\mu\text{L}$  of Coomassie blue solution (750 mM aminocaproic acid, 5% [w/v] Coomassie blue 250 G). Fractions were directly loaded onto a BN gel. BN gel electrophoresis was carried out as described before (Wittig et al., 2006). Basic parameters were as follows: (1) Protean II electrophoresis chamber (Bio-Rad); (2) gel dimensions of 16  $\times$  16 cm; (3) polyacrylamide concentration of the first dimension gradient gel, 4.5% to 16% (top to bottom); and (4) second gel dimension, Tricine SDS-PAGE system (Schägger and von Jagow, 1987), constant polyacrylamide concentration on the separation gel (16.5%), which was overlaid with a 2.5-cm spacing gel as described by Jänsch et al. (1996). Gels were stained according to the Coomassie blue-colloidal protocol (Neuhoff et al., 1988).

### Protein Identification by MS

Spots were cut out from a 2D gel using a manual spot picker (Genetix; spot diameter, 1.4 mm) and were numbered consecutively from 1 to 200. In-gel digestion was carried out as described by Klodmann et al. (2010). Tryptic peptides were resolved in 22  $\mu\text{L}$  of liquid chromatography (LC) sample buffer (2% acetonitrile and 0.1% formic acid in water), and 15  $\mu\text{L}$  was injected into the LC-MS system. Nano-HPLC electrospray ionization quadrupole time of

flight MS analyses were carried out with an Easy-nLC system (Proxeon; Thermo Scientific) coupled to a microTOF Q II MS device (Bruker Daltonics). For LC separation, a two-column setup with a C18 reverse phase for hydrophobic interaction of peptides was used: precolumn, Proxeon EASY-PreColumn (length = 2 cm, i.d. = 100  $\mu\text{m}$ ; ReproSil-Pur C18-AQ, 5  $\mu\text{m}$ , 120 Å); analytical column, Proxeon EASY-Column (length = 10 cm, i.d. = 75  $\mu\text{m}$ ; ReproSil-Pur C18-AQ, 3  $\mu\text{m}$ , 120 Å). The LC gradient started with 95% solution A (water + 0.1% formic acid), and the proportion of solution B (acetonitrile + 0.1% formic acid) was continuously increased for 10 min to 50% B. This ratio was applied for 3 min. Solution B was then continuously increased again for 20 min to 95% B and 5% A. MS/MS fragmentation was carried out automatically. For this, the software selected up to three peptides of highest intensity (with a minimal intensity of 3,000 counts) in the MS precursor scan.

For data processing, DataAnalysis software from Bruker Daltonics was used.

Database search was carried out with ProteinScope 2.0 (Bruker Daltonics) and the Mascot search engine in The Arabidopsis Information Resource (TAIR) 10 database ([www.arabidopsis.org](http://www.arabidopsis.org)). The search was carried out with the following parameters: enzyme, trypsin/P, with up to one missed cleavage allowed; global modification, carbamidomethylation (C), variable modifications, acetyl (N), oxidation (M); precursor ion mass tolerance, 20 ppm; fragment ion mass tolerance, 0.05 D; peptide charge, 1+, 2+, and 3+; instrument type, electrospray ionization quadrupole time of flight. Minimum peptide length was set to 4, and protein and peptide assessments were carried out if the Mascot Score was greater than 25 (for proteins as well as peptides).

Proteins were further validated by comparison with the SUBA II database (Heazlewood et al., 2005, 2007) to determine the proportion of nonmitochondrial proteins in our sample (Supplemental Tables S2 and S3). Therefore, accession numbers of all identified proteins (according to the TAIR 10 database) were used for a search of the SUBA II database. Available proteomic data (MS and GFP data) given in SUBA II were used to assign each protein to its most likely subcellular localization. For four different data subsets (first hit proteins, unique proteins, all proteins, and all peptides), the subcellular distribution as well as the proportion of mitochondrial and nonmitochondrial proteins were determined (Supplemental Table S2).

## Image Processing and Database Generation Using GelMap

Gels were scanned using the Image Scanner III (GE Healthcare) and stored as JPEG files with minimal compression. Image files were loaded into the Delta 2D 4.2 software package (Decodon). Spot detection was carried out by automatic mode of the software package and corrected manually. A file including the coordinates of all spots was generated (coord file) and exported into Excel (Microsoft). Finally, gel image (.jpg) and coord (.txt) files were exported into the GelMap software package available at [www.gelmap.de](http://www.gelmap.de) (Rode et al., 2011). Information on how to use GelMap is given in the how-to area of the GelMap Web site (<http://www.gelmap.de/howto>). For the analyses of 2D BN gels, detailed information for all identified proteins was directly added to the coord file. As a consequence, the GelMap database for mitochondria of *Arabidopsis* only is based on two files.

Furthermore, an optional second table (.txt) file was uploaded that provides peptide data of the MS/MS analyses. Information about the identified peptides of a protein is available via a link for more peptide details in the pop-up windows on the reference gel (Fig. 4).

## Supplemental Data

The following materials are available in the online version of this article.

**Supplemental Figure S1.** Assignment of subunits of complex V (ATP synthase).

**Supplemental Figure S2.** Protein complex visualization by GelMap.

**Supplemental Table S1.** Detail table of the 2D BN/SDS reference map for *Arabidopsis* mitochondrial proteins.

**Supplemental Table S2.** Subcellular localization of the identified proteins according to the SUBA II database.

**Supplemental Table S3.** SUBA II search results.

## Note Added in Proof

The Arabidopsis mitochondrial protein complex proteome reference map ([http://www.gelmap.de/arabidopsis\\_mito](http://www.gelmap.de/arabidopsis_mito)) was integrated into the Arabidopsis proteomics meta portal "MASC P Gator" (<http://gator.masc-proteomics.org/>).

## ACKNOWLEDGMENTS

We thank Dagmar Lewejohann for expert technical assistance and Holger Eubel for critically reading the manuscript.

Received June 23, 2011; accepted August 10, 2011; published August 12, 2011.

## LITERATURE CITED

- Arnold I, Pfeiffer K, Neupert W, Stuart RA, Schagger H (1998) Yeast mitochondrial  $F_1F_0$ -ATP synthase exists as a dimer: identification of three dimer-specific subunits. *EMBO J* 17: 7170–7178
- Baker MJ, Webb CT, Stroud DA, Palmer CS, Frazier AE, Guiard B, Chacinska A, Gulbis JM, Ryan MT (2009) Structural and functional requirements for activity of the Tim9-Tim10 complex in mitochondrial protein import. *Mol Biol Cell* 20: 769–779
- Braun HP, Emmermann M, Kruff V, Schmitz UK (1992) The general mitochondrial processing peptidase from potato is an integral part of cytochrome c reductase of the respiratory chain. *EMBO J* 11: 3219–3227
- Braun HP, Schmitz UK (1995) The bifunctional cytochrome c reductase/processing peptidase complex from plant mitochondria. *J Bioenerg Biomembr* 27: 423–436
- Bykova NV, Egsgaard H, Møller IM (2003a) Identification of 14 new phosphoproteins involved in important plant mitochondrial processes. *FEBS Lett* 540: 141–146
- Bykova NV, Stensballe A, Egsgaard H, Jensen ON, Møller IM (2003b) Phosphorylation of formate dehydrogenase in potato tuber mitochondria. *J Biol Chem* 278: 26021–26030
- Carroll J, Shannon RJ, Fearnley IM, Walker JE, Hirst J (2002) Definition of the nuclear encoded protein composition of bovine heart mitochondrial complex I: identification of two new subunits. *J Biol Chem* 277: 50311–50317
- Delannoy E, Stanley WA, Bond CS, Small ID (2007) Pentatricopeptide repeat (PPR) proteins as sequence-specificity factors in post-transcriptional processes in organelles. *Biochem Soc Trans* 35: 1643–1647
- Douce R, Bourguignon J, Neuburger M, Rébeillé F (2001) The glycine decarboxylase system: a fascinating complex. *Trends Plant Sci* 6: 167–176
- Emmermann M, Braun HP, Schmitz UK (1991) The ADP/ATP translocator from potato has a long amino-terminal extension. *Curr Genet* 20: 405–410
- Eubel H, Jansch L, Braun HP (2003) New insights into the respiratory chain of plant mitochondria: supercomplexes and a unique composition of complex II. *Plant Physiol* 133: 274–286
- Giegé P, Sweetlove LJ, Leaver CJ (2003) Identification of mitochondrial protein complexes in Arabidopsis using two-dimensional blue-native polyacrylamide gel electrophoresis. *Plant Mol Biol Rep* 21: 133–144
- Halperin T, Zheng B, Itzhaki H, Clarke AK, Adam Z (2001) Plant mitochondria contain proteolytic and regulatory subunits of the ATP-dependent Clp protease. *Plant Mol Biol* 45: 461–468
- Heazlewood JL, Howell KA, Millar AH (2003a) Mitochondrial complex I from Arabidopsis and rice: orthologs of mammalian and fungal components coupled with plant-specific subunits. *Biochim Biophys Acta* 1604: 159–169
- Heazlewood JL, Howell KA, Whelan J, Millar AH (2003b) Towards an analysis of the rice mitochondrial proteome. *Plant Physiol* 132: 230–242
- Heazlewood JL, Tonti-Filippini JS, Gout AM, Day DA, Whelan J, Millar AH (2004) Experimental analysis of the Arabidopsis mitochondrial proteome highlights signaling and regulatory components, provides assessment of targeting prediction programs, and indicates plant-specific mitochondrial proteins. *Plant Cell* 16: 241–256
- Heazlewood JL, Tonti-Filippini J, Verboom RE, Millar AH (2005) Combining experimental and predicted datasets for determination of the subcellular location of proteins in Arabidopsis. *Plant Physiol* 139: 598–609
- Heazlewood JL, Verboom RE, Tonti-Filippini J, Small I, Millar AH (2007) SUBA: the Arabidopsis subcellular database. *Nucleic Acids Res* 35: D213–D218
- Heazlewood JL, Whelan J, Millar AH (2003c) The products of the mitochondrial orf25 and orfB genes are FO components in the plant F1FO ATP synthase. *FEBS Lett* 540: 201–205
- Heinemeyer J, Scheibe B, Schmitz UK, Braun HP (2009) Blue native DIGE as a tool for comparative analyses of protein complexes. *J Prot* 72: 539–544
- Huang S, Taylor NL, Narsai R, Eubel H, Whelan J, Millar AH (2010) Functional and composition differences between mitochondrial complex II in Arabidopsis and rice are correlated with the complex genetic history of the enzyme. *Plant Mol Biol* 72: 331–342
- Jansch L, Kruff V, Schmitz UK, Braun HP (1996) New insights into the composition, molecular mass and stoichiometry of the protein complexes of plant mitochondria. *Plant J* 9: 357–368
- Jansch L, Kruff V, Schmitz UK, Braun HP (1998) Unique composition of the preprotein translocase of the outer mitochondrial membrane from plants. *J Biol Chem* 273: 17251–17257
- Jenner HL, Winning BM, Millar AH, Tomlinson KL, Leaver CJ, Hill SA (2001) NAD malic enzyme and the control of carbohydrate metabolism in potato tubers. *Plant Physiol* 126: 1139–1149
- Klodmann J, Braun HP (2011) Proteomic approach to characterize mitochondrial complex I from plants. *Phytochemistry* 72: 1071–1080
- Klodmann J, Sunderhaus S, Nimtz M, Jansch L, Braun HP (2010) Internal architecture of mitochondrial complex I from *Arabidopsis thaliana*. *Plant Cell* 22: 797–810
- Kruff V, Eubel H, Werhahn WH, Jansch L, Braun HP (2001) Proteomic approach to identify novel mitochondrial functions in *Arabidopsis thaliana*. *Plant Physiol* 127: 1694–1710
- Lee CP, Eubel H, O'Toole N, Millar AH (2011) Combining proteomics of root and shoot mitochondria and transcript analysis to define constitutive and variable components in plant mitochondria. *Phytochemistry* 72: 1092–1108
- Lister R, Carrie C, Duncan O, Ho LH, Howell KA, Murcha MW, Whelan J (2007) Functional definition of outer membrane proteins involved in preprotein import into mitochondria. *Plant Cell* 19: 3739–3759
- Lister R, Hulett JM, Lithgow T, Whelan J (2005) Protein import into mitochondria: origins and functions today. *Mol Membr Biol* 22: 87–100
- Meyer EH, Heazlewood JL, Millar AH (2007) Mitochondrial acyl carrier proteins in Arabidopsis thaliana are predominantly soluble matrix proteins and none can be confirmed as subunits of respiratory complex I. *Plant Mol Biol* 64: 319–327
- Meyer EH, Taylor NL, Millar AH (2008) Resolving and identifying protein components of plant mitochondrial respiratory complexes using three dimensions of gel electrophoresis. *J Proteome Res* 2: 786–794
- Michalecka AM, Svensson AS, Johansson FL, Agius SC, Johansson U, Brennicke A, Binder S, Rasmusson AG (2003) Arabidopsis genes encoding mitochondrial type II NAD(P)H dehydrogenases have different evolutionary origin and show distinct responses to light. *Plant Physiol* 133: 642–652
- Millar AH, Eubel H, Jansch L, Kruff V, Heazlewood L, Braun HP (2004a) Mitochondrial cytochrome c oxidase and succinate dehydrogenase contain plant-specific subunits. *Plant Mol Biol* 56: 77–89
- Millar AH, Mittova V, Kiddle G, Heazlewood JL, Bartoli CG, Theodoulou FL, Foyer CH (2003) Control of ascorbate synthesis by respiration and its implications for stress responses. *Plant Physiol* 133: 443–447
- Millar AH, Sweetlove LJ, Giegé P, Leaver CJ (2001) Analysis of the Arabidopsis mitochondrial proteome. *Plant Physiol* 127: 1711–1727
- Millar AH, Trend AE, Heazlewood JL (2004b) Changes in the mitochondrial proteome during the anoxia to air transition in rice focus around cytochrome-containing respiratory complexes. *J Biol Chem* 279: 39471–39478
- Mozo T, Fischer K, Flügge UI, Schmitz UK (1995) The N-terminal extension of the ADP/ATP translocator is not involved in targeting to plant mitochondria in vivo. *Plant J* 7: 1015–1020
- Neuhoff V, Arold N, Taube D, Ehrhardt W (1988) Improved staining of proteins in polyacrylamide gels including isoelectric focusing gels with clear background at nanogram sensitivity using Coomassie Brilliant Blue G-250 and R-250. *Electrophoresis* 6: 255–262
- Peltier JB, Ripoll DR, Friso G, Rudella A, Cai Y, Ytterberg J, Giacomelli L,

Klodmann et al.

- Pillardy J, van Wijk KJ** (2004) Clp protease complexes from photosynthetic and non-photosynthetic plastids and mitochondria of plants, their predicted three-dimensional structures, and functional implications. *J Biol Chem* **279**: 4768–4781
- Peters K, Dukina NV, Jansch L, Braun HP, Boekema EJ** (2008) A structural investigation of complex I and I+III<sub>2</sub> supercomplex from *Zea mays* at 11–13 Å resolution: assignment of the carbonic anhydrase domain and evidence for structural heterogeneity within complex I. *Biochim Biophys Acta (Bioenergetics)* **1777**: 84–93
- Rasmusson AG, Agius SC** (2001) Rotenone-insensitive NAD(P)H dehydrogenases in plants: immunodetection and distribution of native proteins in mitochondria. *Plant Physiol Biochem* **39**: 1057–1066
- Rode C, Senkler M, Klodmann J, Winkelmann T, Braun HP** (2011) GelMap: a novel software tool for the creation and presentation of proteome reference maps. *J Proteomics* **74**: 2214–2219
- Schägger H, von Jagow G** (1987) Tricine-sodium dodecyl sulfate-polyacrylamide gel electrophoresis for the separation of proteins in the range from 1 to 100 kDa. *Anal Biochem* **166**: 368–379
- Schägger H, von Jagow G** (1991) Blue native electrophoresis for isolation of membrane protein complexes in enzymatically active form. *Anal Biochem* **199**: 223–231
- Sunderhaus S, Dudkina N, Jansch L, Klodmann J, Heinemeyer J, Perales M, Zabaleta E, Boekema E, Braun HP** (2006) Carbonic anhydrase subunits form a matrix-exposed domain attached to the membrane arm of mitochondrial complex I in plants. *J Biol Chem* **281**: 6482–6488
- Sunderhaus S, Klodmann J, Lenz C, Braun HP** (2010) Supramolecular structure of the OXPHOS system in highly thermogenic tissue of *Arum maculatum*. *Plant Physiol Biochem* **48**: 265–272
- Taylor N, Heazlewood J, Millar AH** (2011) The *Arabidopsis thaliana* 2D gel mitochondrial proteome: refining the value of reference maps for assessing protein abundance, contaminants and post-translational modifications. *Proteomics* **11**: 1720–1733
- Van Aken O, Whelan J, van Breusegem F** (2010) Prohibitins: mitochondrial partners in development and stress response. *Trends Plant Sci* **15**: 275–282
- Werhahn WH, Braun HP** (2002) Biochemical dissection of the mitochondrial proteome of *Arabidopsis thaliana* by three-dimensional gel electrophoresis. *Electrophoresis* **23**: 640–646
- Werhahn WH, Jansch L, Braun HP** (2003) Identification of novel subunits of the TOM complex from *Arabidopsis thaliana*. *Plant Physiol Biochem* **41**: 407–416
- Werhahn WH, Niemeyer A, Jansch L, Kruft V, Schmitz UK, Braun HP** (2001) Purification and characterization of the preprotein translocase of the outer mitochondrial membrane from *Arabidopsis thaliana*: identification of multiple forms of TOM20. *Plant Physiol* **125**: 943–954
- Winning BM, Sarah CJ, Purdue PE, Day CD, Leaver CJ** (1992) The adenine nucleotide translocator of higher plants is synthesized as a large precursor that is processed upon import into mitochondria. *Plant J* **2**: 763–773
- Wittig I, Braun HP, Schägger H** (2006) Blue-native PAGE. *Nat Protoc* **1**: 418–428
- Zhou ZH, McCarthy DB, O'Connor CM, Reed LJ, Stoops JK** (2001) The remarkable structural and functional organization of the eukaryotic pyruvate dehydrogenase complexes. *Proc Natl Acad Sci USA* **98**: 14802–14807

# Curriculum Vitae

---

Name:	Jennifer Klodmann
Date of Birth:	09.12.1981
Place of Birth:	Hannover, Germany
Citizenship:	Citizen of Germany

---

## SCHOOL EDUCATION

1988 – 1992	Primary school in Holtorf (Nienburg)
1992 – 1994	Orientierungsstufe in Erichshagen (Nienburg)
1994 – 2001	Secondary school ‘Gymnasium Hindenburgschule’ in Nienburg Qualification: ‘Abitur’

## ACADEMIC EDUCATION

Oct. 2001 – Sept. 2002	Student at the Leibniz Universität Hannover, major: Lehramt Gymnasium, subjects: Biology, Chemistry
Oct. 2002 – Oct. 2005	Student at the Leibniz Universität Hannover, major: Plant Biotechnology
Oct. 2005	Bachelor of Science in Plant Biotechnology Thesis: “Submitochondrial localization of carbonic anhydrases in plant mitochondria” Grade: ‘excellent’
Oct. 2005 – Sept. 2007	Student at the Leibniz Universität Hannover, major: Plant Biotechnology
Sept. 2007	Master of Science in Plant Biotechnology Thesis: “Topological analyses of the oxidative phosphorylation system from plants” Grade: ‘excellent’
Since Oct. 2007	PhD student at the Leibniz Universität Hannover, Institute of Plant Genetics, Department Plant Proteomics, Prof. Dr. Hans- Peter Braun



## Publications and Conference contributions

### Publications

Schertl, P., Sunderhaus, S., Klodmann, J., Grozeff, G.E., Bartoli, C.G. and Braun, H.P. (2012)  
L-galactono-1,4-lactone dehydrogenase (GLDH) forms part of three subcomplexes of mitochondrial complex I in *Arabidopsis thaliana*.  
*J. Biol. Chem.* 287: 14412-14419.

Klodmann, J. and Braun, H.P. (2011)  
Proteomic approach to characterize mitochondrial complex I from plants.  
*Phytochemistry* 72: 1071-1080.

Klodmann, J., Lewejohann, D. and Braun, H.P. (2011)  
Low-SDS Blue native PAGE.  
*Proteomics* 11: 1834-1839.

Klodmann, J., Senkler, M., Rode, C. and Braun, H.P. (2011)  
Defining the protein complex proteome of plant mitochondria.  
*Plant Physiol.* 157: 587-598.

Rode, C., Senkler, M., Klodmann, J., Winkelmann, T. and Braun, H.P. (2011)  
GelMap-a novel software tool for building and presenting proteome reference maps.  
*J. Proteomics* 74: 2214-2219.

Welchen, E., Klodmann, J. and Braun, H.P. (2011)  
Biogenesis and supermolecular organization of the oxidative phosphorylation system in plants.  
*In: Plant Mitochondria. Edited by Kempken, F. pp. 327–355. Springer Science + Business Media LLC, New York, NY.*

Zeiser, J.J., Klodmann, J., Braun, H.P., Gerhard, R., Just, I. and Pich, A. (2011)  
Effects of *Clostridium difficile* Toxin A on the proteome of colonocytes studied by differential 2D electrophoresis.  
*J. Proteomics* 75:469-479.

Klodmann, J., Sunderhaus, S., Nimtz, M., Jansch, L. and Braun, H.P. (2010)  
Internal architecture of mitochondrial complex I from *Arabidopsis thaliana*.  
*Plant Cell* 22: 797-810.

Sunderhaus, S., Klodmann, J., Lenz, C. and Braun, H.P. (2010)  
Supramolecular structure of the OXPHOS system in highly thermogenic tissue of *Arum maculatum*.  
*Plant Physiol. Biochem.* 48: 265-272.

Sunderhaus, S., Dudkina, N.V., Jansch, L., Klodmann, J., Heinemeyer, J., Perales, M., Zabaleta, E., Boekema, E.J. and Braun, H.P. (2006)  
Carbonic anhydrase subunits form a matrix-exposed domain attached to the membrane arm of mitochondrial complex I in plants.  
*J. Biol. Chem.* 281: 6482-6488.

## Conference contributions

International Congress on Plant Mitochondrial Biology (ICPMB) (14.-19.05.2011)

Hohenroda, Germany

Poster: *GelMap - A novel software tool for the creation and presentation of proteome reference maps of mitochondria*

Poster: *Structure and subunit composition of NADH ubiquinone oxidoreductase (complex I) from plant mitochondria*

Research Meeting, DFG Forschergruppe „PROMICS” (27.-29.11.2010)

Rostock, Germany

Talk: *Searching for a role of mitochondrial carbonic anhydrases in plants*

24<sup>th</sup> New Phytologist Symposium “Plant respiration and climate change: scaling from mitochondria to the globe” (11.-14.04.2010)

Oxford, United Kingdom

Poster: *Physiological role of mitochondrial gamma carbonic anhydrases in the CO<sub>2</sub> metabolism of plant cells*

16. Arbeitstagung „Mikromethoden in der Proteinchemie“ (22-24.06.2009)

Martinsried, München, Germany

Talk: *Neue Strategie zur Untersuchung der inneren Architektur von großen Proteinkomplexen: Ergebnisse zum Komplex I pflanzlicher Mitochondrien*

International Congress on Plant Mitochondrial Biology (ICPMB) (09.-14.05.2009)

Lake Tahoe, California, USA

Poster, talk: *Internal architecture of the mitochondrial NADH-ubiquinone oxidoreductase (complex I) of plants*

42. Tagung der Deutschen Gesellschaft für Massenspektrometrie (DGMS) (08.-11.03.2009)

Konstanz, Germany

Poster: *Identifizierung von Proteinen des OXPHOS-Systems von *Arum maculatum* durch 2D-Blue Native/SDS-PAGE, QqLIT-Massenspektrometrie und substitutionstolerante Datenbanksuche*

International Congress on Plant Mitochondrial Biology (ICPMB) (25.-29.06.2007)

Nara, Japan

Poster: *Topology and subunit composition of plant mitochondrial OXPHOS complexes*

## Award

Young Investigator Award 2009

16. Arbeitstagung „Mikromethoden in der Proteinchemie“ (22-24.06.2009)

Martinsried, München, Germany

Contribution: *Neue Strategie zur Untersuchung der inneren Architektur von großen Proteinkomplexen: Ergebnisse zum Komplex I pflanzlicher Mitochondrien*



## Danksagung

Zur vorliegenden Dissertation haben viele Menschen beigetragen, ihnen allen danke ich sehr. Im Folgenden möchte ich mich bei den Menschen bedanken, die mich in besonderem Maß in der Forschung aber auch durch ihre Freundschaft unterstützt haben.

**Lieber Hans-Peter**, danke für das interessante Thema, das ich in Deiner Arbeitsgruppe bearbeiten durfte, für Deine engagierte Betreuung meiner Arbeit, sowie für die große Unterstützung bei der Veröffentlichung der entstandenen Daten. Danke, dass Du mir die Teilnahme an so vielen interessanten Konferenzen ermöglicht hast. Danke für Deine Unterstützung, auch in den weniger wissenschaftlichen Dingen des Lebens. Es hat mir viel Spaß gemacht, für Dich und mit Dir zusammen zu arbeiten!

**Prof. Dr. Christoph Peterhänsel** und **Prof. Dr. Udo Schmitz** danke ich, dass sie sich als Korreferenten für meine Dissertation zur Verfügung gestellt haben.

**Der gesamten Abteilung** danke ich für die stete Hilfsbereitschaft und den netten Umgang miteinander.

**Meinen BürokollegInnen** Katrin, Christof, Christina und Christin danke ich für die gegenseitige Hilfe und Diskussionen, für die fröhliche und entspannte Atmosphäre, sowie für die Toleranz meines „Ökosystems Kaffeetasse“ und dafür, dass ihr es doch hin und wieder mal zerstört habt.

**Liebe Dagmar**, danke für Deine große Unterstützung im Labor, für Deine hilfsbereite und souveräne Art, mit der Du mir oft sehr geholfen hast. Danke für Deine Freundschaft.

**Liebe Katrin**, danke für Deine Freundschaft und Deine Unterstützung, in jeder Hinsicht.

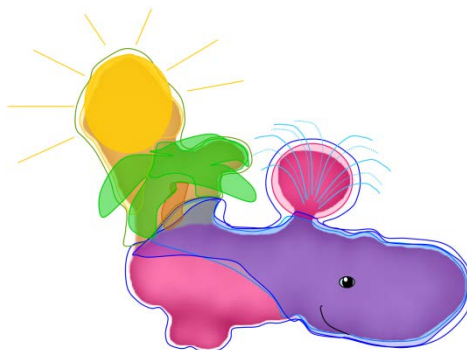
**Liebe Katrin, liebe Steffi**, danke für eine tolle gemeinsame Zeit in den letzten Jahren!

**Liebe Christin**, danke für Dein offenes Ohr und Deine verständnisvolle und hilfsbereite Art, auf die ich gerade in den letzten Wochen nicht hätte verzichten wollen.

**Liebe „core subunits“** der AG, wir haben nun schon einige Jahre mit einander verbracht und vieles gemeinsam erlebt, Kurse ausgerichtet, Konferenzen besucht, aber auch zusammen gegrillt und gefeiert. Danke für diese schöne gemeinsame Zeit!

**Liebe Mama, lieber Papa, lieber Julian**, danke, dass ihr immer hinter mir steht.

**Lieber Michael**, danke für alles.



*So long...and thanks for all the fish!*



## **Erklärung**

Hierdurch erkläre ich, dass ich meine Dissertation mit dem Titel „Structure and function of the mitochondrial NADH ubiquinone oxidoreductase from *Arabidopsis thaliana*“ selbständig verfasst und die benutzten Hilfsmittel und Quellen sowie gegebenenfalls die zu Hilfeleistungen herangezogenen Institutionen vollständig angegeben habe.

Die Dissertation wurde nicht schon als Masterarbeit, Diplomarbeit oder andere Prüfungsarbeit verwendet.

Hannover, den 03.07.2012